Centrum voor Wiskunde en Informatica

REPORT*RAPPORT*

MAS

Modelling, Analysis and Simulation

Modelling, Analysis and Simulation

Homoclinic bifurcations at the onset of pulse self-replication

A. Doelman, T.J. Kaper, L.A. Peletier

REPORT MAS-E0610 FEBRUARY 2006

Centrum voor Wiskunde en Informatica (CWI) is the national research institute for Mathematics and Computer Science. It is sponsored by the Netherlands Organisation for Scientific Research (NWO).
CWI is a founding member of ERCIM, the European Research Consortium for Informatics and Mathematics.

CWI's research has a theme-oriented structure and is grouped into four clusters. Listed below are the names of the clusters and in parentheses their acronyms.

Probability, Networks and Algorithms (PNA)

Software Engineering (SEN)

Modelling, Analysis and Simulation (MAS)

Information Systems (INS)

P.O. Box 94079, 1090 GB Amsterdam (NL)
Kruislaan 413, 1098 SJ Amsterdam (NL)
Telephone +31 20 592 9333
Telefax +31 20 592 4199

ISSN 1386-3703

Homoclinic bifurcations at the onset of pulse self-replication

ABSTRACT
We establish a series of properties of symmetric, N-pulse, homoclinic solutions of the *reduced* Gray-Scott system

$$u'' = uv^2, \qquad v'' = v - uv^2,$$

which play a pivotal role in questions concerning the existence and self-replication of pulse solutions of the full Gray-Scott model. Specifically, we establish the existence, and study properties, of solution branches in the (α,β)-plane that represent multi-pulse homoclinic orbits, where α and β are the central values of $u(x)$ and $v(x)$, respectively. We prove bounds for these solution branches, study their behavior as $\alpha \to \infty$, and establish a series of geometric properties of these branches which are valid throughout the (α,β)-plane. We also establish qualitative properties of multi-pulse solutions and study how they bifurcate, *i.e.*, how they change along the solution branches.

2000 Mathematics Subject Classification: 35K45, 35K57, 35B25, 35B32, 35B35, 35B40, 34C30, 34C37, 92C15, 92E20
Keywords and Phrases: symmetric homoclinic orbits, multi-pulse orbits, homoclinic bifurcations, reaction-diffusion equations, autocatalysis, self-replicating pulses

Homoclinic bifurcations at the onset of pulse self-replication *

Arjen Doelman †
Tasso J. Kaper ‡
Lambertus A. Peletier §

February 10, 2006

Abstract

We establish a series of properties of symmetric, N-pulse, homoclinic solutions of the *reduced* Gray-Scott system

$$u'' = uv^2, \qquad v'' = v - uv^2,$$

which play a pivotal role in questions concerning the existence and self-replication of pulse solutions of the full Gray-Scott model. Specifically, we establish the existence, and study properties, of solution branches in the (α, β)-plane that represent multi-pulse homoclinic orbits, where α and β are the central values of $u(x)$ and $v(x)$, respectively. We prove bounds for these solution branches, study their behavior as $\alpha \to \infty$, and establish a series of geometric properties of these branches which are valid throughout the (α, β)-plane. We also establish qualitative properties of multi-pulse solutions and study how they bifurcate, *i.e.*, how they change along the solution branches.

1 Introduction

In this article, we analyze the existence, nonexistence, bifurcation, and qualitative properties of positive, symmetric, N-pulse, homoclinic orbits of the following system of ordinary differential equations:

$$u'' = uv^2 \qquad \text{and} \qquad v'' = v - uv^2, \tag{1.1}$$

*Key words: symmetric homoclinic orbits, multi-pulse orbits, homoclinic bifurcations, reaction-diffusion equations, autocatalysis, self-replicating pulses. **AMS (MOS) subject classifications:** 35K45, 35K57, 35B25, 35B32, 35B35, 35B40, 34C30, 34C37, 92C15, 92E20.

†C.W.I. Centrum voor Wiskunde en Informatica, Kruislaan 413, 1098 SJ Amsterdam, the Netherlands, & Korteweg-de Vries Institute, University of Amsterdam, Plantage Muidergracht 24, 1018 TV Amsterdam, the Netherlands, doelman@cwi.nl

‡Department of Mathematics & Center for BioDynamics, Boston University, 111 Cummington Street, Boston, MA 02215, U.S.A. tasso@math.bu.edu

§Mathematical Institute, Leiden University, P.O. Box 9512, 2300 RA Leiden, the Netherlands. & C.W.I. Centrum voor Wiskunde en Informatica, Kruislaan 413, 1098 SJ Amsterdam, the Netherlands, peletier@math.leidenuniv.nl

where $x \in \mathbb{R}$, $u = u(x)$, $v = v(x)$, and prime denotes d/dx. Symmetric solutions of (1.1) are identified by their values at the origin,

$$u(0) = \alpha \qquad \text{and} \qquad v(0) = \beta, \tag{1.2}$$

where α and β are positive constants. Moreover, since $u' = 0$ and $v' = 0$ at the origin for symmetric solutions, any pair (α, β) determines a unique local solution of (1.1).

For some values of (α, β) the corresponding solution (u, v) exists for all $x \in \mathbb{R}$ and has the property that

$$v(x) \to 0 \qquad \text{as} \qquad x \to \pm\infty. \tag{1.3}$$

Although $u(x) \to \infty$ as $x \to \pm\infty$ with $u'(x) \to \pm p_\infty$ for some p_∞ for such solutions, we refer to solutions endowed with the property (1.3) as *homoclinic orbits.* Let us denote the set of such points by Σ, *i.e.,*

$$\Sigma = \{(\alpha, \beta) \in \mathbb{R}^+ \times \mathbb{R}^+ : \text{ the corresponding solution } (u, v) \text{ is homoclinic}\}. \tag{1.4}$$

Our main objectives in this article are to study fundamental aspects of:

(i) the location of the set Σ in the (α, β)-plane,

(ii) the structure of Σ as a family of curves, including their bifurcations, and

(iii) qualitative properties of the different homoclinic orbits.

In order to determine the location of Σ, we define the family of hyperbolas

$$\mathcal{K}_\lambda = \{(\alpha, \beta) : \alpha > 0,\ \beta = \lambda/\alpha\}, \qquad \lambda > 0. \tag{1.5}$$

We will show that the set Σ lies below $\mathcal{K}_{3/2}$ and that it straddles $\mathcal{K}_1$. In Figure 1, we display some of the curves from the set Σ in the (α, β)-plane, as well as portions of the hyperbolas $\mathcal{K}_1$ and $\mathcal{K}_{3/2}$.

It follows from the equation for v in (1.1) that $v''(0) < 0$ if $\beta > 1/\alpha$, whereas $v''(0) > 0$ if $\beta < 1/\alpha$. Thus, for points in Σ which lie above $\mathcal{K}_1$, the graph of $v(x)$ must have an odd number of local maxima; while, for those lying below $\mathcal{K}_1$, the number of local maxima must be even. In Figure 2, we present the graph of $v(x)$ of several homoclinic orbits, two starting at points above $\mathcal{K}_1$ and two starting from points below $\mathcal{K}_1$.

The location of the set Σ may be determined more precisely by analyzing homoclinic orbits with an odd number of local maxima and those with an even number of local maxima separately, and by defining admissible sets $\mathcal{A}_{\text{odd}}$ and $\mathcal{A}_{\text{even}}$, respectively. Plainly, $\mathcal{A}_{\text{odd}}$ lies between the curves $\mathcal{K}_{3/2}$ and $\mathcal{K}_1$, and $\mathcal{A}_{\text{even}}$ must lie below $\mathcal{K}_1$. We then obtain an explicit curve which connects $\mathcal{K}_{3/2}$ and $\mathcal{K}_1$ and which serves as an upper bound for $\mathcal{A}_{\text{odd}}$. Bounding $\mathcal{A}_{\text{even}}$ is a more delicate operation; here, we prove the existence of an upper bound and a positive lower bound. See Figure 1 for an illustration of these sets.

The second objective concerns the structure of the set Σ as a family of curves of initial conditions corresponding to symmetric, N-pulse, homoclinic orbits. We begin with the regime where α is large and use ideas and methods which have been developed

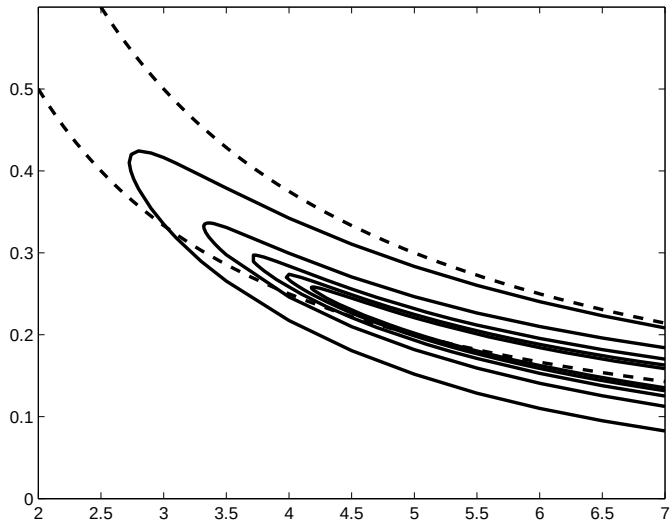

Figure 1: In the (α, β)-plane, several branches of symmetric, N-pulse, homoclinic orbits obtained from numerical simulations of (1.1) (solid curves) and the hyperbolas $\mathcal{K}_1$ and $\mathcal{K}_{3/2}$ (dashed curves). All of the branches lie below $\mathcal{K}_{3/2}$. For large α, they are ordered as $\mathcal{C}_1^\infty$, $\mathcal{C}_3^\infty$, $\mathcal{C}_5^\infty$, $\mathcal{C}_7^\infty$, $\mathcal{C}_9^\infty$, $\mathcal{C}_{10}^\infty$, $\mathcal{C}_8^\infty$, $\mathcal{C}_6^\infty$, $\mathcal{C}_4^\infty$, $\mathcal{C}_2^\infty$ from top to bottom.

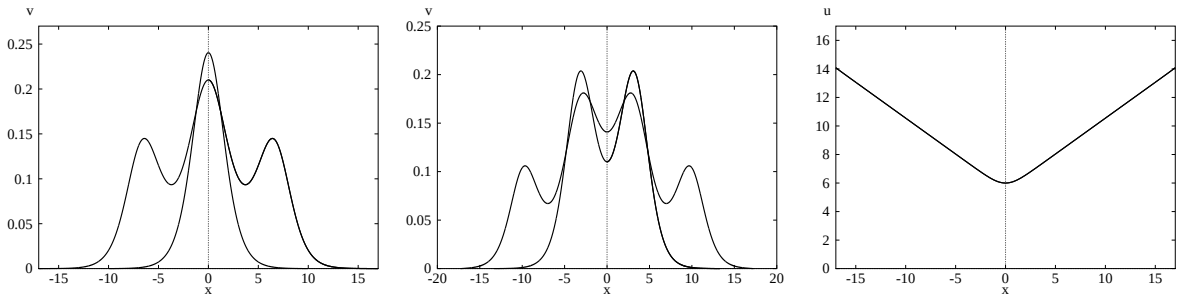

Figure 2: Left frame: the graphs of $v(x)$ for a 1-pulse solution and a 3-pulse solution lying on $\mathcal{C}_1^\infty$ and $\mathcal{C}_3^\infty$, respectively, the first and the second branches from the top in Figure 1. Here, $\beta \approx 0.2404422$ and $\beta \approx 0.2100454$, respectively. Middle frame: the graphs of $v(x)$ for a 2-pulse solution and a 4-pulse solution, lying on $\mathcal{C}_2^\infty$ and $\mathcal{C}_4^\infty$, respectively, the first and the second branches from the bottom in Figure 1. Here, $\beta \approx 0.1101287$ and $\beta \approx 0.14084$, respectively. Right frame: the graph of $u(x)$ for the same 1-pulse solution as in the left frame with $p_\infty = u'(\infty) \approx 0.5033$. In all frames $\alpha = 6$.

in [11] and [7] for the purpose of studying the asymptotic properties of stationary pulse solutions of the Gray-Scott system (1.14) and more general systems. For each $N \geq 1$, and for α sufficiently large, *i.e.,* greater than some $\tilde{\alpha}(N)$, we find that Σ consists of a

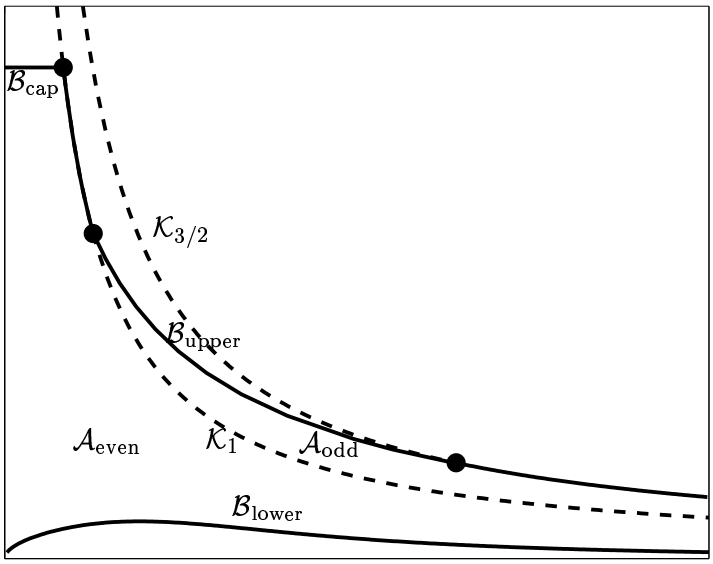

Figure 3: A sketch in the (α,β)-plane of the curves $\mathcal{K}_{3/2}$ (upper hyperbola – partly dashed and partly solid), $\mathcal{K}_1$ (lower hyperbola – partly dashed and partly solid), $\mathcal{B}_{\rm upper}$ (the solid curve segment connecting the two hyperbolae between the middle and lower dots), $\mathcal{B}_{\rm cap}$ (the solid line segment connecting $\mathcal{K}_1$ at the upper dot to the β-axis), and $\mathcal{B}_{\rm lower}$ (solid curve at the bottom). The boundaries on the admissible sets $\mathcal{A}_{\rm odd}$ and $\mathcal{A}_{\rm even}$ are given, respectively, by the solid portion of $\mathcal{K}_{3/2}$, the solid curve segment $\mathcal{B}_{\rm upper}$, and the lower, dashed portion of $\mathcal{K}_1$, and by the solid portion of $\mathcal{K}_1$ between the upper and middle dots, the solid line segment $\mathcal{B}_{\rm cap}$, a piece of the vertical (β) axis, and the solid curve $\mathcal{B}_{\rm lower}$.

series of unique branches

$$\mathcal{C}_N^\infty = \{(\alpha,\beta) : \alpha > \tilde{\alpha}(N),\ \beta = \beta_N(\alpha)\}, \qquad N = 1,2,3,\ldots \tag{1.6}$$

of homoclinic orbits such that $v(x)$ has N local maxima on $\mathcal{C}_N^\infty$. These branches must lie above $\mathcal{K}_1$ if N is odd and below $\mathcal{K}_1$ if N is even. Specifically,

$$\beta_N(\alpha) = \frac{3}{2\alpha} - \frac{3}{2\alpha^3}\left(\frac{11}{8} + \frac{8}{5}(N^2-1)\right) + o(\alpha^{-3}) \quad \text{as} \quad \alpha \to \infty \quad \text{if } N \text{ is odd} \tag{1.7}$$

and

$$\beta_N(\alpha) = \frac{3\sqrt{2}}{\sqrt{5}} N \frac{1}{\alpha^2} + o(\alpha^{-2}) \quad \text{as} \quad \alpha \to \infty \quad \text{if } N \text{ is even.} \tag{1.8}$$

Moreover, in the process of establishing these results, we show for each N that the N-pulse homoclinic orbits with initial conditions on $\mathcal{C}_N^\infty$ lie in the transverse intersections

of invariant manifolds of system (1.1) when $\alpha \gg 1$. Finally, in the special cases of $N = 1$ and $N = 2$, these results agree with the matched asymptotic results obtained in [24] for one- and two-pulse solutions of the system (1.1).

The geometric construction and the resulting asymptotic expansions (1.7) and (1.8) imply that for each α large enough there exists an $\tilde{N}$ large such that the set Σ consists of a family of curves $\mathcal{C}_N^\infty$, with $N = 1, 2, \ldots, \tilde{N}$. These curves are neatly ordered like a mille-feuille cake; alternating being near the hyperbola $\mathcal{K}_{3/2}$ and near the α-axis. See Figure 1. Moreover, the asymptotics also allow us to conclude that the bounds on the regimes $\mathcal{A}_{\text{odd}}$ and $\mathcal{A}_{\text{even}}$ are optimal for large enough α.

The geometry of the curves $\mathcal{C}_N^\infty$ anchors the main results of this article about the structure of Σ, which we now describe. The invariant manifolds, in whose transverse intersections the N-pulse orbits lie for α large, can be continued to $\mathcal{O}(1)$ values of α into the region of the (α, β)-plane in which there is no longer a small parameter in the governing equations (1.1) and in which the four variables (u, u', v, v') evolve on the same scale. Moreover, by continuing these invariant manifolds and by using some of the qualitative properties of homoclinic orbits, we will be able to track the intersections of these manifolds, and hence the curves $\mathcal{C}_N^\infty$ as well, into the region in which α and β are both $\mathcal{O}(1)$.

For each N, let Σ_N denote the subset of Σ containing symmetric, N-pulse homoclinic orbits, *i.e.,* the orbits (u, v) with the property that the function $v(x)$ has N local maxima, and let us additionally assume that the maxima (and minima) are non-degenerate. We shall prove the following series of results about Σ_N, for each N:

(1) The set Σ_N consists of a finite collection of smooth segments $\mathcal{C}_{k,N}$, $k = 1, 2, \ldots, K_N$, where $\mathcal{C}_{1,N} = \mathcal{C}_N^\infty$.

(2) The segments $\mathcal{C}_{k,N}$ are bounded in length when $k \geq 2$. In particular, if we parameterize the segments $\mathcal{C}_{k,N} = \{(\alpha_{k,N}(s), \beta_{k,N}(s)) : s \in I_{k,N}\}$ then the intervals $I_{k,N}$ are finite when $k \geq 2$. By contrast, the intervals $I_{1,N}$ are semi-infinite.

(3) The functions $\alpha_{k,N}(s)$ and $\beta_{k,N}(s)$, as well as their first derivatives, have finite, nonzero limits as $s \to \partial I_{k,N}$, when $\partial I_{k,N}$ is finite.

(4) At the finite endpoints of the segments $\mathcal{C}_{k,N}$ – referred to as *bifurcation points* – the number of pulses changes and different segments begin.

(5) If a bifurcation point lies on $\mathcal{K}_1$, then the adjacent segments correspond to symmetric homoclinic orbits with $2n - 1$ and $2n$ pulses, respectively.

These results also enable us to rule out a number of different bifurcation scenarios, For example, result (3) implies that a curve $\mathcal{C}_N^\infty$ cannot spiral into an accumulation point or approach some type of nontrivial limit set. Also, along the way to establishing these results, we show that bifurcations between homoclinic orbits with $2n$ and $2n + 1$ are not possible (note the contrast with result (5) above) and that bifurcations between a curve $\mathcal{C}_{1,N}$ and a curve $\mathcal{C}_{k,N\pm n}$ for $n \geq 2$ and any k are also not possible (where we restrict

to $N \pm n \geq 1$). We remark that these results do not say anything about bifurcations to asymmetric homoclinic orbits, which may occur.

In numerical simulations, we observed the following continuation results:

(*i*) The curves $\mathcal{C}_1^\infty$, $\mathcal{C}_3^\infty$, and $\mathcal{C}_5^\infty$ continue all the way until they hit $\mathcal{K}_1$, where they meet the curves $\mathcal{C}_2^\infty$, $\mathcal{C}_4^\infty$, and $\mathcal{C}_6^\infty$, respectively, at the points $P_{1,2} \approx (3.02, 0.3314)$, $P_{3,4} \approx (3.83, 0.2612)$, and $P_{5,6} \approx (4.40, 0.2274)$. These are also illustrations of results (2) – (5) above.

(*ii*) For decreasing α, the curve $\mathcal{C}_7^\infty$ becomes a new branch of 5-pulse orbits, $\mathcal{C}_{2,5}$, at $(5.0, 0.2248)$, changes back into a branch, $\mathcal{C}_{2,7}$, of 7-pulse orbits at $(4.065, 0.26)$, and then hits $\mathcal{K}_1$, meeting the curve $\mathcal{C}_8^\infty$, at the point $P_{7,8} \approx (4.86, 0.2058)$. The set $\mathrm{cl}\,(\mathcal{C}_7^\infty \cup \mathcal{C}_{2,5} \cup \mathcal{C}_{2,7} \cup \mathcal{C}_8^\infty)$ appears as one smooth branch in Figure 1, where cl denotes the closure of a set. At the first transition point, the local minima on either side of the origin and closest to it merge with the local maxima that are further from the origin and that are immediately adjacent to them. Hence, there is a loss of two local maxima. At the second transition point, there is a gain of two (symmetric) local maxima. These are also illustrations of results (2) – (5) above.

(*iii*) As α decreases, the curve $\mathcal{C}_9^\infty$ becomes a new branch, $\mathcal{C}_{3,7}$, of 7-pulse orbits at $(6.0, 0.1842)$, then becomes a new branch, $\mathcal{C}_{2,9}$, of 9-pulse orbits at $(5.2, 0.1926)$, before merging with $\mathcal{C}_{10}^\infty$ at $P_{9,10} \approx (5.24, 0.1908)$ on $\mathcal{K}_1$. The set $\mathrm{cl}\,(\mathcal{C}_9^\infty \cup \mathcal{C}_{3,7} \cup \mathcal{C}_{2,9} \cup \mathcal{C}_{10}^\infty)$ is a smooth branch in Figure 1.

Note that the numerical simulations indicate that there are (at least) three different disconnected branches of 7-pulse orbits, and two branches of 5- and 9-pulse orbits, *i.e.*, $K_7 \geq 3$ and $K_N \geq 2$ for $N = 5, 9$. The simulations also suggest that $K_N = 1$ if N is even. Thus, the bifurcational structure of the set Σ is surprisingly complex, and Σ has more structure than suggested by Figure 1.

The third objective concerns qualitative properties of homoclinic orbits. There is a monotonicity property; namely, the maxima and the minima in the graph of $v(x)$ decrease as one moves away from the origin, as is also illustrated in Figure 2. We prove that this is a general property of homoclinic orbits of (1.1). In particular, we show that if (u, v) is a homoclinic orbit of the system (1.1) and v has local maxima (minima) at the points ξ_1 and ξ_2, then

$$0 < \xi_1 < \xi_2 \qquad \Longrightarrow \qquad v(\xi_1) > v(\xi_2). \tag{1.9}$$

Our analysis of this monotonicity property, and that of other qualitative properties, is inspired by methods for fourth-order systems of ordinary differential equations presented in [35].

A useful qualitative property of (1.1) is the energy-type function

$$\mathcal{H} = \mathcal{H}(u, u', v, v') = \frac{1}{2}(v')^2 - \frac{1}{2}v^2 + \frac{1}{3}uv^3, \tag{1.10}$$

which is naturally suggested by the v equation in (1.1). It is important to emphasize, however, that this function $\mathcal{H}$ is *not* a conserved quantity for the full system. Writing

$\mathcal{H} = \mathcal{H}(x)$, we see via a direct calculation that

$$\frac{d\mathcal{H}}{dx} = \frac{1}{3}u'(x)\{v(x)\}^3 \tag{1.11}$$

along orbits. More precisely, on $x > 0$, $\mathcal{H}$ is increasing along orbits whenever $v > 0$, because $u' > 0$ along orbits. The function $\mathcal{H}$ plays a crucial role in the construction of the admissible regions $\mathcal{A}_{\text{even}}$ and $\mathcal{A}_{\text{odd}}$ (Figure 3).

The asymptotic results (1.7) and (1.8) and the continuation results are strongly based on Fenichel theory for normally hyperbolic invariant manifolds, see [16, 39, 23] and [15], respectively. Writing (1.1) as a system of four first-order differential equations,

$$\left\{ \begin{array}{rcl} u' &=& p \\ p' &=& uv^2 \\ v' &=& q \\ q' &=& v - uv^2, \end{array} \right. \tag{1.12}$$

we see that the plane

$$\mathcal{M} = \{(u,p,v,q) | v = 0, q = 0\} \tag{1.13}$$

is normally hyperbolic. The stable and unstable manifolds of $\mathcal{M}$ intersect transversely, as we will show, and the various homoclinic orbits connecting $(u,p,v,q) = (\infty, -p_\infty, 0, 0)$ to $(u,p,v,q) = (\infty, p_\infty, 0, 0)$ lie in these intersections, where the value of p_∞ depends on the orbit. Thus, the homoclinic orbits studied in this paper are homoclinic to the invariant manifold $\mathcal{M}$. Moreover, the demonstration of the existence of these homoclinic orbits will rely also on the reversibility symmetry $(u,p,v,q,t) \to (u,-p,v,-q,-t)$ that (1.12) inherits from the symmetry of (1.1).

Overall, our analysis of system (1.1) represents a blending of analytical and geometric methods for differential equations. We found it fruitful and essential to combine the analytically-obtained and geometrically-derived results in order to prove the main existence and bifurcation results (see especially Theorem 7.1).

Finally, we describe our deeper motivation for studying system (1.1). System (1.1) plays an important role in the analysis of the Gray-Scott model,

$$\left\{ \begin{array}{rcll} U_t &=& U_{xx} - UV^2 + A(1-U), & A > 0 \\ V_t &=& DV_{xx} + UV^2 - BV, & D > 0, \quad B > 0 \end{array} \right. \tag{1.14}$$

[18]. The Gray-Scott model was the first system of reaction-diffusion equations in which the phenomenon of self-replicating pulses was observed [29, 34, 36, 37]. In recent years, the phenomenon of self-replication of pulses and spots in the Gray-Scott model has become an active subject of research [5, 6, 11, 13, 24, 25, 26, 30, 31, 33, 34, 36, 38, 40]. It is known from numerical simulations that there is a saddle-node bifurcation of homoclinic orbits, which plays a central role in initiating the pulse self-replication process [6, 5, 24, 25, 26, 30, 33, 40]. The reduced Gray-Scott system (1.1) governs the leading order ('spatial') dynamics near the onset of self-replication [6, 30, 24, 25, 26]. From the existence of the families of multi-pulse homoclinic orbits for (1.1) constructed and studied in this paper, one can show that there are also associated families of stationary, multi-pulse patterns of the Gray-Scott model (see also [24]). Therefore, we will describe the

relation between the reduced and the full Gray-Scott systems. In addition, the relevance of the bifurcations of the homoclinic orbits studied here for the process of self-replication of pulses in the full Gray-Scott model is explained.

Finally, we discuss the phenomenon of pulse self-replication in a more general setting, since it has become clear recently that it is not restricted to the Gray-Scott model. Self-replication of pulses has for instance also been observed in generalizations of the Gray-Scott model, see [38], and in the classical and generalized Gierer-Meinhardt equations, see [10, 12, 25], where we refer the reader to [17, 32] for references on this equation, as well as to other equations of this type. It is known from numerical simulations that there is a structure of homoclinic orbits and bifurcations in the stationary problem associated to the Gierer-Meinhardt equations for parameter values near the onset of pulse self-replication that is, from a geometrical view point, remarkably similar to the structure of homoclinic orbits studied here. Moreover, as in the case of the Gray-Scott equations, it plays a central role in organizing the dynamics in the self-replication regime [12, 25].

This article is organized as follows. In Section 2, we show that Σ must lie below $\mathcal{K}_{3/2}$, we establish the monotonicity property of local extrema, and we prove the first nonbifurcation result for symmetric homoclinic orbits. In Sections 3 and 4, we establish the bounds on the admissible sets $\mathcal{A}_{\text{odd}}$ and $\mathcal{A}_{\text{even}}$, respectively, in which Σ lies. In Section 5, we state the asymptotic results for $\alpha \to \infty$ quoted in (1.7) and (1.8). Then, in Section 6, we prove the continuation results; and, in Section 7, we establish the homoclinic bifurcation theorems. Finally, in Section 8, we discuss the relation between the Gray-Scott model (1.14) and the reduced system (1.1), and some generic features of the process of pulse self-replication.

Numerical solutions of (1.1) were computed using XPPAUT [14], with the fourth-order Runge-Kutta method and $dt = 0.01$; and, a numerical shooting procedure was used to find the initial conditions for the homoclinic orbits.

2 Qualitative properties

In this section, we prove a few general properties of solutions of the initial value problem problem

$$\text{(IVP)} \begin{cases} u'' = uv^2, \qquad v'' = v - uv^2 & \text{for} \quad x > 0 \\ u = \alpha, \quad u' = 0, \qquad \text{and} \qquad v = \beta, \quad v' = 0 & \text{at} \quad x = 0 \end{cases} \tag{2.1}$$

Specifically, we look for values of α and β for which there exists a solution (u, v) such that $v > 0$ on $\mathbb{R}^+$ and $v(x) \to 0$, i.e. for which the system (1.1) possesses a nondegenerate, symmetric, homoclinic orbit with central values (α, β).

First, we prove that the hyperbola $\mathcal{K}_{3/2}$ is a universal upper bound in the (α, β)-plane for homoclinic orbits to exist, and then we prove a monotonicity property for the local maxima and minima of $v(x)$, when (u, v) is a homoclinic orbit.

Lemma 2.1 *Let (u, v) be the solution of Problem (IVP). If $\alpha\beta \geq 3/2$, then there exists a point $a > 0$ such that*

$$v(x) > 0 \quad \text{for} \qquad 0 \leq x < a, \quad v(a) = 0, \tag{2.2}$$

$$v'(x) < 0 \quad \text{for} \qquad 0 < x \leq a. \tag{2.3}$$

Proof First, we derive an upper bound for v''. Since $u'(x) > 0$ for $x > 0$, it follows that $u(x) > \alpha$ for $x > 0$. Hence,

$$v'' = v - uv^2 < v - \alpha v^2 \qquad \text{for} \quad x > 0. \tag{2.4}$$

Second, we derive an upper bound for v'. Since $\alpha\beta \geq 3/2$ by assumption, we find

$$v''(0) = \beta(1 - \alpha\beta) \leq -\frac{1}{2}\beta < 0.$$

Hence, $v' < 0$ in a right-neighborhood of the origin.

Third, we define the point

$$x_0 = \sup\{x > 0 : vv' < 0 \ \text{ on } \ (0, x)\}.$$

To finish the proof, it suffices to show that

$$v(x_0) = 0 \qquad \text{and} \qquad v'(x_0) < 0,$$

because then (2.2) holds with $a = x_0$.

Thus, suppose to the contrary that $v'(x_0) = 0$ as well as $v(x_0) \geq 0$. Multiplying the inequality (2.4) by $2v'$ and integrating over $(0, x_0)$, we find that

$$0 > v_0^2 - \beta^2 - \frac{2\alpha}{3}(v_0^3 - \beta^3), \qquad v_0 = v(x_0),$$

since $v'(x) < 0$ on $(0, x_0)$. When we divide both sides by $(v_0 - \beta) < 0$ and rearrange the terms, we obtain

$$\frac{2\alpha}{3}v_0^2 < \left(1 - \frac{2\alpha\beta}{3}\right)(v_0 + \beta).$$

Recalling that, by assumption, $\alpha\beta \geq 3/2$, we conclude that

$$\frac{2\alpha}{3}v_0^2 < 0,$$

a contradiction. Therefore, (2.3) holds with $a = x_0$, as claimed. □

This lemma and the fact that $v(x)$ must be strictly positive for all x in order for the solution to be a homoclinic orbit immediately imply:

Corollary 2.1 *In order for the orbit through the initial condition* $(\alpha, 0, \beta, 0)$ *to be a symmetric* N*-pulse homoclinic orbit, for any* $N \geq 1$*, the pair* (α, β) *must lie below the curve* $\mathcal{K}_{3/2}$.

Next, we show in the following lemma that the hyperbola $\mathcal{K}_1$ is a separating curve:

Lemma 2.2 *In order for the orbit through the initial condition* $(\alpha, 0, \beta, 0)$ *to be a symmetric* N*-pulse homoclinic orbit with* N *odd, the pair* (α, β) *must lie above* $\mathcal{K}_1$*; while for the orbit through the initial condition* $(\alpha, 0, \beta, 0)$ *to be a symmetric* N*-pulse homoclinic orbit with* N *even, the pair* (α, β) *must lie below* $\mathcal{K}_1$.

Proof From the v equation in (IVP), one sees that $v''(0) = \beta(1 - \alpha\beta)$. Hence, for $\alpha\beta > 1$, $v(x)$ has a non-degenerate local maximum at $x = 0$, so that any symmetric homoclinic orbit must have an odd number of pulses. By contrast, for $\alpha\beta < 1$, $v(0)$ is a non-degenerate local minimum, so that any symmetric homoclinic orbit must have an even number of pulses. □

In the next lemma, we prove a useful monotonicity property for solutions of (IVP) with multiple distinct local extrema. We show that successive minima must be strictly decreasing as $|x|$ increases. The same holds for successive maxima.

Lemma 2.3 *Let* (u, v) *be the solution of Problem (IVP) for initial data* α *and* β*, and let* v *have distinct positive local minima at* η_1 *and* η_2*, respectively, where* $0 \leq \eta_1 < \eta_2$*. and no local minima in the interval* (η_1, η_2)*. Then,*

$$v(\eta_1) > v(\eta_2).$$

Similarly, distinct, successive local maxima must decrease strictly.

Proof The proof is based on an analysis of the energy function $\mathcal{H}(x)$, which is known to be increasing on $\mathbb{R}^+$.

Suppose, to the contrary, that $v(\eta_2) \geq v(\eta_1) > 0$. By integrating (1.11), we find

$$\frac{d\mathcal{H}}{dx}(x) = \frac{1}{3}u'(x)v^3(x)$$

over the interval (x, η_2); and, using $v(x) > v(\eta_2)$, we obtain

$$\begin{aligned} \mathcal{H}(\eta_2) - \mathcal{H}(x) &= \frac{1}{3}\int_x^{\eta_2} u'(t)v^3(t)\,dt \\ &> \frac{1}{3}v^3(\eta_2)\int_x^{\eta_2} u'(t)\,dt \\ &= \frac{1}{3}v^3(\eta_2)\{u(\eta_2) - u(x)\}. \end{aligned} \tag{2.5}$$

Now, let

$$\eta^* = \inf\{x < \eta_2 : v > v(\eta_2) \ \text{ on } \ (x, \eta_2)\}.$$

Then, in view of our assumption,

$$\eta_1 \leq \eta^* < \eta_2 \qquad \text{and} \qquad v(\eta^*) = v(\eta_2).$$

We substitute $x = \eta^*$ into (2.5) and evaluate the left member using the definition of $\mathcal{H}$. This yields

$$\frac{1}{3}v^3(\eta_2)\{u(\eta_2) - u(\eta^*)\} - \frac{1}{2}(v'(\eta^*))^2 > \frac{1}{3}v^3(\eta_2)\{u(\eta_2) - u(\eta^*)\},$$

because $v(\eta^*) = v(\eta_2)$. Hence, $\frac{1}{2}(v'(\eta^*))^2 < 0$, which is a contradiction. The fact that the local maxima also decrease monotonically is proven in the same way. □

Corollary 2.2 *For any N-pulse homoclinic orbit (u, v) of the Problem (IVP) with $N \geq 1$, the central local maximum will be the largest if N is odd, while if N is even the central two (symmetric) local maxima will be the largest.*

In the next lemma, we prove results about solutions (u, v) of Problem (IVP) for which v has degenerate extrema, *i.e.,* for which $v'(a) = v''(a) = 0$ either at $a = 0$ or at some $a > 0$.

Lemma 2.4 *Let $(u(x), v(x))$ be the solution of Problem (IVP) on $x \geq 0$, and let $a \geq 0$ be a critical point of v. Then,*
(a) $v'''(a) = 0$ *if* $a = 0$, *whereas* $v'''(a) < 0$ *if* $a > 0$.
(b) *If also* $v''(a) = 0$, *then* $v^{(iv)}(a) < 0$, *irrespective of whether* $a = 0$ *or* $a > 0$.

Proof From the second equation in (1.1), one computes

$$v''' = v' - u'v^2 - 2uvv'.$$

Hence, $v'''(a) = -u'(a)v^2(a)$. Since $u'(a) = 0$ if $a = 0$ and $u'(a) > 0$ if $a > 0$, the assertion in part (a) follows.

Next, we calculate

$$v^{(iv)} = v'' - u''v^2 - 4u'vv' - 2u(v')^2 - 2uvv''.$$

Hence, if $v''(a) = 0$, then

$$v^{(iv)}(a) = -u''(a)v^2(a) = -u(a)v^4(a) < 0,$$

as claimed in part (b). □

Next, we exclude certain bifurcations of symmetric multi-pulse orbits, namely those that go from an odd number $(2n + 1)$ of pulses *down* to an even number $(2n)$ of pulses. The proof of this result relies on the previous lemma.

Lemma 2.5 *Let $n \geq 1$. A symmetric $(2n+1)$-pulse orbit cannot bifurcate into a symmetric $2n$-pulse orbit (or vice versa).*

Proof Suppose, to the contrary, that a branch $\mathcal{C}_{2n+1}$ of symmetric $(2n+1)$ pulse orbits does bifurcate into a symmetric $2n$ pulse orbit at some point (α_0, β_0). Let us parametrize the orbits on $\mathcal{C}_{2n+1}$ by σ such that $(\alpha_\sigma, \beta_\sigma) \to (\alpha_0, \beta_0)$ as $\sigma \to 0$. Since $2n+1$ is an odd number, the graph of $v(x)$ has a local maximum at the origin. Let us denote the two adjacent local minima by $\pm\eta_1$ ($\eta_1 > 0$) and the nearest local maxima by $\pm\xi_1$ ($\xi_1 > \eta_1 > 0$). Plainly, η_1 and ξ_1 depend continuously on σ. Moreover, since $\mathcal{C}_{2n+1}$ approaches $\mathcal{C}_{2n}$ as $\sigma \to 0$, it follows that

$$\eta_1(\sigma) \to 0 \qquad \text{and} \qquad v(\pm\eta_1, \sigma) \to v(0, \sigma) \qquad \text{as} \quad \sigma \to 0.$$

By Lemma 2.3,

$$v(\pm\eta_1, \sigma) < v(\pm\xi_1, \sigma) < v(0, \sigma).$$

Therefore,

$$v(\pm\xi_1, \sigma) \to v(0, 0) \qquad \text{as} \quad \sigma \to 0.$$

This implies that

$$v^{(i)}(0, 0) = 0 \qquad \text{for} \qquad i = 1, 2, 3, 4, \text{ and } 5.$$

However, by Lemma 2.4, this is impossible, so that we have a contradiction. □

Remark 2.1 As we will show below in Lemma 7.6, along the hyperbola $\mathcal{K}_1$, orbits with an odd number, $(2n-1)$, of pulses bifurcate into orbits with an even number, $2n$, of pulses, in contrast to the situation described in Lemma 2.5.

Remark 2.2 At this stage, one can already see that $\mathcal{K}_{3/2}$ is a sharp upper bound – at least in the regime of large α – on the domain in which initial conditions for N-pulse orbits with N odd may lie, since the curve of $1-$pulse orbits, given by (1.8) with $N = 1$ for large α, lies just underneath it.

Remark 2.3 The nonexistence of homoclinic orbits through initial conditions that lie above $\mathcal{K}_{3/2}$ also follows directly from analyzing the energy function (1.10) introduced above. We recall from (1.11) that $\mathcal{H}'(x) > 0$ along homoclinic orbits, since $u'(x) > 0$ for all $x > 0$ along homoclinic orbits. Also,

$$\lim_{x \to \infty} \mathcal{H}(u(x), u'(x), v(x), v'(x)) = 0$$

for homoclinic orbits, since $v(x)$ and $v'(x)$ vanish exponentially for solutions that are backward and forward asymptotic to $(v, v') = (0, 0)$. Therefore, $\mathcal{H}(0)$ must be negative along homoclinic orbits, but $\mathcal{H}(0) = (\beta^2/3)(\alpha\beta - (3/2))$, which is positive for $\alpha\beta > 3/2$. Hence, there is a contradiction.

3 Boundaries on $\mathcal{A}_{\text{odd}}$, the region in which N-pulse orbits with N odd can lie

We have seen that the region in the (α, β)-plane in which we may find N-pulse homoclinic orbits with N odd is bounded above by $\mathcal{K}_{3/2}$ and bounded below by $\mathcal{K}_1$. However, the region between these two hyperbolas is unbounded as $\alpha \to 0$. In this section, we find an upper bound on this region for small values of α.

It will be convenient to introduce the variable $\gamma = \alpha\beta$. For points between the two hyperbolas, we have $\gamma \in [1, 3/2]$. We shall construct a curve

$$\mathcal{B}_{\text{upper}} = \{(\alpha^*(\gamma), \beta^*(\gamma)) : 1 \leq \gamma \leq 3/2\},$$

which connects $\mathcal{K}_1$ and $\mathcal{K}_{3/2}$.

We introduce the following quantities: let $T(\gamma) = \cosh^{-1}(2/\gamma)$ and let $\mu^* = \mu^*(\gamma)$ be the unique solution of the equation

$$\cosh(\mu T(\gamma)) = 1 + \frac{3 - 2\gamma}{2\gamma\mu^3} \qquad \text{for} \qquad 1 \leq \gamma < \frac{3}{2}. \tag{3.1}$$

See Figure 4 for a plot of the function $\mu^*(\gamma)$. Asymptotically,

$$\mu^*(\gamma) \sim \left(\frac{4}{3T^2(3/2)}\right)^{\frac{1}{5}} \left(\frac{3}{2} - \gamma\right)^{\frac{1}{5}}, \text{ as } \gamma \to \frac{3}{2}^-.$$

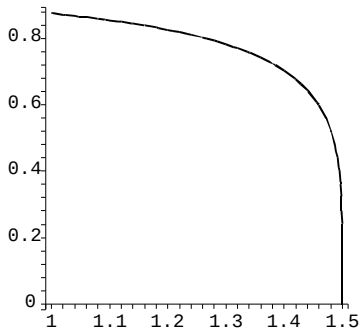

Figure 4: Graph of the function $\mu^*(\gamma)$, as given by formula (3.1).

Lemma 3.1 *Let $(u(x), v(x))$ be a homoclinic orbit with an odd number of local maxima and with initial data $(\alpha, 0, \beta, 0)$. Then the point (α, β) must lie below the curve $\mathcal{B}_{\text{upper}}$ defined by*

$$\alpha^*(\gamma) = \frac{\gamma\sqrt{2(1 - \mu^*(\gamma))}}{T(\gamma)}, \qquad \beta^*(\gamma) = \frac{T(\gamma)}{\sqrt{2(1 - \mu^*(\gamma))}} \qquad \text{for} \quad 1 \leq \gamma < \frac{3}{2}. \tag{3.2}$$

γ	$T(\gamma)$	$\mu^*(\gamma)$	$\beta^*(\gamma)$	$\alpha^*(\gamma)$
1.0	1.317	0.876	2.647	0.378
1.1	1.205	0.856	2.243	0.490
1.2	1.099	0.827	1.868	0.642
1.3	0.996	0.783	1.513	0.859
1.4	0.896	0.704	1.163	1.203
1.5	0.795	0.000	0.562	2.667

Table 1. The values of the functions $T(\gamma)$, $\mu^*(\gamma), \beta^*(\gamma)$, and $\alpha^*(\gamma)$ in Lemma 3.1 for a series of values of $\gamma \in [1, 3/2]$.

Proof As a preparatory step, we scale the variables by setting

$$u(x) = \alpha y(t), \qquad v(x) = \beta z(t), \qquad \text{and} \qquad t = \beta x. \tag{3.3}$$

The equations (1.1) then become

$$\ddot{y} = yz^2, \qquad \ddot{z} = \sigma^2 z(1 - \gamma yz), \qquad \gamma = \alpha\beta, \qquad \sigma = \frac{1}{\beta}, \tag{3.4}$$

where an overdot in the remainder of this section denotes a derivative with respect to t. Also, the initial data at $t = 0$ are $y = 1, \dot{y} = 0, z = 1$, and $\dot{z} = 0$.

First, we obtain upper bounds on $z(t)$ and $y(t)$. We already know that $z(t) < 1$ for all t, by Corollary 2.2. Equation (3.4) then implies that $\ddot{y} < y$, and in turn integration reveals that

$$y(t) < \cosh(t), \qquad \dot{y}(t) < \sinh(t).$$

Next, we use these upper bounds to derive *lower* bounds for $z(t)$ and $y(t)$. Substitution of the upper bounds into (3.4) directly yields

$$\ddot{z} > \sigma^2 z\{1 - \gamma \cosh(t)\}.$$

For each γ choose $T = T(\gamma) > 0$ such that $\gamma \cosh(T) = 2$. Then, $1 - \gamma \cosh(t) > -1$ for all $t \in (0, T)$, since $\cosh(t)$ is an increasing function. Hence, the upper bound on z implies that

$$\ddot{z} > -\sigma^2 z > -\sigma^2 \qquad \text{for} \qquad 0 < t < T. \tag{3.5}$$

Integration of this inequality and use of the initial conditions leads to the desired lower bound,

$$z(t) > 1 - \frac{1}{2}\sigma^2 t^2 \qquad \text{for} \qquad 0 < t < T. \tag{3.6}$$

Moreover, $z > 0$ on $[0, T)$ if $\sigma T < \sqrt{2}$, *i.e.*, if $\beta > T/\sqrt{2}$. Also, a lower bound on $y(t)$ is now readily at hand. Substitution of (3.6) into (3.4) implies

$$\ddot{y} > \left(1 - \frac{1}{2}\sigma^2 T^2\right)^2 y, \tag{3.7}$$

so that

$$y(t) \geq \cosh(\mu t) \qquad \text{for} \quad 0 < t < T, \qquad \text{where} \quad \mu \equiv 1 - \frac{1}{2}\sigma^2 T^2. \tag{3.8}$$

Finally, we use the energy function

$$H(t) \equiv H(y(t), \dot{y}(t), z(t), \dot{z}(t)) = \frac{1}{2}(\dot{z})^2 - \frac{\sigma^2}{2} z^2 + \frac{\sigma^2 \gamma}{3} y z^3,$$

where we emphasize that H is not a conserved quantity of the full system (3.4). Instead, $\dot{H} = (\sigma^2\gamma/3)\dot{y}z^3$; and, we find that

$$H(T) = \frac{1}{3}\sigma^2 \Big\{ \gamma \int_0^T \dot{y}(s) z^3(s)\, ds - \Big(\frac{3}{2} - \gamma \Big) \Big\},$$

because $H(0) = (-\sigma^2/3)((3/2) - \gamma)$. We will show that $H(T) > 0$, which implies that $z(t)$ cannot be a homoclinic orbit, in contradiction to the hypotheses. Indeed, because $z(t) > \mu$ on $(0, T)$ by (3.6) and $\dot{y} > \mu \sinh(\mu t)$ by (3.7), we have

$$\int_0^T \dot{y}(s) z^3(s)\, ds > \mu^3 \{\cosh(\mu T) - 1\}.$$

Hence, $H(T) > 0$ if

$$\gamma\, \mu^3 \{\cosh(\mu T) - 1\} > \frac{3}{2} - \gamma,$$

or equivalently if

$$\cosh(\mu T) > 1 + \frac{3 - 2\gamma}{2\gamma \mu^3}. \tag{3.9}$$

Now, there exists a unique value μ^* of μ such that

$$\cosh(\mu^* T) = 1 + \frac{1}{2(\mu^*)^3},$$

because $\cosh(\mu T)$ is increasing and $1/2\mu^3$ is decreasing in μ. Thus, (3.9) certainly holds for $\mu > \mu^*$, *i.e.*, for

$$1 - \frac{1}{2}\sigma^2 T^2 > \mu^*,$$

or equivalently

$$\sigma^2 T^2 < 2(1 - \mu^*) \qquad \Longrightarrow \qquad \beta < \beta^* \equiv \frac{T}{\sqrt{2(1 - \mu^*)}},$$

where we recall that $T = T(\gamma)$, and hence also $\mu^* = \mu^*(\gamma)$ and $\beta^* = \beta^*(\gamma)$. □

Corollary 2.1 and Lemmas 2.2 and 3.1 now directly imply

Corollary 3.1 *In order for the orbit through the initial condition $(\alpha, 0, \beta, 0)$ to be a symmetric N-pulse homoclinic orbit with N odd, the pair (α, β) must lie in the connected set $\mathcal{A}_{\rm odd}$ bounded above by $\mathcal{K}_{3/2}$ and $\mathcal{B}_{\rm upper}$ and bounded below by $\mathcal{K}_1$.*

See also the illustration in Figure 1.

4 Boundaries on $\mathcal{A}_{\text{even}}$, the region in which N-pulse orbits with N even can lie

We consider symmetric, N-pulse homoclinic orbits with N even. We already know that the initial conditions (α, β) for these orbits satisfy $\alpha\beta < 1$ and that they must lie below the separating curve $\mathcal{K}_1$, by Lemma 2.2. However, $\mathcal{K}_1$ has a vertical asymptote at $\alpha = 0$, so that it does not provide a finite upper bound for all α down to zero.

In this section, we show that there is a finite upper bound valid as $\alpha \to 0$. More precisely, we show that there exists a constant $\beta_{\text{cap}} > \beta^*(\gamma = 1)$ (where $\beta^*(\gamma)$ is defined in the previous section) such that the horizontal line segment $\mathcal{B}_{\text{cap}} \equiv \{(\alpha, \beta) | \beta = \beta_{\text{cap}}, \alpha \in (0, 1/\beta_{\text{cap}}]\}$ is the desired finite upper bound. See Lemma 4.3 in Section 4.1 below.

In addition, we show that there exists a function $\beta = \beta_{\text{L}}(\alpha)$ for all $\alpha > 0$ such that the curve $\mathcal{B}_{\text{lower}} \equiv \{(\alpha, \beta) | \beta = \beta_{\text{L}}(\alpha)\}$ is a nontrivial lower bound on the set of initial conditions that can correspond to these orbits. See Lemma 4.5 in Section 4.2 below. The results of this section are summarized in Corollary 4.1 below.

4.1 The cap $\mathcal{B}_{\text{cap}}$

In this section, we establish the desired cap, $\mathcal{B}_{\text{cap}}$. As a preparatory step, we change variables in (IVP) so that α and β appear in the equations and in the energy function. Let

$$u(x) = \alpha y(x) \qquad \text{and} \qquad v(x) = \beta z(x). \tag{4.1}$$

This is the same change of dependent variables used in the previous section; however, we do not rescale the independent variable here. The equations become

$$y'' = \beta^2 y z^2 \qquad \text{and} \qquad z'' = z - \alpha\beta y z^2, \tag{4.2}$$

with initial conditions $(y(0), y'(0), z(0), z'(0)) = (1, 0, 1, 0)$ and energy function

$$\mathcal{H}(y, y', z, z') = \frac{(z')^2}{2} - \frac{z^2}{2} + \frac{\alpha\beta}{3} y z^3,$$

with a slight abuse of notation (note $\mathcal{H}(y, y', z, z') = \beta^2 \mathcal{H}(u, u', v, v')$). Equivalently,

$$\mathcal{H}(x) = \mathcal{H}(0) + \int_0^x \mathcal{H}'(s) ds = -\frac{1}{2} + \frac{\alpha\beta}{3} + \frac{\alpha\beta}{3} \int_0^x y'(s) z^3(s) ds. \tag{4.3}$$

Also, we emphasize that $\mathcal{H}(0) < 0$ for $\alpha\beta < 1$ and that $d\mathcal{H}/dx > 0$ along orbits.

Our strategy for establishing the cap, $\mathcal{B}_{\text{cap}}$, is to show that there exists a value of $\beta = \beta_{\text{cap}}$ so that $\mathcal{H}(x)$ vanishes at some x_0 for each (α, β) with $\alpha \in (0, \frac{1}{\beta_{\text{cap}}})$ and $\beta = \beta_{\text{cap}}$. In turn, to show that $\mathcal{H}$ must vanish, we derive a lower bound on $\mathcal{H}$ and show that it has a finite zero, which then, in turn, forces $\mathcal{H}$ through zero.

We employ the following explicitly computable lower bounds for $z(x)$, $y(x)$, and $y'(x)$. Let

$$z_0(x) = \cosh(x) \tag{4.4}$$

and let $y_0(x) = C_0(\beta \sinh(x))$ be the solution of the problem,

$$y_0'' = \beta^2(\cosh^2(x))y_0, \qquad y_0(0) = 1, \quad y_0'(0) = 0. \tag{4.5}$$

This is a modified Mathieu equation. See Remark 4.1 below. A lower bound for $z(x)$ is given in the following lemma:

Lemma 4.1 *We have*

$$z(x) > z_1(x) \equiv z_0(x) - \alpha\beta\zeta_1(x), \qquad \text{as long as} \quad z_1(x) > 0, \tag{4.6}$$

where

$$\zeta_1(x) = \int_0^x \sinh(x-s)\cosh(\beta \sinh(s))z_0^2(s)ds. \tag{4.7}$$

The condition that z_1 be positive is needed, since z_1 will have a first zero due to the fact that ζ_1 eventually grows faster than z_0. This will be shown in the proof of the lemma. In fact, it will be useful to introduce the notation $\xi(z_1)$ and $\xi(z)$ for the first, positive roots of $z_1(x)$ and $z(x)$, respectively.

Lower bounds for $y(x)$ and $y'(x)$ are given in the following lemma:

Lemma 4.2 *We have*

$$y(x) > y_1(x) \qquad \text{and} \qquad y'(x) > y_1'(x), \tag{4.8}$$

again as long as $z_1(x) > 0$, where y_1 is the solution of the following problem:

$$y_1'' - \beta^2 z_0^2(x)y_1 = -2\alpha\beta^3 \cosh(\beta \sinh(x))z_0(x)\zeta_1(x), \qquad y_1(0) = 1, \quad y_1'(0) = 0. \tag{4.9}$$

The proofs of Lemmas 4.1 and 4.2 are presented in Appendix A.

The following lemma gives the desired cap:

Lemma 4.3 *There exists a value of β, β_{cap}, which is greater than $\beta^*(\gamma = 1)$, such that for each $\alpha \in (0, \frac{1}{\beta_{\text{cap}}}]$ there exists an $x_0 = x_0(\alpha)$ such that $\mathcal{H}(x_0) = 0$. Moreover, the solutions of (IVP) with the initial conditions $(\alpha, 0, \beta_{\text{cap}}, 0)$ cannot be symmetric N-pulse homoclinic orbits.*

Proof of Lemma 4.3 Substituting the lower bounds from Lemmas 4.1 and 4.2 into the formula (4.3) for $\mathcal{H}$, we find the following, explicitly computable, lower bound on $\mathcal{H}$:

$$\mathcal{H}(x) > \mathcal{H}_1(x) \equiv -\frac{1}{2} + \frac{\alpha\beta}{3} + \frac{\alpha\beta}{3}\int_0^x y_1'(s)z_1^3(s)ds, \tag{4.10}$$

as long as $0 < x < \xi(z_1)$. Moreover, there exists a value of β, which we label $\beta_{\rm cap}$, such that, for each $\alpha < 1/\beta_{\rm cap}$, $\mathcal{H}_1$ first vanishes at some $x = \xi(\mathcal{H}_1)$, where $\xi(\mathcal{H}_1)$ depends on α and $\xi(\mathcal{H}_1) < \xi(z_1)$. Specifically, direct evaluation shows that the value $\beta_{\rm cap} = 4$ works, and this value is greater than $\beta^*(\gamma = 1)$, as may be checked from formula (3.2). Hence, for each $\alpha < 1/\beta_{\rm cap}$, the energy function itself, $\mathcal{H}$, must also first vanish for some $x = \xi(\mathcal{H})$, where $\xi(\mathcal{H}) < \xi(\mathcal{H}_1)$, since $\mathcal{H}_1$ is a lower bound on $\mathcal{H}$. In turn, therefore, the orbit through the initial condition $(\alpha, \beta_{\rm cap})$ cannot be a homoclinic orbit, because along homoclinic orbits $\mathcal{H}(x) < 0$ for all x and $\lim_{x\to\infty} \mathcal{H}(x) = 0$.

To complete the proof, we need to show that the above results continue to hold in the limit as $\alpha \to 0^+$. We establish the following lemma, which contains the asymptotics of the zeroes $\xi(\mathcal{H}_1)$ and $\xi(z_1)$ in the limit as $\alpha \to 0^+$. Define ξ^* implicitly by

$$\beta \sinh(\xi^*) = \ln\left(\frac{1}{\alpha}\right), \tag{4.11}$$

and observe that, as $\alpha \to 0^+$,

$$\xi^* \sim \left(\ln\left[\frac{2}{\beta}\ln\left(\frac{1}{\alpha}\right)\right]\right). \tag{4.12}$$

Then, we have

Lemma 4.4 *In the limit that $\alpha \to 0^+$,*

$$\xi(z_1) \sim \left(\ln\left[\frac{2}{\beta}\ln\left(\frac{1}{\alpha}\right)\right]\right)\left(1 + \left[\ln\left(\frac{1}{\alpha}\right)\right]^{-1}\right), \tag{4.13}$$

$$\xi(\mathcal{H}_1) \sim \ln\left[\frac{2}{\beta}\ln\left(\frac{1}{\alpha}\right)\right] - \frac{5}{2}\left[\ln\left[\ln\left(\frac{1}{\alpha}\right)\right]\right]\left[\ln\left(\frac{1}{\alpha}\right)\right]^{-1} + [\ln(K)]\left[\ln\left(\frac{1}{\alpha}\right)\right]^{-1}. \tag{4.14}$$

Moreover, for α sufficiently small, $y_1'(x)$, $z_1(x)$, and $\mathcal{H}_1(x)$ are all positive at $x = \xi^*$.

This lemma is proven in Appendix B. It implies that, also in the limit $\alpha \to 0^+$, the zeroes $\xi(z_1)$ and $\xi(\mathcal{H}_1)$ exist and remain ordered as $\xi(\mathcal{H}_1) < \xi(z_1)$. Hence, the functions $\mathcal{H}(x)$ and $z(x)$ also have zeroes for all α down to zero, and they are ordered as $\xi(\mathcal{H}) < \xi(\mathcal{H}_1) < \xi(z_1) < \xi(z)$. This completes the proof of the lemma.

□

The data presented in Table 2 below are the values of the zeroes $\xi(\mathcal{H})$, $\xi(\mathcal{H}_1)$, $\xi(z_1)$, and $\xi(z)$ for a series of values of α between zero and $1/\beta_{\rm cap}$. Here, $\mathcal{H}$ and $\xi(z)$ were evaluated via direct numerical simulation of the differential equations and $\mathcal{H}_1$ and $\xi(z_1)$ via symbolic algebra. They are ordered from smallest to largest. We see that $\xi(\mathcal{H}) < \xi(\mathcal{H}_1)$, confirming that the energy function $\mathcal{H}$ vanishes (and becomes nonnegative) before the lower bound $\mathcal{H}_1$ does so. Also, the data confirms that $\xi(z_1) < \xi(z)$, *i.e.,* that the z component vanishes (and becomes nonpositive) only after the lower bound z_1 does so. Finally, $\xi(\mathcal{H}_1) < \xi(z_1)$, confirming the analytical result that $\mathcal{H}_1$ must first increase through zero before z_1 can decrease through zero.

α	$\xi(\mathcal{H})$ (num)	$\xi(\mathcal{H}_1)$ (symb)	$\xi(z_1)$ (symb)	$\xi(z)$ (num)
0.01	0.8561	0.8571	1.390	1.614
0.05	0.6090	0.6098	1.155	1.424
0.10	0.4758	0.4763	1.037	1.315
0.25	0.3839	0.3842	0.962	1.242
0.20	0.3087	0.3088	0.906	1.186
0.25	0.2409	0.2410	0.863	1.134

Table 2. The values of the zeroes $\xi(\mathcal{H}_1)$ and $\xi(z_1)$ as obtained from symbolic algebra (symb) for the functions $\mathcal{H}_1(x)$ and $z_1(x)$ and the values of the zeroes $\xi(\mathcal{H})$ and $\xi(z)$ from numerical simulation (num) of the differential equations for a series of values of α, again using XPPAUT [14]. The zeroes are ordered from smallest to largest, confirming the analytical results, as discussed in the text. Note that here $\beta = 4$.

Remark 4.1 The equation $y'' = \beta^2(\cosh^2(x))y$ may be put into the standard form for modified Mathieu equations, $y'' - (a - 2q\cosh(2x))y = 0$, with $a = \beta^2/2$ and $q = -\beta^2/4$, because $(\cosh(x))^2 = \frac{1}{2}(\cosh(2x) + 1)$. See Chapter 20 of [1]. To obtain the equation in algebraic form, set $t = \beta\sinh(x)$ and $\eta(t) = y(x)$ in the original equation. This yields $\ddot{\eta} + (t/(\beta^2 + t^2))\dot{\eta} - \eta = 0$, and the fundamental two linearly independent solutions are $E_0(t)$ and $E_0(-t)$, where $E_0(t)$ is defined in terms of a series, satisfies $E_0(0) = 1$ and $E_0'(t) > 0$ for all t, diverges as $t \to \infty$, and vanishes as $t \to -\infty$. They are the analogs of the exponential functions that satisfy $w'' - w = 0$. We also define $C_0(t) = \frac{1}{2}(E_0(t) + E_0(-t))$, which is the analog of $w(t) = \cosh(t)$. Moreover, from this form of the equation, one sees that it has regular singular points at $t = \pm i\beta$ and an irregular singular point at $t = \infty$. Finally, it reduces to a modified Bessel equation in the limit as $t \to \infty$, and $C_0(t) \sim I_0(t) \sim \frac{1}{\sqrt{2\pi t}}e^t(1 + \frac{1}{8}t^{-1})$ as $t \to \infty$, where I_0 is the zeroth order modified Bessel function.

Remark 4.2 The value of $\beta_{\rm cap}$ is not unique, and there are many other values greater than $\beta^*(\gamma = 1)$. There may even be values of $\beta_{\rm cap}$ less than $\beta^*(\gamma = 1)$. However, the result of Lemma 4.3 with $\beta_{\rm cap} = 4$ suffices for our purposes here.

4.2 The lower bound $\mathcal{B}_{\rm lower}$

In this section, we establish the desired, nontrivial lower bound, $\beta = \beta_{\rm L}(\alpha)$.

Lemma 4.5 *For each $\alpha > 0$ there exists a constant $\beta_L = \beta_L(\alpha) > 0$ independent of N such that, if $\beta \in (0, \beta_L)$, then the solution of (IVP) with the initial condition $(\alpha, 0, \beta, 0)$ cannot be a symmetric N-pulse homoclinic orbit with N even. Moreover, $\beta_L(\alpha)$ varies continuously with α.*

The proof of Lemma 4.5 is given in Appendix C. We shall use $\mathcal{B}_{\rm lower}$ to denote the curve $\beta_L(\alpha)$ in the parameter plane given by this lemma, see Figure 1. Homoclinic orbits can only exist for initial conditions (α, β) that lie above it.

Lemmas 2.2, 4.3, and 4.5 now immediately imply

Corollary 4.1 *In order for the orbit through the initial condition* $(\alpha, 0, \beta, 0)$ *to be a symmetric* N*-pulse homoclinic orbit with* N *even, the pair* (α, β) *must lie inside the connected set* $\mathcal{A}_{\rm even}$ *bounded above by* $\mathcal{K}_1$ *and* $\mathcal{B}_{\rm cap}$*, bounded to the left by a segment of the* β*-axis, and bounded below by the curve* $\mathcal{B}_{\rm lower}$*.*

Remark 4.3 The asymptotics for $\beta_L(\alpha)$ as $\alpha \to \infty$ imply that the boundary $\mathcal{B}_{\rm lower}$ is a sharp lower bound on $\mathcal{A}_{\rm even}$ in the regime with α large given the asymptotic location of the curve $\mathcal{C}_2^\infty$ (recall (1.8) with $N = 2$) and given the fact that the curve $\mathcal{C}_2^\infty$ lies below all of the other $\mathcal{C}_N^\infty$. See the end of Appendix C.

Remark 4.4 The conclusion of Lemma 4.5 also holds for N-pulse homoclinic orbits with N odd, since the proof is independent of the number of pulses.

5 Existence of multi-pulse orbits for large α

In this section, we demonstrate the existence of symmetric N-pulse homoclinic orbits for large α. Specifically, we establish the existence of the curves $\mathcal{C}_N^\infty$ for $\alpha > \tilde{\alpha}(N)$, where $\tilde{\alpha}(N)$ is sufficiently large, and determine their leading order approximations in this limit. These results follow directly from Theorem 4.1 in [11], where the existence of symmetric N-pulse homoclinic orbits in the Gray-Scott model is shown. Nevertheless, we present the proof here, because it is based on concepts that will be essential to the forthcoming sections. Also, the proof we present here differs in several important respects from that given in [11]. Most significantly, we follow the approach used in Theorem 2.1 of [7], where the existence of symmetric N-pulse homoclinic orbits for a class of generalized Gierer-Meinhardt equations is shown, because this approach more readily lends itself to generalization to other systems with hierarchies of homoclinic orbits.

We assume $\alpha \gg 1$. Moreover, based on the bounds on the sets $\mathcal{A}_{\rm odd}$ and $\mathcal{A}_{\rm even}$, we see that it suffices to examine the regime in which $\beta = \mathcal{O}(1/\alpha) \ll 1$. Hence, we scale u and v accordingly,

$$u(x) = \alpha y(x), \quad v(x) = \frac{z(x)}{\alpha}. \tag{5.1}$$

Thus, y and z are taken to be $\mathcal{O}(1)$ with respect to the small parameter $\delta \equiv \frac{1}{\alpha} \ll 1$; and, by equations (1.1), they satisfy the system,

$$y'' = \delta^2 y z^2 \qquad \text{and} \qquad z'' = z - y z^2. \tag{5.2}$$

The coupled equations (5.2) are equivalent to the singularly perturbed, fourth-order dynamical system,

$$\left\{ \begin{array}{rcl} y' &=& \delta p \\ p' &=& \delta y z^2 \\ z' &=& q \\ q' &=& z - y z^2, \end{array} \right. \tag{5.3}$$

where the variables y and z differ from those used in Sections 1 and 2, and the variables p and q differ from those used above. The reversibility symmetry is given, just as in (1.12), by

$$x \to -x,\ p \to -p, q \to -q. \tag{5.4}$$

5.1 The manifolds $\mathcal{M}$, $W^s(\mathcal{M})$, $W^u(\mathcal{M})$

Both for $\delta = 0$ and $\delta \neq 0$, the system (5.3) has a 2-dimensional invariant manifold, $\mathcal{M}$, given by

$$\mathcal{M} = \{(y, p, z, q) : z = 0, q = 0\}, \tag{5.5}$$

because the third and fourth components of the vector field vanish identically on this set.

For $\delta = 0$, $\mathcal{M}$ is the collection of saddle fixed points of the fast reduced system

$$y \equiv y_0,\ \ p \equiv p_0,\ \ z' = q,\ \ q' = z - y_0 z^2, \tag{5.6}$$

where y_0 and p_0 are real constants, and we will be interested in the half plane $\{(y_0, p_0) : y_0 > 0\}$. The unions of the stable and unstable manifolds of these individual saddle fixed points over all y_0 and p_0 are the stable and unstable manifolds, $W_0^s(\mathcal{M})$ and $W_0^u(\mathcal{M})$, respectively, of $\mathcal{M}$.

We are interested only in the branches that lie in the regime with $z \geq 0$. For $\delta = 0$, these two branches coincide in a homoclinic manifold,

$$W_{0,h}^s(\mathcal{M}) = W_{0,h}^u(\mathcal{M}) = \{(y, p, z, q) : y = y_0 > 0, p = p_0 \in \mathbb{R}, z = Z_h(y_0), q = Z_h'(y_0)\}, \tag{5.7}$$

where

$$Z_h(y_0) = Z_h(x; y_0) = \frac{3}{2y_0}\text{sech}^2\left(\frac{1}{2}x\right) \tag{5.8}$$

is the homoclinic orbit of (5.6) that connects the saddle fixed point to itself. In addition, the limiting stable and unstable manifolds $W_0^s(\mathcal{M})$ and $W_0^u(\mathcal{M})$ can equivalently be seen as part of the level set $\mathcal{H}(y, p, z, q) = 0$ of the energy function

$$\mathcal{H}(y, p, z, q) = \frac{1}{2}q^2 - \frac{1}{2}z^2 + \frac{1}{3}yz^3, \tag{5.9}$$

with $y, z > 0$, which is a scaled version of the energy function.

By contrast, for $\delta > 0$, orbits on $\mathcal{M}$ evolve slowly according to the shear flow,

$$y' = \delta p, \qquad \text{and} \qquad p' = 0, \tag{5.10}$$

and $\mathcal{M}$ is a normally hyperbolic slow manifold of (5.3). It has 3-dimensional stable and unstable manifolds, $W^s(\mathcal{M})$ and $W^u(\mathcal{M})$. The local components of these manifolds are $C^r - \mathcal{O}(\delta)$ close to $W_0^{s,u}(\mathcal{M})$, respectively. Orbits that are forward asymptotic to $\mathcal{M}$ must lie in $W_0^s(\mathcal{M})$, and similarly orbits that are backward asymptotic to $\mathcal{M}$ must lie in $W_0^u(\mathcal{M})$. Hence, these orbits asymptotically satisfy $y(x) \to \pm\infty$ and $p(x) \to$ constant as

$x \to \pm\infty$, since $z(x) \to 0$ exponentially and $p(x)$ grows only linearly for any orbit that is forward/backward asymptotic to orbits on $\mathcal{M}$, such as these orbits are.

Remark 5.1 The coincidence of the manifolds $\mathcal{M}$ for $\delta = 0$ and $\delta \neq 0$ is special, since in general there is a family of slow manifolds each of which is only $\mathcal{O}(\delta)$ close to its singular (or reduced) limit, [16]. Moreover, $W^s(\mathcal{M})$ and $W^u(\mathcal{M})$ are uniquely determined here, as well, since $\mathcal{M}$ is given explicitly, and hence known uniquely.

5.2 The proofs of (1.7) and (1.8)

Since $W^s_{0,h}(\mathcal{M})$ and $W^u_{0,h}(\mathcal{M})$, which coincide, transversely intersect the hyperplane $\{q = 0\}$, the local components of the perturbed manifolds $W^s(\mathcal{M})$ and $W^u(\mathcal{M})$ also intersect the hyperplane $\{q = 0\}$ transversely in one or more 2-dimensional manifolds for all δ sufficiently small, see [16]. We define the 2-dimensional manifold $\mathcal{I}^{+1}$ to be the the first intersection of $W^u(\mathcal{M})$ with $\{q = 0\}$, and similarly the 2-dimensional manifold $\mathcal{I}^{-1}$ to be the first intersection of $W^s(\mathcal{M})$ with $\{q = 0\}$.

Lemma 5.1 *The manifolds $\mathcal{I}^{+1}$ and $\mathcal{I}^{-1}$ are given by*

$$\mathcal{I}^{\pm 1} = \{(y, p, z, q) : y = y_0 > 0, p = p_0, z = z_{\pm 1}(y_0, p_0), q = 0\}, \tag{5.11}$$

where $z_1(y, p)$ and $z_{-1}(y, p)$ are smooth functions of p and y such that

$$\begin{aligned} z_{-1}(y, p) &< z_1(y, p) \quad \text{for} \quad p > 0, \\ z_{-1}(y, p) &> z_1(y, p) \quad \text{for} \quad p < 0, \\ z_{-1}(y, 0) &= z_1(y, 0) \quad \text{for} \quad p = 0, \end{aligned}$$

and where $z_{\pm 1}(y_0, p_0) = \frac{3}{2y_0} + \mathcal{O}(\delta)$. Moreover,

$$\mathcal{I}^{+1} \cap \mathcal{I}^{-1} = \{(y, p, z, q) : y = y_0 > 0, p = 0, z = z_{\pm 1}(y_0, 0), q = 0\}. \tag{5.12}$$

From this lemma, we see that the 2-dimensional manifolds $\mathcal{I}^{\pm 1}$ are parameterized by y_0 and p_0, and we see how their relative orientations vary with p, specifically on which side of the unperturbed homoclinic orbit, $z = 3/2y_0$, the manifolds $\mathcal{I}^{\pm 1}$ lie. Also, we see that the intersection $\mathcal{I}^{+1} \cap \mathcal{I}^{-1}$ is a subset of $\{p = 0\}$, and it is parameterized by y_0.

Proof We first prove the latter statement, (5.12). A homoclinic orbit $\Gamma = (y, p, z, q) \in W^u(\mathcal{M}) \cap W^s(\mathcal{M})$ must satisfy

$$\triangle\mathcal{H} = \int_{-\infty}^{\infty} \mathcal{H}'|_{\Gamma(x)} dx = \frac{1}{3}\delta \int_{-\infty}^{\infty} p(x) z^3(x) dx = 0, \tag{5.13}$$

since $\mathcal{H}|_{\mathcal{M}} \equiv 0$. Note that $\triangle\mathcal{H}$ is in essence the Melnikov function that measures the distance between $W^s(\mathcal{M})$ and $W^u(\mathcal{M})$ in $\{q = 0\}$, [11, 7], and we remark that the improper integral converges, because $z(x)$ decays exponentially for these solutions, while

$p(x)$ grows only linearly. Equation (5.13) is exact; and, it can be approximated by setting $p(x) = p_0 + \mathcal{O}(\delta)$ and $z(x) = Z_h(x; y_0) + \mathcal{O}(\delta)$,

$$\triangle\mathcal{H} = \frac{1}{3}\delta p_0 \int_{-\infty}^{\infty} Z_h^3(x; y_0)dx + \mathcal{O}(\delta^2) = 0.$$

Hence, the p-coordinate of $W^s(\mathcal{M}) \cap W^u(\mathcal{M}) \cap \{q = 0\} = \mathcal{I}^{+1} \cap \mathcal{I}^{-1}$ must satisfy $p = p_0 = \mathcal{O}(\delta)$, because otherwise it would not be possible for a zero of $\triangle\mathcal{H}$ to exist.

We now go further and show that p_0 must actually vanish. In fact, by the reversibility symmetry (5.4), an orbit that has initial conditions in $W^s(\mathcal{M}) \cap \{p = q = 0\}$ is also homoclinic to $\mathcal{M}$, *i.e.,* the initial conditions are necessarily in $W^s(\mathcal{M}) \cap W^u(\mathcal{M}) \cap \{q = 0\} = \mathcal{I}^{+1} \cap \mathcal{I}^{-1}$. Moreover, if $p_0(y_0)$ is not identically 0, then we can apply the reversibility symmetry (5.4) to obtain a second intersection $\mathcal{I}^{+1} \cap \mathcal{I}^{-1}$, given by $p = -p_0(y_0)$. However, such a second intersection cannot exist, because $W^s(\mathcal{M})$ and $W^u(\mathcal{M})$ are uniquely determined and the local manifolds are $C^r - \mathcal{O}(\delta)$ close to $W^s_{0,h}(\mathcal{M})$ and $W^u_{0,h}(\mathcal{M})$, respectively, as stated above. Thus, $\triangle\mathcal{H} = 0$ for $p_0 \equiv 0$, and the desired result, (5.12), follows.

Next, the 2-dimensional manifolds $\mathcal{I}^{\pm 1}$ can be parameterized by $p = p_0$ and $y = y_0$ with $y_0 > 0$ as in (5.11), because there are unique fast stable and unstable fibers for each basepoint (y_0, p_0) on $\mathcal{M}$. Also, the z-components $z_{\pm 1}(y_0, p_0)$ must be $\mathcal{O}(\delta)$-close to $3/2y_0$, because this is the z-coordinate of $W^s_{0,h}(\mathcal{M}) \cap \{q = 0\} = W^u_{0,h}(\mathcal{M}) \cap \{q = 0\}$, which has $\mathcal{H} = 0$.

Finally, we consider the orbits $\Gamma_{+1}(x) = (y_1(x), p_1(x), z_1(x), q_1(x))$ which lie in $W^u(\mathcal{M})$ with initial conditions $(y_0, p_0, z_1(p_0, y_0), 0) \in \mathcal{I}^{+1}$, and we consider the homoclinic orbits $\Gamma_{-1}(x) = (y_{-1}(x), p_{-1}(x), z_{-1}(x), q_{-1}(x))$ which lie in $W^s(\mathcal{M})$ with initial conditions $(y_0, p_0, z_{-1}(p_0, y_0), 0) \in \mathcal{I}^{-1}$. Let

$$\begin{aligned}
\triangle\mathcal{H}_{-1} &\equiv \int_0^{\infty} \mathcal{H}'|_{\Gamma_{-1}} dx = \frac{1}{3}\delta \int_0^{\infty} p_{-1}(x) z_{-1}^3(x) dx, \\
\triangle\mathcal{H}_{+1} &\equiv \int_{-\infty}^{0} \mathcal{H}'|_{\Gamma_1} dx = \frac{1}{3}\delta \int_{-\infty}^{0} p_1(x) z_1^3(x) dx.
\end{aligned}$$

Both $\triangle\mathcal{H}_{-1}$ and $\triangle\mathcal{H}_{+1}$ exist, since $\mathcal{H}|_{\mathcal{M}} = 0$. Therefore, if $p_0 > 0$, then $\triangle\mathcal{H}_{-1} > 0$, since $p' > 0$ by (5.3). In turn, $\mathcal{H}(y_0, p_0, z_{-1}(p_0, y_0), 0) < 0$. Similarly, $\mathcal{H}(y_0, p_0, z_1(p_0, y_0), 0) > 0$. Hence, by (5.9), $z_{-1}(p_0, y_0) < z_1(p_0, y_0)$. The case $p_0 < 0$ follows by applying the symmetry (5.4). □

Remark 5.2 In the subsequent analysis, we will often choose $p_0 = \delta\tilde{p}_0$ in (5.11). It immediately follows from the above arguments that

$$\frac{3}{2y_0} + \mathcal{O}(\delta^2) = z_{-1}(y_0, \delta\tilde{p}_0) < z_1(y_0, \delta\tilde{p}_0) = \frac{3}{2y_0} + \mathcal{O}(\delta^2). \tag{5.14}$$

The stable and unstable manifolds $W^s(\mathcal{M})$ and $W^u(\mathcal{M})$ may have additional intersections with the hyperplane $\{q = 0\}$. In fact, the flow generated by (5.3) defines a 'half' Poincaré map,

$$\mathcal{P} : \{q = 0\} \to \{q = 0\}, \tag{5.15}$$

where the image of (y_0, p_0, z_0) under $\mathcal{P}$ is the point (y, p, z) corresponding to the next intersection of the orbit $\Gamma_0(x)$ with $\{q = 0\}$ and $\Gamma_0(0) = (y_0, p_0, z_0, 0)$. With this definition, $\mathcal{P}^2$ defines a more standard Poincaré map. We also define $\mathcal{I}^n \subset W^u(\mathcal{M}) \cap \{q = 0\}$ $(n \geq 1)$ to be the n-th intersection of $W^u(\mathcal{M})$ with $\{q = 0\}$ and $\mathcal{I}^{-m} \subset W^s(\mathcal{M}) \cap \{q = 0\}$ $(m \geq 1)$ to be the m-th intersection of $W^s(\mathcal{M})$ with $\{q = 0\}$, *i.e.,*

$$\mathcal{P}(\mathcal{I}^n) = \mathcal{I}^{n+1}, \quad \mathcal{P}^{-1}(\mathcal{I}^{-m}) = \mathcal{I}^{-m-1}, \quad n, m \geq 1, \tag{5.16}$$

where $\mathcal{P}^{-1}$ is the inverse map (backwards time) that is naturally related to $\mathcal{P}$ through the symmetry (5.4). In general, $\mathcal{P}^{-1}(\mathcal{I}^n) \subsetneqq \mathcal{I}^{n-1}$ $(n \geq 2)$, because $\mathcal{P}$ might not be defined on parts of $\mathcal{I}^{n-1}$, and, similarly, $\mathcal{P}(\mathcal{I}^{-m}) \subsetneqq \mathcal{I}^{-m+1}$ $(m \geq 2)$, since $\mathcal{P}^{-1}$ might not be defined on parts of $\mathcal{I}^{-m+1}$ (see the proof of Lemma 5.2 below). However, by construction,

$$\begin{aligned} \mathcal{P}(\mathcal{I}^n \cap \mathcal{I}^{-m}) &= \mathcal{I}^{n+1} \cap \mathcal{I}^{-m+1} \quad (n \geq 1, m \geq 2), \\ \mathcal{P}^{-1}(\mathcal{I}^n \cap \mathcal{I}^{-m}) &= \mathcal{I}^{n-1} \cap \mathcal{I}^{-m-1} \quad (n \geq 2, m \geq 1). \end{aligned} \tag{5.17}$$

Next, it is also not clear *a priori* whether $\mathcal{I}^n$ and $\mathcal{I}^{-m}$ exist, because we have not yet shown that $\mathcal{P}$ is defined on $\mathcal{I}^{n-1}$ or that $\mathcal{P}^{-1}$ is defined on $\mathcal{I}^{-m+1}$. However, due to the singularly perturbed nature of (5.3), we have a certain control over the intersections of $W^s(\mathcal{M})$ and $W^u(\mathcal{M})$ with $\{q = 0\}$; and, hence, we can establish the nonemptiness of these intersections in the following lemma:

Lemma 5.2 *Fix any $n, m \geq 1$. There exists a positive $\delta_0 = \delta_0(n, m)$ sufficiently small such that, for all $\delta \in (0, \delta_0)$, $\mathcal{I}^n \neq \emptyset$ and $\mathcal{I}^{-m} \neq \emptyset$. Their asymptotic expansions are given by*

$$\mathcal{I}^n, \mathcal{I}^{-m} = \{y = y_0 > 0, p = p_0, z = z_{n,-m}(y_0, p_0) = \frac{3}{2y_0} + \mathcal{O}(\delta)\}, \qquad \textit{for} \quad n, m \quad \textit{odd} \tag{5.18}$$

$$\mathcal{I}^n, \mathcal{I}^{-m} = \{y = y_0 > 0, p = p_0, z = z_{n,-m}(y_0, p_0) = \mathcal{O}(\sqrt{\delta})\}, \qquad \textit{for} \quad n, m \quad \textit{even}. \tag{5.19}$$

Furthermore, for $p \geq 0$, they are ordered, as follows:

$$\begin{aligned} z_2(y,p) < z_4(y,p) < z_6(y,p) < .... \quad \ll \quad ... < z_5(y,p) < z_3(y,p) < z_1(y,p), \\ z_{-2}(y,p) < z_{-4}(y,p) < z_{-6}(y,p) < .... \quad \ll \quad ... < z_{-5}(y,p) < z_{-3}(y,p) < z_{-1}(y,p), \end{aligned} \tag{5.20}$$

and

$$z_{-n}(y,p) < z_n(y,p) \quad \text{for } n \geq 1 \text{ odd, while } z_{-n}(y,p) > z_n(y,p) \quad \text{for } n \geq 2 \text{ even,}$$

where the ordering for $p < 0$ follows by (5.4).

In addition, $\mathcal{I}^n \cap \mathcal{I}^{-m} \neq \emptyset$ when either both n and m are odd, or when both are even. More specifically, for any fixed $N \geq 1$ there exists a $\tilde{\delta}_0$ sufficiently small such that $\mathcal{I}^k$ exists for $k = -2N, -2N+1, \ldots, -1$, and for $k = 1, \ldots, 2N-1, 2N$, and such that

$$\mathcal{I}^{+N} \cap \mathcal{I}^{-N} = \{y = y_0 > 0, p = 0, z = z_{\pm N}(y_0, 0), q = 0\} \tag{5.21}$$

for $\delta \in (0, \tilde{\delta}_0)$. *Moreover, for* $-N < j < N$,

$$\mathcal{I}^{+N+j} \cap \mathcal{I}^{-N+j} = \{y = y_0 > 0, p = \frac{3j}{y_0}\delta + \mathcal{O}(\delta^2), z = z_{N\pm j}(y_0, p), q = 0\}, \qquad (5.22)$$

so that $\mathcal{I}^{+N+j} \cap \mathcal{I}^{-N+j} \subset \{p > 0\}$ *for* $j > 0$ *and* $\mathcal{I}^{+N+j} \cap \mathcal{I}^{-N+j} \subset \{p < 0\}$ *for* $j < 0$.

This lemma gives more details than are necessary for the proof of (1.7) and (1.8). However, the information on the structure of $\mathcal{I}^n$ for all n, $\mathcal{I}^{-m}$ for all m, and their intersections $\mathcal{I}^n \cap \mathcal{I}^{-m}$ will be useful below.

Proof First, we need to determine which part (if any) of $\mathcal{I}^{+1} \in \{q = 0\}$ is mapped by $\mathcal{P}$ to $\{q = 0\}$. Therefore, we consider an orbit $\Gamma_1(x) = (y_1(x), p_1(x), z_1(x), q_1(x))$ with $\Gamma_1(0) = (y_1^0, \delta\tilde{p}_1^0, z_1^0, 0) \in \mathcal{I}^{+1}$, where $\delta\tilde{p}_1^0$ is strictly $\mathcal{O}(\delta)$. For such an orbit, $\Gamma_1(0)$ is not too close to $\mathcal{I}^{-1}$. Thus, $\Gamma_1(x)$ has its minimal distance $(=\mathcal{O}(\sqrt{\delta}))$ from $\mathcal{M}$ at some point $x = X$, where $X = \mathcal{O}(|\log\delta|)$, because Γ_1 is $\mathcal{O}(\delta)$-close to an unperturbed homoclinic solution of (5.6). Then, we see that

$$\mathcal{H}(\Gamma_1(X)) = \int_{-\infty}^{X} \mathcal{H}'|_{\Gamma_1(x)} dx = \frac{1}{3}\delta^2\tilde{p}_1^0 \int_{-\infty}^{\infty} Z_h^3(x; y_0)dx + \mathcal{O}(\delta^{2+\rho}), \qquad (5.23)$$

for some $\rho > 0$, because $\Gamma_1(x) \to \mathcal{M}$ as $x \to -\infty$ and because $\mathcal{H}|_{\mathcal{M}} = 0$. Moreover, $\text{signum}(\mathcal{H}(\Gamma_1(X))) = \text{signum}(\tilde{p}_1^0)$, which implies that only those $\Gamma_1(x)$ with $\tilde{p}_1^0 < 0$ have $\mathcal{H} < 0$ when they approach $\mathcal{M}$, *i.e.,* only those $\Gamma_1(x)$ with $\tilde{p}_1^0 < 0$ are inside the family of unperturbed homoclinic orbits (5.7) as they return to $\mathcal{M}$. Therefore, the return map $\mathcal{P}$ is only defined for points with $\tilde{p}_1^0 < 0$, because orbits with $\tilde{p}_1^0 > 0$ are outside $\mathcal{H} = 0$ and do not return to $\mathcal{M}$. Also, one finds that the p-coordinate $\delta\tilde{p}_2$ of $\mathcal{P}(y_1, \delta\tilde{p}_1, z_1)$ is

$$\delta\tilde{p}_2 = \delta\tilde{p}_1 + \int_0^X (p_1)'dx = \delta\left[\tilde{p}_1 + y_1\int_0^\infty Z_h^2(x; y_1)dx + \mathcal{O}(\delta^\rho)\right] = \delta\left[\tilde{p}_1 + \frac{3}{y_1} + \mathcal{O}(\delta^\rho)\right] \qquad (5.24)$$

for some $\rho > 0$ (by (5.8)). Hence, both $\delta\tilde{p}_2 < 0$ and $\delta\tilde{p}_2 > 0$ are possible. Although $\mathcal{P}$ is only defined on $\mathcal{I}^{+1}$ for $p < 0$, its image $\mathcal{I}^{+2}$ is unbounded in the p-coordinate. This is due to the singular character of the flow, that stretches the part $\mathcal{I}^{+1} \cap \{p < 0\}$ near $(y, p) = (0, 0)$. By increasing p_1 (or $\delta\tilde{p}_1$) toward 0, the orbit $\Gamma_1(x)$ remains near $\mathcal{M}$ for an arbitrarily long time. During this period, p approaches the limit value given by (5.24) – recall that $p' = 0$ on $\mathcal{M}$ (5.10) – that becomes arbitrarily large by choosing y_1 small enough. The y-coordinate grows along with the (slow) flow on $\mathcal{M}$ (5.10), and becomes arbitrarily large by taking $p_1 < 0$ close enough to 0 (i.e. by increasing the 'time' that $\Gamma_1(x)$ remains near $\mathcal{M}$). See [9] for a detailed analysis of this stretching mechanism in singularly perturbed systems.

It also follows from the above analysis and the character of (5.3) that $\mathcal{P}(y_1, p_1, z_1) = (y_2, p_2, z_2) \in \mathcal{I}^{+2}$ with $y_2 = y_1 + \mathcal{O}(\delta) > 0$, $p_2 = p_1 + \mathcal{O}(\delta)$ and $z_2 = \mathcal{O}(\sqrt{\delta})$. This establishes (5.19) for $n = 2$. Moreover, (5.24) implies that $p_2 = 0$ if

$$p_1 = \delta\tilde{p}_1 = -\delta y_1 \int_0^\infty Z_h^2(x; y_1)dx + \mathcal{O}(\delta^\rho) = -\frac{3}{y_1}\delta + \mathcal{O}(\delta^\rho) < 0 \qquad (5.25)$$

for some $\rho > 0$.

The proofs of the existence of the third intersection, $\mathcal{I}^{+3}$, of $W^u(\mathcal{M})$ and $\{q = 0\}$ and of the fact that it is an unbounded manifold run along essentially the same lines. Moreover, the third intersection of $W^u(\mathcal{M})$ with $\{q = 0\}$ must lie in between the first and the second intersections, $\mathcal{I}^{+1}$ and $\mathcal{I}^{+2}$, respectively, because $W^u(\mathcal{M})$ cannot have self-intersections and because $W^u(\mathcal{M})$ is of co-dimension one. In terms of the z coordinates, this translates into $z_2(y,p) < z_3(y,p) < z_1(y,p)$, with $z_2(y,p) = \mathcal{O}(\sqrt{\delta})$ and $z_1(y,p), z_3(y,p) = 3/2y + \mathcal{O}(\delta)$, because the third intersection $W^u(\mathcal{M}) \cap \{q = 0\}$ must also be $C^r - \mathcal{O}(\delta)$ close to the unperturbed homoclinic family (5.7).

Statements (5.18), (5.19), and (5.20) follow inductively by the above arguments (in backwards time in the case of $-m < 0$).

To show that $\mathcal{I}^n \cap \mathcal{I}^{-m} \neq \emptyset$, we first show that $\mathcal{I}^{+2} \cap \mathcal{I}^{-2}$ exists by mimicking the proof of (5.12) in Lemma 5.1. We observe that $\mathcal{I}^{+2} \cap \{p = 0\} = \{p = 0\}$ by (5.24), so it follows immediately that $\mathcal{I}^{+2} \cap \mathcal{I}^{-2} \supset \{p = 0\}$, by the symmetry (5.4). To show that $\{p = 0\}$ is the unique intersection of $\mathcal{I}^{+2}$ and $\mathcal{I}^{-2}$, we observe that (5.13) must hold for all orbits that are homoclinic to $\mathcal{M}$, and hence it holds in particular for those homoclinic orbits that have their initial conditions in $\mathcal{I}^{+2} \cap \mathcal{I}^{-2}$, which is the second intersection $W^s(\mathcal{M}) \cap W^u(\mathcal{M}) \cap \{q = 0\}$. These orbits make two full circuits through the fast field between touch-down and take-off from $\mathcal{M}$. During this excursion, they are $\mathcal{O}(\delta)$-close to a homoclinic orbit of the fast reduced system (5.6). Hence, (5.13) can again be approximated by setting $p(x) = p_0 + \mathcal{O}(\delta)$ and $z(x) = Z_h(x; y_0) + \mathcal{O}(\delta)$ so that

$$\triangle\mathcal{H} = 2\left(\frac{1}{3}\delta p_0 \int_{-\infty}^{\infty} Z_h^3(x; y_0)dx\right) + \mathcal{O}(\delta^2),$$

which implies that the p_0-coordinate $\mathcal{I}^{+2} \cap \mathcal{I}^{-2}$ must satisfy $p = p_0(y_0) = \mathcal{O}(\delta)$ in order for $\triangle\mathcal{H}$ to vanish at $\mathcal{O}(\delta^2)$. The $C^r - \mathcal{O}(\delta)$-closeness of $W^s(\mathcal{M})$ and $W^u(\mathcal{M})$ to $W^s_{0,h}(\mathcal{M})$ and $W^u_{0,h}(\mathcal{M})$ implies that $p_0(\delta) \equiv 0$. Similar arguments may be used to show that $\mathcal{I}^{+N} \cap \mathcal{I}^{-N} \neq \emptyset$ and that $\mathcal{I}^{+N} \cap \mathcal{I}^{-N} \subset \{p = 0\}$ for all $N \geq 1$.

Finally, we note that (5.25) can be interpreted as the leading order approximation of the p-coordinate of the curve in $\mathcal{I}^{+1}$ that is mapped by $\mathcal{P}$ to $\mathcal{I}^{+2} \cap \{p = 0\} = \mathcal{I}^{+2} \cap \mathcal{I}^{-2}$. Thus, by (5.17), (5.25) represents $\mathcal{P}^{-1}(\mathcal{I}^{+2} \cap \mathcal{I}^{-2}) = \mathcal{I}^{+1} \cap \mathcal{I}^{-3}$, *i.e.,* we have obtained (5.22) for $N = 2$ and $j = -1$. The above leading order calculation (5.24) of the image of p under the map $\mathcal{P}$, *i.e.,* over a half-circuit of the unperturbed homoclinic orbit, holds for any $\Gamma_N(x)$ with initial conditions in $\mathcal{I}^{+N}$. Hence, for $j = 1$, (5.22) follows immediately from the fact that $\mathcal{I}^{+N} \cap \mathcal{I}^{-N} \subset \{p = 0\}$ and that $\mathcal{P}(\mathcal{I}^{+N} \cap \mathcal{I}^{-N}) = \mathcal{I}^{+N+1} \cap \mathcal{I}^{-N+1}$, where we recall (5.17). The general statement in (5.22) follows by induction, through repetitive applications of $\mathcal{P}$ or $\mathcal{P}^{-1}$. □

Proof of (1.7) and (1.8) The key to the proof lies in defining the curves $\mathcal{C}^\infty_N$ for any given N in the (α, β) parameter space in terms of the intersection manifold $\mathcal{I}^n \cap \mathcal{I}^{-m}$ for certain n and m. First, we observe that an orbit $\Gamma_N(x)$ that is homoclinic to $\mathcal{M}$ must be in $W^s(\mathcal{M}) \cap W^u(\mathcal{M})$, *i.e.,* the intersections of such an orbit with $\{q = 0\}$ must be points in $\mathcal{I}^n \cap \mathcal{I}^{-m}$ for some n and m. Moreover, a symmetric homoclinic orbit with initial condition $\Gamma_N(0) = (\alpha_N, 0, \beta_N, 0)$ in $\mathcal{I}^{+N} \cap \mathcal{I}^{-N}$ ($\subset \{q = 0\}$) makes N half-circuits

through the fast field associated to (5.3) before touching down on $\mathcal{M}$. Thus, such an orbit $\Gamma_N(x)$ makes N full loops through the fast field between taking off and touching down on $\mathcal{M}$. During each of these loops, the $z_N(x)$ coordinate of $\Gamma_N(x)$ has one non-degenerate maximum (at the intersection of $\Gamma_N(x)$ with $\{q(=z')=0\}$ where $z_N(x)=3/2y_0+\mathcal{O}(\delta)$ by (5.18)). Thus, by definition, $\Gamma_N(x)$ must have its initial conditions in $\mathcal{C}_N^\infty$, and hence $\mathcal{I}^{+N}\cap\mathcal{I}^{-N}$ corresponds identically to $\mathcal{C}_N^\infty$. Finally, we unscale (5.1) and find

$$\mathcal{I}^{+N}\cap\mathcal{I}^{-N}=\{(y_0,0,z_{\pm N}(y_0,0),0)=\left(\frac{\alpha_N}{\alpha},0,\alpha\beta_N,0\right):(\alpha_N,\beta_N)\in\mathcal{C}_N^\infty\},\qquad(5.26)$$

by (5.21). Therefore, both the existence of the curves $\mathcal{C}_N^\infty$ for all $N\geq 1$ and their leading order approximations, see (1.7) and (1.8), follow from Lemma 5.2. This completes all but one part of the proof. It only remains to derive the higher order terms, which give more accurate formulas for the locations of the curves $\mathcal{C}_N^\infty$ for large α. We do so in the next lemma. □

5.3 Higher order approximations of $\mathcal{I}^{+N}\cap\mathcal{I}^{-N}$ and of $\mathcal{C}_N^\infty$

Apart from giving a more accurate description of $\mathcal{I}^{+N}\cap\mathcal{I}^{-N}$ and of $\mathcal{C}_N^\infty$, the following result also gives analytic confirmation (for $u'=0$) of the ordering (5.20) obtained above by geometric arguments.

Lemma 5.3 *Fix any $N\geq 1$. and let $\mathcal{I}^{+N}\cap\mathcal{I}^{-N}$ be represented by $\{(y,p,z,q):y=y_0,p=0,z=z_{\pm N}(y_0,0),q=0\}$, recall (5.21). Then, there exists a $\delta_0(N)$ sufficiently small such that for $\delta<\delta_0(N)$*

$$\begin{aligned}
&z_{\pm N}(y_0,0)=\tfrac{3}{2y_0}\left\{1-\tfrac{\delta^2}{y_0^2}(\tfrac{11}{8}+k(k-1)\tfrac{32}{5})+\mathcal{O}(\delta^{2+\rho})\right\},\quad\text{if}\quad N=2k-1,\quad k\geq 1,\\
&z_{\pm N}(y_0,0)=\tfrac{6\sqrt{2}}{\sqrt{5}}k\tfrac{\delta}{y_0^2}+\mathcal{O}(\delta^{1+\rho}),\qquad\qquad\text{if}\quad N=2k,\qquad k\geq 1,
\end{aligned}\qquad(5.27)$$

for some $\rho>0$. Equivalently, by (5.26), if $\mathcal{C}_N^\infty=\{(\alpha,\beta):\beta=\beta_N(\alpha)\}$, then for $\alpha\gg\tilde{\alpha}(N)$,

$$\begin{aligned}
&\beta_N(\alpha)=\tfrac{3}{2\alpha}\left\{1-\tfrac{1}{\alpha^2}(\tfrac{11}{8}+k(k-1)\tfrac{32}{5})+\mathcal{O}(\tfrac{1}{\alpha^{2+\rho}})\right\},\quad\text{if}\quad N=2k-1,\quad k\geq 1,\\
&\beta_N(\alpha)=\tfrac{6\sqrt{2}}{\sqrt{5}}k\tfrac{1}{\alpha^2}+\mathcal{O}(\tfrac{1}{\alpha^{2+\rho}}).\qquad\qquad\text{if}\quad N=2k,\qquad k\geq 1.
\end{aligned}\qquad(5.28)$$

Proof The result follows by computing in two independent ways the value of $\mathcal{H}|_{\mathcal{I}^{+N}\cap\mathcal{I}^{-N}}$ for orbits $\Gamma_{\pm N}(x)=(y_{\pm N}(x),p_{\pm N}(x),z_{\pm N}(x),q_{\pm N}(x))$ for which the initial condition, $\Gamma_{\pm N}(0)=(y_0,0,z_{\pm N}(y_0,0),0)$, lies in the intersection $\mathcal{I}^{+N}\cap\mathcal{I}^{-N}$. First,

$$\mathcal{H}|_{\mathcal{I}^{+N}\cap\mathcal{I}^{-N}}=\frac{1}{3}(z_{\pm N}(y_0,0))^2\left(-\frac{3}{2}+y_0z_{\pm N}(y_0,0)\right)\qquad(5.29)$$

by (5.9). Second, we also have

$$\mathcal{H}|_{\mathcal{I}^{+N}\cap\mathcal{I}^{-N}}=-\int_0^\infty\mathcal{H}'|_{\Gamma_{\pm N}(x)}dx=-\frac{1}{3}\delta\int_0^\infty p_{\pm N}(x)z_{\pm N}^3(x)dx,\qquad(5.30)$$

because $\mathcal{H}|_{\mathcal{M}} = 0$. In this second formula, we expand $\Gamma_{\pm N}(x)$ in δ^2,

$$\begin{aligned} y_{\pm N}(x) &= y_0 + \delta^2 y_1(x) + \mathcal{O}(\delta^{2+\rho}), & p_{\pm N}(x) &= \tfrac{1}{\delta}(y_{\pm N})'(x), \\ z_{\pm N}(x) &= Z_h(x;y_0) + \delta^2 Z_1(x) + \mathcal{O}(\delta^{2+\rho}), & q_{\pm N}(x) &= (z_{\pm N})'(x) \end{aligned} \tag{5.31}$$

by (5.14) for some $\rho > 0$. Hence, from (5.2) and (5.8), we see that $y_1(x)$ satisfies

$$y_1'' = \frac{9}{4y_0}\operatorname{sech}^4\left(\frac{1}{2}x\right),$$

to leading order, which yields

$$y_1'(x) = \frac{3}{2y_0}\left[3\tanh\frac{1}{2}x - \tanh^3\frac{1}{2}x\right] + y_1'(0). \tag{5.32}$$

Now, we observe that we have (in general) shifted the position of $x = 0$ by setting $z_{\pm N}(x) = Z_h(x;y_0) + \mathcal{O}(\delta^2)$ in (5.31); with this leading order approximation of $z_{\pm N}(x)$ we necessarily have $z_{\pm N}(0) = 3/2y_0 + \mathcal{O}(\delta^2)$. Of course, this is exactly the correct choice for $N = 1$, and hence for $N = 1$ we set $y_1'(0) = 0$ in (5.32) and approximate (5.30) as

$$\begin{aligned} \mathcal{H}|_{\mathcal{I}^{+1}\cap\mathcal{I}^{-1}} &= -\frac{1}{3}\delta^2\int_0^\infty y_1'(x)Z_h^3(x;y_0)dx + \mathcal{O}(\delta^{2+\rho}) \\ &= -\frac{1}{3}\delta^2\left(\frac{3}{2y_0}\right)^4\int_0^\infty\left[3\tanh\frac{1}{2}x - \tanh^3\frac{1}{2}x\right]\operatorname{sech}^6\left(\frac{1}{2}x\right)dx + \mathcal{O}(\delta^{2+\rho}) \\ &= -\frac{\delta^2}{y_0^4}\left(\frac{3}{2}\right)^3\frac{11}{24} + \mathcal{O}(\delta^{2+\rho}). \end{aligned}$$

Therefore, equating the two expressions (5.29) and (5.33) and using the approximation $z_{\pm1}(y_0,0) = 3/2y_0 + \mathcal{O}(\delta^2)$ obtained in (5.14) in the expression (5.29), we find

$$\frac{1}{3}\left(y_0 z_{\pm1}(y_0,0) - \frac{3}{2}\right)\left(\frac{3}{2y_0} + \mathcal{O}(\delta^2)\right)^2 = -\frac{\delta^2}{y_0^4}\left(\frac{3}{2}\right)^3\frac{11}{24} + \mathcal{O}(\delta^{2+\rho}),$$

which is equivalent to (5.27) for $N = 1$.

Next, we consider the case $N = 2$. We have to translate the initial condition to the next intersection of $\Gamma_{\pm2}(x)$ with $\{q = 0\}$, because $z_{\pm2}(x) = 3/2y_0 + \mathcal{O}(\delta^2)$ at this intersection. This intersection lies in $\mathcal{P}(\mathcal{I}^{+2}\cap\mathcal{I}^{-2}) = \mathcal{I}^{+3}\cap\mathcal{I}^{-1}$ by construction. Now, the only information we need on the initial conditions in the above analysis is the value of $y_1'(0)$ (in the shifted coordinates). It follows from (5.22), with $N = 2$ and $j = 1$, that the p-coordinate of $\Gamma_{\pm2}\cap\{q = 0\}$ is $3\delta/y_0 + \mathcal{O}(\delta^2)$. Hence, for $N = 2$, we have to set $y_1'(0) = 3/y_0$ in (5.32). We introduce the return time $X_-^1 < 0$ as the value of x for which (the translation of) $\Gamma_{\pm2}(x)$ intersects $\{q = 0\}$, *i.e.*, $X_-^1 < 0$ exactly defines the translation of $x = 0$, $\Gamma_{\pm2}(X_-^1) \in \mathcal{I}^{+2}\cap\mathcal{I}^{-2}$. Thus, by (5.30),

$$\mathcal{H}|_{\mathcal{I}^{+2}\cap\mathcal{I}^{-2}} = -\frac{1}{3}\delta^2\int_{X_-^1}^\infty y_1'(x)Z_h^3(x;y_0)dx + \mathcal{O}(\delta^{2+\rho})$$

$$
\begin{aligned}
&= -\frac{1}{3}\delta^2\left(\frac{3}{2y_0}\right)^4\int_{-\infty}^{\infty}\left[(3\tanh\frac{1}{2}x-\tanh^3\frac{1}{2}x)+2\right]\operatorname{sech}^6\left(\frac{1}{2}x\right)dx+\mathcal{O}(\delta^{2+\rho})\\
&= -\frac{2}{3}\delta^2\left(\frac{3}{2y_0}\right)^4\int_{-\infty}^{\infty}\operatorname{sech}^6\left(\frac{1}{2}x\right)dx+\mathcal{O}(\delta^{2+\rho})\\
&= -\frac{\delta^2}{y_0^4}\left(\frac{3}{2}\right)^3\frac{32}{15}+\mathcal{O}(\delta^{2+\rho}),
\end{aligned}
$$

where we used the property that $y_1'(x)-y_1'(0)$ is an odd function of x. We now equate the expressions (5.29) and (5.33) to obtain

$$
\frac{1}{3}z_{\pm 2}^2(y_0,0)\left(-\frac{3}{2}+\mathcal{O}(\delta)\right)=-\frac{\delta^2}{y_0^4}\left(\frac{3}{2}\right)^3\frac{32}{15}+\mathcal{O}(\delta^{2+\rho}),
$$

which yields (5.27) for $N=2$.

Finally, we prove (5.27) for general values of N. Since the approximation $z_{\pm N}(x)=Z_h(x;y_0)+\mathcal{O}(\delta^2)$ in (5.31) is valid over at most a full circuit through the fast field, we have to approximate the orbit $\Gamma_{\pm N}(x)$ for $N\geq 3$ separately over each of its several circuits/loops. The orbit $\Gamma_{\pm 2k}(x)$ makes k circuits through the fast field between $\Gamma_{\pm 2k}(0)\in\mathcal{I}^{+N}\cap\mathcal{I}^{-N}$ and at its touch down on $\mathcal{M}$. Therefore, we split $\Gamma_{\pm 2k}(x)$ into k parts: $\Gamma_{\pm 2k}^j(x)$, $j=1,2,...,k$. For each $\Gamma_{\pm 2k}^j(x)$, we translate the point $x=0$ to the intersection of $\Gamma_{\pm 2k}^j(x)$ with $\mathcal{I}^{+N+2j-1}\cap\mathcal{I}^{-N+2j-1}=\mathcal{P}^{2j-1}(\mathcal{I}^{+N}\cap\mathcal{I}^{-N})$, $j=1,2,...,k$, so that we can use expansion (5.31). Also, we recall that $\mathcal{I}^{n,-m}$ is only $\mathcal{O}(\delta)$-close to $3/2y_0$ for n,m odd by (5.18). Hence, it follows from (5.22) that the approximation $(y_1^j)'(x)$ given by (5.32) has a (translated) initial condition $(y_1^j)'(0)=3(2j-1)/y_0$. We define $X_\pm^j=\mathcal{O}(|\log\delta|)$, $X_-^j<0<X_+^j$, as the values of x for which $\Gamma_{\pm 2k}^j(x)$ has its (first) intersections with $\{q=0\}$, $\mathcal{O}(\sqrt{\delta})$ near $\mathcal{M}$ (with $X_+^k=\infty$), *i.e.*, $\Gamma_{\pm 2k}^j(X_\pm^j)\in\mathcal{I}^{+N+2j-1\pm 1}\cap\mathcal{I}^{-N+2j-1\pm 1}$ $(j<k)$. Hence, up to terms of $\mathcal{O}(\delta^{2+\rho})$,

$$
\begin{aligned}
\mathcal{H}|_{\mathcal{I}^{+2k}\cap\mathcal{I}^{-2k}} &= -\frac{1}{3}\delta^2\sum_{j=1}^{k}\int_{X_-^j}^{X_+^j}(y_1^j)'(x)Z_h^3(x;y_0)dx\\
&= -\frac{1}{3}\delta^2\left(\frac{3}{2y_0}\right)^4\sum_{j=1}^{k}\int_{-\infty}^{\infty}\left[(3\tanh\frac{1}{2}x-\tanh^3\frac{1}{2}x)+2(2j-1)\right]\operatorname{sech}^6\left(\frac{1}{2}x\right)dx\\
&= -\frac{2}{3}\delta^2\left(\frac{3}{2y_0}\right)^4\sum_{j=1}^{k}(2j-1)\int_{-\infty}^{\infty}\operatorname{sech}^6\left(\frac{1}{2}x\right)dx\\
&= -\frac{\delta^2}{y_0^4}\left(\frac{3}{2}\right)^3\frac{32}{15}\sum_{j=1}^{k}(2j-1)\\
&= -\frac{\delta^2}{y_0^4}\left(\frac{3}{2}\right)^3\frac{32}{15}k^2.
\end{aligned}
$$

Equating this expression with (5.29) yields (5.27) for $N = 2k$. The result for $N = 2k-1$ is obtained by a similar decomposition of $\Gamma_{\pm(2k-1)}(x)$, and we note that $\tilde{\alpha}(N)$ may be taken to be $1/\tilde{\delta}_0(N)$. This completes the proofs of this lemma and of the validity of (1.7) and (1.8). □

Remark 5.3 This lemma implies that the first order corrections are of higher order than can be expected from (5.18) and (5.19). However, the result (5.14) can be applied, because the p-coordinate of an orbit with initial conditions in $\mathcal{I}^{+N} \cap \mathcal{I}^{-N}$ is $\mathcal{O}(\delta)$, so that the first-order corrections are indeed of higher order than expected.

6 Continuation of the invariant manifolds

In this section, we study the invariant manifolds of the original system (1.12) for general values of α and β. All four components of the vector field (1.12) are of the same size, *a priori*. Nevertheless, we can derive sufficient information about the existence and geometry of the invariant manifolds to continue the intersection manifolds $\mathcal{I}^{+N} \cap \mathcal{I}^{-N}$ obtained in the preceding section for $\alpha \gg \tilde{\alpha}(N)$ and $\beta \ll 1$ to the regime here in which $\alpha, \beta > 0$. Hence, we may continue the curves $\mathcal{C}_N^\infty$ of N-pulse homoclinic orbits, as well.

6.1 The invariant manifolds $\mathcal{M}$, $W^u_{\rm loc}(\mathcal{M})$, and $W^s_{\rm loc}(\mathcal{M})$

The manifold

$$\mathcal{M} \equiv \{(u,p,v,q) | v = 0, q = 0\} \tag{6.1}$$

is invariant under the flow ϕ_x of the original system (1.12). The restricted vector field on $\mathcal{M}$ is

$$u' = p, \qquad p' = 0. \tag{6.2}$$

In addition, $\mathcal{M}$ is normally hyperbolic, with Lyapunov type numbers $\nu^s = e^{-1}$, $\lambda^u = e^{-1}$, and $\sigma^s(m) = 0$ for all $m \in \mathcal{M}$ (where the general definitions of these type numbers are given in Chapter V of [15]). Hence, by the unstable manifold theory presented there, $\mathcal{M}$ has local stable and unstable manifolds, denoted again by $W^s_{\rm loc}(\mathcal{M})$ and $W^u_{\rm loc}(\mathcal{M})$, respectively. The manifolds $W^s_{\rm loc}(\mathcal{M})$ and $W^u_{\rm loc}(\mathcal{M})$ are three-dimensional and consist of all of the initial conditions near $\mathcal{M}$ such that solutions through them approach $\mathcal{M}$ exponentially in forward and backward time, respectively. More finely, let ϕ_x^* denote the restriction of the flow map to points on $\mathcal{M}$. Then, we have

$$W^s_{\rm loc}(\mathcal{M}) = \bigcup_{(u,p,0,0)\in\mathcal{M}} \mathcal{F}^s_{(u,p)}, \qquad W^u_{\rm loc}(\mathcal{M}) = \bigcup_{(u,p,0,0)\in\mathcal{M}} \mathcal{F}^u_{(u,p)}, \tag{6.3}$$

where $\mathcal{F}^s_{(u,p)}$ is the stable fiber with base point $(u,p,0,0) \in \mathcal{M}$ consisting of initial conditions that are (exponentially) forward asymptotic to $\phi_x^*(u,p,0,0)$ as $x \to \infty$ and $\mathcal{F}^u_{(u,p)}$ is the unstable fiber with base point $(u,p,0,0) \in \mathcal{M}$ consisting of initial conditions that are asymptotic to $\phi_x^*(u,p,0,0)$ as $x \to -\infty$. These fibers are invariant as a family. For example,

$$\phi_x \mathcal{F}^s_{(u,p)} = \mathcal{F}^s_{\phi_x^*(u,p)}. \tag{6.4}$$

Remark 6.1 The invariant manifold $\mathcal{M}$ given by (6.1) is not compact, and the u components of the orbits of interest on $\mathcal{M}$ grow without bound in the limits $x \to \pm\infty$. Moreover, no compact subset of $\mathcal{M}$ is overflowing invariant. Hence, in order to apply invariant manifold theory, which is developed for compact manifolds and which requires the manifold to be overflowing invariant if it has a boundary, we take the standard preparatory steps. One needs to work with sufficiently large compact sets of $\mathcal{M}$ that contain the portions relevant to the homoclinic orbits under consideration. Also, one needs to employ C^∞ bump functions at the boundaries of these compact sets to make the reduced vector field (6.2) point outward along these boundaries. Moreover, the notion of solutions approaching a compact set on $\mathcal{M}$ exponentially in time only makes sense as long as the orbits of the basepoints stay in that same compact set. (Alternatively, one may analyze a version of the original vector field (1.12) in which the u variable has been compactified.)

Remark 6.2 Any initial condition $Q = (u(t_0), p(t_0), v(t_0), q(t_0))$ on $W^s_{\rm loc}$, with $|v(t_0)|$ and $|q(t_0)|$ small but nonzero, must lie on a fiber $\mathcal{F}^s_{b_0}$ for some base point $b_0 = (u_0, p_0, 0, 0)$. Also, the image of any such base point satisfies $\pi_p \phi^*_x(u_0, p_0) = p_0$ for all x due to the simple flow on $\mathcal{M}$. Therefore,

$$u(t) \to \infty \qquad \text{and} \qquad p(t) \to p_0, \tag{6.5}$$

which are conditions homoclinic orbits must satisfy.

6.2 Continuation of the manifolds $\mathcal{I}^{+N} \cap \mathcal{I}^{-N}$ and of the curves $\mathcal{C}^\infty_N$

In proving (1.7) and (1.8) in Section 5, we showed that for each $N \geq 1$ there exists an $\tilde{\alpha}(N)$ sufficiently large such for each $\alpha > \tilde{\alpha}$, there is a unique symmetric N-pulse homoclinic orbit. The good initial conditions lie on the curves $\mathcal{C}^\infty_N$, and the asymptotics of their locations were determined up to sufficiently high order for $\alpha > \tilde{\alpha}(N)$. In this section, we continue the curves $\mathcal{C}^\infty_N$ into the regime where α is not large.

The main result of this section, see Theorem 6.1 below, states that if it is known that there is a symmetric N-pulse homoclinic orbit through a given initial condition $(\alpha_0, 0, \beta_0, 0)$ for which (α_0, β_0) is on $\mathcal{C}^\infty_N$, then there exists a segment of a smooth 1-D path in the (α, β)-plane such that solutions through the initial conditions on this segment are also symmetric N-pulse homoclinic orbits and such that this segment contains the given (α_0, β_0) pair. Specifically, the theorem states that there exists an $s > 0$ such that the curve $\mathcal{C}^\infty_N$ can be extended to a point that is a Euclidean distance of s away from (α_0, β_0), and that this is a balanced extension, which is locally flat to first order in s. It is reminiscent of continuation results obtained from the Implicit Function Theorem.

Theorem 6.1 *Fix an arbitrary $N \geq 1$ and consider the curve $\mathcal{C}^\infty_N$ that exists for $\alpha > \tilde{\alpha}(N)$. Assume that $\mathcal{C}^\infty_N$ has been extended to $(\alpha_0, \beta_0) \in \mathcal{C}^\infty_N$, i.e., assume that there is a smooth parametrization $(\alpha(\sigma), \beta(\sigma))$ of $\mathcal{C}^\infty_N$ for $\sigma \geq \sigma_0$ with $(\alpha(\sigma_0), \beta(\sigma_0)) = (\alpha_0, \beta_0)$ and $\alpha(\sigma) \to \infty$ as $\sigma \to \infty$. Then, there exist $\sigma_1, \tilde{\sigma}_1 > 0$ such that the parametrization $(\alpha(\sigma), \beta(\sigma))$ of $\mathcal{C}^\infty_N$ can be extended smoothly to $\sigma \in [\sigma_0 - \sigma_1, \infty)$ with $\|(\alpha(\sigma_0 - \sigma_1), \beta(\sigma_0 -$*

$\sigma_1)) - (\alpha_0, \beta_0)\| = s$, *and such that there is a point* $(\alpha(\sigma_0 + \tilde{\sigma}_1), \beta(\sigma_0 + \tilde{\sigma}_1))$ *on the known segment of* $\mathcal{C}_N^\infty$ *with* $\|(\alpha(\sigma_0 + \tilde{\sigma}_1), \beta(\sigma_0 + \tilde{\sigma}_1)) - (\alpha_0, \beta_0)\| = s$ *and* $\|(\alpha(\sigma_0 - \sigma_1), \beta(\sigma_0 - \sigma_1)) - (\alpha(\sigma_0 + \tilde{\sigma}_1), \beta(\sigma_0 + \tilde{\sigma}_1))\| \approx 2s$.

Remark 6.3 Here, the extension may be said to be balanced because the new point $(\alpha(\sigma_0 - \sigma_1), \beta(\sigma_0 - \sigma_1))$ is at the same Euclidean distance from $(\alpha(\sigma_0), \beta(\sigma_0))$ as is the point $(\alpha(\sigma_0 + \tilde{\sigma}_1), \beta(\sigma_0 + \tilde{\sigma}_1))$, which is on that part of the curve $\mathcal{C}_N^\infty$ whose existence was already known, and because all three points are almost collinear.

Remark 6.4 We trust that the parametrization variable σ here will not be confused with the $\sigma \equiv 1/\beta$ used in Section 3.

The proof of Theorem 6.1 will depend strongly on the normally hyperbolic character of the invariant manifold $\mathcal{M}$ and on the corresponding structure of the flow near $\mathcal{M}$. First, we introduce some notation and establish a proposition about tubes of solutions that contain a solution through an initial condition of the type $(\alpha_0, 0, \beta_0, 0)$. Let $r > 0$ be small enough and consider the 3-dimensional ball $B_0^3(r) \subset \{q = 0\}$ of radius r centered at $(\alpha_0, 0, \beta_0, 0)$. Solutions $\Gamma(x; (u_0, p_0, v_0, 0))$ of (1.12) through initial conditions $(u_0, p_0, v_0, 0) \in B_0^3(r)$ constitute an open, 4-dimensional set $\mathcal{T}_+$, which is topologically a tube; *i.e.*,

$$\mathcal{T}_+ = \{(u, p, v, q) : \exists\, x > 0 \text{ and } (u_0, p_0, v_0, 0) \in B_0^3(r); (u, p, v, q) = \Gamma(x; (u_0, p_0, v_0, 0))\}. \tag{6.6}$$

Proposition 6.1 *Define* $\Gamma_0(x)$ *by* $\Gamma_0(x) = \Gamma(x; (\alpha_0, 0, \beta_0, 0))$ *with* $\Gamma_0(0) = (\alpha_0, 0, \beta_0, 0)$ *and let* $\Gamma_0(x)$ *be in* $\mathcal{T}_+$. *There exists an* $\tilde{r} > 0$ *such that for each* $x_1 > 0$ *the* 4*-dimensional ball* $B_1^4(\tilde{r})$ *of radius* $\tilde{r}$ *centered at* $\Gamma_0(x_1)$ *lies inside* $\mathcal{T}_+$.

Proof of Proposition 6.1 Fix an $\tilde{r} > 0$ small. For each $x < 0$, consider the set of initial conditions inside the 4-dimensional ball $B_1^4(\tilde{r})$ centered at $\Gamma_0(x)$. Now, flow each initial condition in each of these balls forward for all x, and label the union of all of these forward solutions by $\mathcal{T}_-^1$. Clearly, $\mathcal{T}_-^1$ is a 4-dimensional tube, an open set, and forward invariant under the flow of the differential equation. In particular, $\Gamma_0(x + x_1) \in \mathcal{T}_-^1$ for any $x_1 > 0$, and this solution intersects the hyperplane $\{q = 0\}$ at $x = -x_1$ at the point $(\alpha_0, 0, \beta_0, 0)$, by definition. Moreover, this intersection is transverse if $\alpha_0\beta_0 \neq 1$, because then $q'|_{x=-x_1} \neq 0$, recall (1.12); whereas, if $\alpha_0\beta_0 = 1$, then this intersection is still topologically transverse, because then $q''|_{x=-x_1} = 0$ but $q'''|_{x=-x_1} \neq 0$ by Lemma 2.4. Therefore, in both cases ($\alpha_0\beta_0 \neq 1, = 1$), the orbits through all of the initial conditions in $B_1^4(\tilde{r})$ must also intersect $\{q = 0\}$, as long as $\tilde{r}$ is small enough. In addition, the distance between the intersection of such an orbit with $\{q = 0\}$ and the point $(\alpha_0, 0, \beta_0, 0)$ can be made arbitrarily small, by continuous dependence on initial conditions. Of course, there can be additional intersections of $\mathcal{T}_-^1$ with $\{q = 0\}$. However, for the intersection nearest $(\alpha_0, 0, \beta_0, 0)$, $\mathcal{T}_-^1 \cap \{q = 0\} \subset B_0^3(r)$, for the value of r fixed in Theorem 6.1, as long as $\tilde{r}$ is taken to be small enough. This proves the proposition. □

Remark 6.5 Theorem 6.1 above concerns symmetric N-pulse homoclinic orbits that have nondegenerate local extrema, due to the definition of these orbits given in the Introduction. Hence, in the proof below it is the case that $\alpha_0\beta_0 \neq 1$. The other case,

$\alpha_0\beta_0 = 1$, which corresponds to orbits with degenerate extrema, will be treated separately in Corollary 6.1 below.

Remark 6.6 The statement of the proposition might be false if the intersection of $\Gamma_0(x + x_1)$ with $\{q = 0\}$ is not at least topologically transverse.

Proof of Theorem 6.1 Fix an arbitrary $N \geq 1$. Let $\Gamma_0(x) = \Gamma(x; (\alpha_0, 0, \beta_0, 0))$ denote the symmetric N-pulse homoclinic orbit through $(\alpha_0, 0, \beta_0, 0)$.

There is a well-defined, closed neighborhood $\Sigma_{\mathcal{M}}$ of $\mathcal{M}$ in which the flow generated by (1.12) can be transformed smoothly into Fenichel normal form,

$$\begin{aligned} \dot{a} &= \Lambda_u(a, b, c_1, c_2)a, \\ \dot{b} &= -\Lambda_s(a, b, c_1, c_2)b, \\ \dot{c}_1 &= f_1(a, b, c_1, c_2)ab + g_1(c_1, c_2), \\ \dot{c}_2 &= f_2(a, b, c_1, c_2)ab + g_2(c_1, c_2), \end{aligned} \tag{6.7}$$

where $\Lambda_{u,s}(a, b, c_1, c_2)$ are C^∞, $\Lambda_{u,s}(0, 0, c_1, c_2) = 1$, and $\Lambda_{u,s}(a, b, c_1, c_2) > 0$, for all $(a, b, c_1, c_2) \in \Sigma_{\mathcal{M}}$, [15, 16] and [23]. Note that one may also use the results presented in [21]. These transformed coordinates are chosen so that the invariant manifold $\mathcal{M}$ is given by $\{a = b = 0\}$, and so that $W^s(\mathcal{M}) = \{a = 0\}$ and $W^u(\mathcal{M}) = \{b = 0\}$. The neighborhood $\Sigma_{\mathcal{M}}$ can be represented by $\Sigma_{\mathcal{M}} = \{-\Sigma \leq a, b \leq \Sigma\}$ for some $\Sigma > 0$, and we will use $\tilde{\mathcal{T}}_+$ to denote the transformation of the tube $\mathcal{T}_+$ given by (6.6) in Fenichel coordinates.

The forward orbit $\Gamma_0(x)$, which lies in $W^s(\mathcal{M})$ for $x > 0$, can be represented in $\Sigma_{\mathcal{M}}$ by $\tilde{\Gamma}_0(\xi) = (0, b_0(\xi), c_{1,0}(\xi), c_{2,0}(\xi))$, where we note that sometimes a rescaling of the independent variable is needed [15, 16], so that here ξ is a rescaling of x (and we trust there will be no confusion with the different variable ξ used in earlier sections). This orbit $\tilde{\Gamma}_0(\xi)$ enters $\Sigma_{\mathcal{M}}$ through the hyperplane $\{b = \Sigma\}$.

Now, by Proposition 6.1, the intersection $\tilde{\mathcal{T}}_+ \cap \{b = \Sigma\}$ defines an open 3-dimensional neighborhood, $\tilde{\mathcal{U}}^3_+$, of $\tilde{\Gamma}_0(\xi) \cap \{b = \Sigma\}$ in the $\{b = \Sigma\}$ hyperplane. Then, the intersection $\tilde{\mathcal{U}}^3_+ \cap \{a = 0\}$ is non-empty, because $\tilde{\Gamma}_0(\xi) \subset \{a = 0\}$, and we can define the following set

$$\tilde{\mathcal{S}}^2_+ = \tilde{\mathcal{U}}^3_+ \cap W^s(\mathcal{M}) = \tilde{\mathcal{T}}_+ \cap \{b = \Sigma\} \cap \{a = 0\} \neq \emptyset. \tag{6.8}$$

The set $\tilde{\mathcal{S}}^2_+$ is 2-dimensional, and it is open as subset of $\{a = 0, b = \Sigma\}$. The forward orbits of initial conditions in it generate a sub-tube, $\tilde{\mathcal{T}}^s_+$, of $\tilde{\mathcal{T}}_+$ consisting of solutions $\tilde{\Gamma}(\xi)$ of (6.7) that are forward asymptotic to $\mathcal{M}$. This implies that, back in the original coordinate space, there is an open 3-dimensional sub-tube $\mathcal{T}^s_+$ of $\mathcal{T}_+$ that consists of orbits $\Gamma(x; (u_0, p_0, v_0, 0)) \in W^s(\mathcal{M})$. Clearly, $\Gamma_0(x) \in \mathcal{T}^s_+$. The intersection $\mathcal{T}^s_+ \cap \{q = 0\}$ defines the 2-dimensional subset $\mathcal{S}^2_+ \subset B^3_0(r)$ of initial conditions of solutions of (1.12) in $W^s(\mathcal{M})$. See Figure 5 for a schematic illustration. Of course, $\mathcal{T}^s_+$ may intersect $\{q = 0\}$ several times; and, here, we focus on the intersection centered at $(\alpha_0, 0, \beta_0, 0)$. (Also, we remark that whereas the tilde always denotes the set transformed into the Fenichel coordinates, there is one exception. Namely, $\mathcal{S}^2_+$ and $\tilde{\mathcal{S}}^2_+$ are not the same set under the transformation to Fenichel coordinates.)

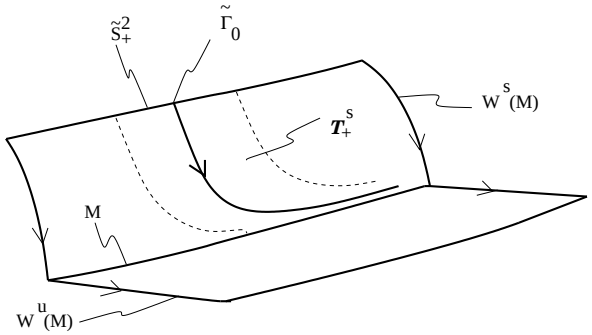

Figure 5: A schematic illustration of a portion of the normally hyperbolic invariant manifold $\mathcal{M}$, portions of its local stable and unstable manifolds, the orbit Γ_0, the set $\mathcal{S}^2_+$, and the tube τ^S_+. Note that the dimension of each set in the figure is one less than it is in reality in this projective drawing.

Now, let $\tilde{s} > 0$ be small enough and consider the 2-dimensional ball $\tilde{B}^2_+(\tilde{s}) \subset \tilde{\mathcal{S}}^2_+$ of radius $\tilde{s}$, centered at $\tilde{\Gamma}_0(\xi) \cap \{b = \Sigma\}$. The image of $\tilde{B}^2_+(\tilde{s})$ under the transformation from the Fenichel coordinates back into the original coordinates of (1.12) is a transformed ball, which we denote by $F^{-1}(\tilde{B}^2_+(\tilde{s}))$. This transformed ball, $F^{-1}(\tilde{B}^2_+(\tilde{s}))$, is a smooth 2-dimensional manifold that is flat to leading order, *i.e.,* it is linear in $\tilde{s}$ to leading order, because the Fenichel transformation is smooth and because $\tilde{s}$ is small enough. Next, let F^{-2}_+ denote the 2-dimensional subset of $\mathcal{S}^2_+ \subset \{q = 0\}$ of initial conditions of orbits that pass through $F^{-1}(\tilde{B}^2_+(\tilde{s}))$. This subset is also smooth and linear in $\tilde{s}$ to leading order, because the time-of-flight along $\Gamma_0(x)$ from $(\alpha_0, 0, \beta_0, 0)$ to $\Sigma_{\mathcal{M}}$ is bounded. We can now choose an $s > 0$ and a closed 3-dimensional ball $\overline{B^3_0(s)}$ of radius s, centered at $(\alpha_0, 0, \beta_0, 0)$ such that $\overline{B^3_0(s)} \cap \mathcal{S}^2_+ \subset F^{-2}_+$. This 2-dimensional set can be represented by

$$\overline{B^3_0(s)} \cap \mathcal{S}^2_+ = \{(u_s(s_1, s_2), p_s(s_1, s_2), v_s(s_1, s_2), 0) \text{ with } s_1^2 + s_2^2 \leq s^2\}, \tag{6.9}$$

where

$$\begin{aligned} u_s(s_1, s_2) &= \alpha_0 + c^u_1 s_1 + c^u_2 s_2 + \mathcal{O}(s^2), \\ p_s(s_1, s_2) &= \quad\; c^p_1 s_1 + c^p_2 s_2 + \mathcal{O}(s^2), \\ v_s(s_1, s_2) &= \beta_0 + c^v_1 s_1 + c^v_2 s_2 + \mathcal{O}(s^2); \end{aligned} \tag{6.10}$$

and $c^{u,p,v}_{1,2}$ are constants. Note that $(u_s(0,0), p_s(0,0), v_s(0,0), 0) = (\alpha_0, 0, \beta_0, 0)$ by construction.

Exactly the same construction can be made in backwards 'time', *i.e.,* for $x < 0$. This leads to a subset $\mathcal{S}^2_-$ of $B^3_0(r)$ of initial conditions of orbits that lie in $W^u(\mathcal{M})$, *i.e.,* of solutions of (1.12) that are backward asymptotic to $\mathcal{M}$. It follows by the reversibility symmetry of (1.12) that

$$\overline{B^3_0(s)} \cap \mathcal{S}^2_- = \{(u_s(s_1, s_2), -p_s(s_1, s_2), v_s(s_1, s_2), 0) \text{ with } s_1^2 + s_2^2 \leq s^2\}, \tag{6.11}$$

with u_s, p_s, v_s as in (6.10). Solutions of (1.12) with initial conditions in $\mathcal{S}^2_+ \cap \mathcal{S}^2_-$ are homoclinic to $\mathcal{M}$. Most significantly, within the ball $\overline{B^3_0(s)}$, the intersection $\mathcal{S}^2_+ \cap \mathcal{S}^2_-$ is

explicitly given by

$$p_s(s_1, s_2) = c_1^p s_1 + c_2^p s_2 + \mathcal{O}(s^2) = 0. \tag{6.12}$$

We now show that the coefficients c_1^p and c_2^p are non-zero, so that (6.12) defines a linear relation between s_1 and s_2 to leading order, which, in turn, can be substituted into the components u_s and v_s to obtain the desired balanced extension of the curve $\mathcal{C}_N^\infty$.

The orbit $\Gamma_0(x)$ intersects the hyperplane $\{q = 0\}$ $2N - 1$ times, because $(\alpha_0, \beta_0) \in \mathcal{C}_N^\infty$. These intersections correspond to N non-degenerate maxima and $N - 1$ non-degenerate minima of the v-component of $\Gamma_0(x)$ by the definition of $\mathcal{C}_N^\infty$. Hence, all intersections of $\Gamma_0(x)$ with $\{q = 0\}$ are transverse, and thus, by choosing s small enough, all intersections with $\{q = 0\}$ of orbits homoclinic to $\mathcal{M}$ that have initial conditions that are determined by (6.12), (6.10) and (6.9)/(6.11), are also transverse. As a consequence, the local curve

$$\{(\alpha(s_1, s_2), \beta(s_1, s_2)) = (u_s(s_1, s_2), v_s(s_1, s_2)) \text{ with } s_1^2 + s_2^2 \leq s^2 \text{ such that } p_s(s_1, s_2) = 0\} \tag{6.13}$$

must be part of $\mathcal{C}_N^\infty$. The smooth parametrization assumption, which guarantees that there is a smooth parametrization of the set of solutions of (6.12) that is given by $(\alpha(\sigma), \beta(\sigma))$ for $\sigma \in [\sigma_0, \sigma_0 + \tilde{\sigma}_1]$, therefore also implies that this parametrization is linear to leading order with $(\alpha(\sigma_0), \beta(\sigma_0)) = (\alpha_0, \beta_0)$ and $(\alpha(\sigma_0 + \tilde{\sigma}_1), 0, \beta(\sigma_0 + \tilde{\sigma}_1)) \in \partial B_0^3(s)$. Hence, $(c_1^p, c_2^p) \neq (0, 0)$; and, in turn, we see directly that (6.12) defines – to leading order – a linear relation between s_1 and s_2. Thus, the local parametrization $(\alpha(\sigma), \beta(\sigma))$ can be extended to all $\sigma \in [\sigma_0 - \sigma_1, \sigma_0 + \tilde{\sigma}_1]$ for some $\sigma_1 > 0$ so that also $(\alpha(\sigma_0 - \sigma_1), 0, \beta(\sigma_0 - \sigma_1)) \in \partial B_0^3(s)$ with $\|(\alpha(\sigma_0 - \sigma_1), 0, \beta(\sigma_0 - \sigma_1)) - (\alpha(\sigma_0 + \tilde{\sigma}_1), 0, \beta(\sigma_0 + \tilde{\sigma}_1))\| = 2s$, to leading order. □

The second result, see Corollary 6.1 below, concerns possible accumulation points of initial conditions for which symmetric N-pulse homoclinic orbits are known to exist. These accumulation points may lie on the curve $\mathcal{K}_1$ or *a priori* also anywhere inside the regions $\mathcal{A}_{\text{odd}}$ or $\mathcal{A}_{\text{even}}$, and for now our treatment of accumulation points is general. Specifically, we show that the initial condition corresponding to such an accumulation point also gives rise to a homoclinic orbit, although it need not be a homoclinic orbit of exactly the same type, because it may have degenerate maxima/minima. We also show that, by an argument similar to that used above in proving Theorem 6.1, homoclinic orbits even exist past such accumulation points. This situation arises for example at the point on $\mathcal{K}_1$ where the curves $\mathcal{C}_1^\infty$ and $\mathcal{C}_2^\infty$ meet, as we will see in Section 7.

Remark 6.7 It is also possible, *a priori*, that more than two curves $\mathcal{C}_N$ meet at such an accumulation point. However, the arguments of Section 7 can be used to show that this cannot occur.

Corollary 6.1 *Fix an arbitrary $N \geq 1$. Let (α_j, β_j) lie on $\mathcal{C}_N$ for $j = 1, 2, 3, \ldots$ and assume that $\lim_{j\to\infty}(\alpha_j, \beta_j) = (\alpha^*, \beta^*)$ exists. Let $\Gamma^*(x) = \Gamma(x; (\alpha^*, 0, \beta^*, 0))$ be the solution of (1.12) that is determined by (α^*, β^*). Then, $\Gamma^*(x) \in W^u(\mathcal{M}) \cap W^s(\mathcal{M})$, i.e., $\Gamma^*(x)$ is homoclinic to $\mathcal{M}$. Furthermore, there are $s > 0$, $\sigma_1, \tilde{\sigma}_1 > 0$, and at least one curve $(\alpha(\sigma), \beta(\sigma))$ through (α^*, β^*), parameterized by $\sigma \in [-\sigma_1, \tilde{\sigma}_1]$, so that the solution*

$\Gamma_\sigma(x) = \Gamma(x;(\alpha(\sigma),0,\beta(\sigma),0))$ *is homoclinic to* $\mathcal{M}$ *for all* $\sigma \in [-\sigma_1,\tilde{\sigma}_1]$. *The curve* $(\alpha(\sigma),\beta(\sigma)) \in \mathcal{C}_N$ *for* $\sigma \in [-\sigma_1,0)$, *and* $(\alpha(0),\beta(0)) = (\alpha^*,\beta^*)$. *There is a sequence* $\{\tilde{\sigma}_j\}_{j=2}^{\infty} \subset [-\sigma_1,0)$ *such that* $(\tilde{\alpha}_j,\tilde{\beta}_j) = (\alpha(\tilde{\sigma}_j),\beta(\tilde{\sigma}_j))$ *is a subsequence of the* (α_j,β_j)*'s;* $\|(\alpha(-\sigma_1),\beta(-\sigma_1)) - (\alpha^*,\beta^*)\| = \|(\alpha(\tilde{\sigma}_1),\beta(\tilde{\sigma}_1)) - (\alpha^*,\beta^*)\| = s$. *The parametrization of* $(\alpha(\sigma),\beta(\sigma))$ *is smooth for* $\sigma \in [-\sigma_1,0)$ *and for* $\sigma \in (0,\tilde{\sigma}_1]$, *but not necessarily at* $\sigma \neq 0$*; the limits* $\lim_{\sigma\uparrow 0}(\alpha(\sigma),\beta(\sigma))$ *and* $\lim_{\sigma\downarrow 0}(\alpha(\sigma),\beta(\sigma))$ *exist, but are not necessarily equal.*

Proof Define the ball $B^3_*(r)$, centered around $(\alpha^*,0,\beta^*)$ and the tube $\mathcal{T}_+$ (6.6) around $\Gamma^*(x)$ as in the proof of Theorem 6.1. By the convergence of the sequence (α_j,β_j), there is a J such that $\Gamma_j(x) = \Gamma(x;(\alpha_j,0,\beta_j,0)) \subset \mathcal{T}_+$ for all $j \geq J$. The orbits $\Gamma_j(x)$ are all asymptotic to $\mathcal{M}$, thus, the tube $\mathcal{T}_+$ has to intersect the neighborhood $\Sigma_{\mathcal{M}}$ of $\mathcal{M}$ in which the flow can be given in Fenichel normal form (6.7). As a consequence, the transformed tube $\tilde{\mathcal{T}}_+$ and the transformed solutions $\tilde{\Gamma}(\xi)$ can be defined as in the proof of Theorem 6.1. Moreover, the 2-dimensional set $\tilde{S}^2_+$ (6.8) also exists and is non-empty.

The orbit $\Gamma^*(x)$ is asymptotic to $\mathcal{M}$ if it can be shown that the transformed orbit $\tilde{\Gamma}^*(\xi)$ intersects $\tilde{S}^2_+$, *i.e.,* that there is a certain value ξ^* of ξ such that $\tilde{\Gamma}^*(\xi^*) \in \tilde{S}^2_+$. Since the $\tilde{\Gamma}_j(\xi)$-orbits are homoclinic to $\mathcal{M}$ there exist ξ_j's such that $\tilde{\Gamma}_j(\xi_j) \in \tilde{S}^2_+$ (for $j \geq J$). By the continuous dependence of initial data and by the fact that the time-of-flight between $B^3_*(r)$ and $\Sigma_{\mathcal{M}}$ is bounded, it follows that $\xi_j \to \xi^*$ and $\tilde{\Gamma}_j(\xi_j) \to \tilde{\Gamma}^*(\xi^*) \in \overline{\tilde{S}^2_+}$ as $j \to \infty$ (recall that $\tilde{S}^2_+$ is open as subset of $\{a = 0, b = \Sigma\}$). Proposition 6.1 implies that $\tilde{\Gamma}^*(\xi^*) \in \tilde{S}^2_+$, so that $\Gamma^*(x) \in W^s(\mathcal{M}) \cap W^u(\mathcal{M})$ by the reversibility symmetry of (1.12).

As a consequence, the next steps in the proof of Theorem 6.1 can also be mimicked. The 'locally flat' 2-dimensional sets $\overline{B^3_*(s)} \cap \mathcal{S}^2_+$ and $\overline{B^3_*(s)} \cap \mathcal{S}^2_-$ can be defined as in (6.9) and (6.11). Moreover, the intersection $\mathcal{S}^2_+ \cap \mathcal{S}^2_-$ within the (closed) ball $\overline{B^3_*(s)}$ is also given by (6.12), so that the subset $\{(\alpha(s_1,s_2),\beta(s_1,s_2))\}$ of the (α,β)-plane given in (6.13) indeed defines initial conditions of orbits that are homoclinic to $\mathcal{M}$. However, here it cannot be concluded that $(c^p_1,c^p_2) \neq (0,0)$. In general, the expression $p_s(s_1,s_2)$ in (6.12) will, at leading order, be a homogeneous polynomial in s_1 and s_2 of degree $k \geq 1$. The expression $p_s(s_1,s_2) = 0$ must have (countably many) zeroes, because $(\alpha_j,\beta_j) \in (\mathcal{S}^2_+ \cap \mathcal{S}^2_-) \cap \overline{B^3_*(s)}$ for $j \geq J_s$ for some J_s (and $(\alpha^*,\beta^*) \in (\mathcal{S}^2_+ \cap \mathcal{S}^2_-) \cap \overline{B^3_*(s)}$). Hence, (6.11) may define up to $k \geq 1$ curves through the point $(s_1,s_2) = (0,0)$, so that there may be up to k parameterized curves $(\alpha_l(\sigma),\beta_l(\sigma))$, $l = 1,2,...$ through the point (α^*,β^*). By picking one of these curves, one may show that the statement of the corollary follows by the same type of arguments as used in the proof of Theorem 6.1. □

Remark 6.8 It *cannot* be concluded that the parametrization of $(\alpha(\sigma),\beta(\sigma))$ is generally smooth at $\sigma = 0$, *i.e.,* at (α^*,β^*). For instance, it cannot be excluded by the above arguments that the manifolds $\mathcal{S}^2_\pm$ have a fold structure and that (6.12) is given by $s_1^2 = s_2^3 + \mathcal{O}(s^4)$.

7 Homoclinic bifurcations

In this section, we prove Theorem 7.1, which for each N establishes the five results about Σ_N, the subset of the set Σ corresponding to N-pulse orbits. These results were labelled (1)–(5) in the Introduction. In brief, for each N, this Theorem establishes that there are finitely many components of Σ_N, that all of the curves $\mathcal{C}_{1,N} \equiv \mathcal{C}_N^\infty$ inside Σ_N are semi-infinite in length, that the components $\mathcal{C}_{k,N}$ with $k \geq 2$ have finite length, that the curves $\mathcal{C}_{k,N}$ remain locally flat at their endpoints, and that there are allowable and nonallowable bifurcations between different types of multi-pulse orbits.

Many of these results are established in a sequence of lemmas (see Lemmas 7.1–7.4 below), which in turn build on earlier results from Sections 2 – 6. Hence, this Theorem is the culmination and fruitful blending of the analytic and geometric methods employed in Sections 2 – 6.

7.1 Bifurcations along the curves $\mathcal{C}_N$

In this section, we introduce a definition of a bifurcation on a curve $\mathcal{C}_N$, a definition which agrees with the natural idea that the v-component of a bifurcating homoclinic orbit must have degenerate critical points, and we show that bifurcations must be nondegenerate, see Lemma 7.1 below.

A symmetric N-pulse homoclinic orbit $\Gamma_N(x;(\alpha,\beta)) = (u_N(x), p_N(x), v_N(x), q_N(x)) \subset W^u(\mathcal{M}) \cap W^s(\mathcal{M})$ intersects the hyper-plane $\{q = 0\}$ in $2N-1$ points, G_N^j, $j = -N+1, ..., N-1$; the v-components of the G_N^j's correspond to the maxima and minima of $v_N(x)$ as function of x. The homoclinic orbit $\Gamma_N(x;(\alpha,\beta))$ is assumed to be non-degenerate, which by definition means that all maxima and minima of $v_N(x)$ are non-degenerate, i.e. that $v_N(x)$ has non-vanishing second derivatives at its extremal points – see Remark 7.1. The center (or point of symmetry) of $\Gamma_N(x;(\alpha,\beta))$ is represented by $G_N^0 = (u_N(0), 0, v_N(0)) = (\alpha, 0, \beta)$. In general, the coordinates x_N^j are defined by $q_N(x_N^j) = 0$ so that

$$G_N^j = (u_N(x_N^j), p_N(x_N^j), v_N(x_N^j)),\ j = -N+1, ..., N-1. \tag{7.1}$$

Note that $x_N^j = -x_N^{-j}$ by the reversibility symmetry. By definition, $G_N^j \in \mathcal{I}^{+N+j} \cap \mathcal{I}^{-(N-j)}$, $j = -N+1, ..., N-1$. Here, $\mathcal{I}^n$, respectively $\mathcal{I}^{-m}$, are the 2-dimensional manifolds in (u,p,v)-space as defined in Section 5, i.e. the n-th intersection of $W^u(\mathcal{M})$ with $\{q=0\}$, resp. the m-th intersection of $W^s(\mathcal{M})$ with $\{q=0\}$. Note that $\mathcal{I}^{n,-m}$ are defined in a scaled context in Section 5 (5.1), here we consider the unscaled equivalents of $\mathcal{I}^{n,-m}$ (see also (5.26)). In fact,

$$\mathcal{I}^{+N+j} \cap \mathcal{I}^{-(N-j)} \equiv \cup_{\Gamma_N} G_N^j,\ j = -N+1, ..., N-1, \tag{7.2}$$

i.e. $\mathcal{I}^{+N+j} \cap \mathcal{I}^{-(N-j)}$ consists of the union over the (u,p,v)-coordinates of the j-th extremes of the v-components of all symmetric N-pulse homoclinic orbits $\Gamma_N(x)$ (again counting from the center of $\Gamma_N(x)$). The family of all symmetric homoclinic N-pulse

orbits can be identified as

$$\Sigma_N = \cup_{\Gamma_N} G_N^0 = \cup_{\Gamma_N} (u_N(0), v_N(0)), \tag{7.3}$$

see also (5.26). This family will consist – in general – of several branches, *i.e.*,

$$\Sigma_N = \bigcup_{k=1}^{K_N} \mathcal{C}_{k,N}. \tag{7.4}$$

It follows from Lemma 5.2 that $K_N \geq 1$ for every N, and we recall that $\mathcal{C}_{1,N} = \mathcal{C}_N^\infty$ was defined to be the unique branch that extends to $\alpha \to \infty$ for every N. The numerical simulations presented in Figure 1 show three distinct branches $\mathcal{C}_{k,7}$, *i.e.* $K_7 \geq 3$, while so far $K_1 = K_3 = 1$, $K_5 = 2$, $K_9 = 2$, and $K_{2n} = 1$, at least. We plan to carry out a more extensive search using AUTO with HomCont.

As the initial condition $(\alpha, 0, \beta, 0)$ varies, a non-degenerate, symmetric, N-pulse, homoclinic orbit $\Gamma_N(x)$ may bifurcate into a symmetric M-pulse orbit $\Gamma_M(x)$ $(N \neq M)$ when maxima and minima of $v_N(x)$ are created or annihilated. More precisely, we define a point (α^*, β^*) as a bifurcation point of the branch $\mathcal{C}_{k,N}$ if $(\alpha^*, \beta^*) \in \overline{\mathcal{C}}_{k,N}$ while $(\alpha^*, \beta^*) \notin \mathcal{C}_{k,N}$, so that $\Gamma_N(x; (\alpha^*, \beta^*))$, the orbit with initial conditions $(\alpha^*, 0, \beta^*, 0)$, is homoclinic to $\mathcal{M}$ – see Remark 7.1.

There are two kinds of generic bifurcations. At both flanks of the graph of $v_N(x; \alpha, \beta)$, a maximum may merge with a minimum (in a symmetric fashion), so that $(\alpha^*, \beta^*) \in \overline{\mathcal{C}}_N \cap \overline{\mathcal{C}}_{N+2}$ for some $N \geq 1$, but $(\alpha^*, \beta^*) \notin \mathcal{C}_N \cup \mathcal{C}_{N+2}$. At the bifurcation, $v_N(x; (\alpha^*, \beta^*))$ has two degenerate extrema, *i.e.* there is an $x^* > 0$ such that $v_N'(\pm x^*; (\alpha^*, \beta^*)) = v_N''(\pm x^*; (\alpha^*, \beta^*)) = 0$. The bifurcation may also occur at the center of the graph, which corresponds to $(\alpha^*, \beta^*) \in \overline{\mathcal{C}}_N \cap \overline{\mathcal{C}}_{N+1}$ for some odd $N \geq 1$ (Lemma 2.5). In this case, $v_N'(0; (\alpha^*, \beta^*)) = v_N''(0; (\alpha^*, \beta^*)) = v_N'''(0; (\alpha^*, \beta^*)) = 0$. A bifurcation is degenerate (by definition) if also either $v_N'''(\pm x^*; (\alpha^*, \beta^*)) = 0$ with $x^* > 0$ or $v_N^{(iv)}(0; (\alpha^*, \beta^*)) = 0$ at the bifurcation point.

Lemma 7.1 *The bifurcation associated to a bifurcation point (α^*, β^*) of a branch $\mathcal{C}_{k,N}$, $k, N \geq 1$, cannot be degenerate.*

Proof This is an immediate consequence of Lemma 2.4. □

Corollary 7.1 *Let (α^*, β^*) be a bifurcation point of a branch $\mathcal{C}_{k,N}$. The v-component of the homoclinic orbit $\Gamma_N(x; (\alpha^*, \beta^*))$ has a degenerate maximum in the point of symmetry $x = 0$ if $(\alpha^*, \beta^*) \in \mathcal{K}_1$. If $(\alpha^*, \beta^*) \notin \mathcal{K}_1$, then the v-component of $\Gamma_N(x; (\alpha^*, \beta^*))$ has degenerate extrema in two points $x = \pm x^*$, $x^* > 0$.*

Remark 7.1 The definitions of non-degenerate homoclinic curves Γ_N and their bifurcations are based on the character of the graphs of the v-components $v_N(x)$ of Γ_N as functions of x and on how these graphs change as the initial conditions (α, β) vary.

Therefore, the concepts of non-degeneracy and bifurcation of homoclinic curves we introduced here differ from the standard definitions in dynamical systems theory (see for instance [28]). In that more general setting, the bifurcations of Γ_N as a homoclinic orbit in the phase space are considered as functions of the problem parameters. There is in general no 'classical' homoclinic bifurcation associated to the transition from an N-pulse orbit Γ_N to an M-pulse orbit Γ_M that we are aware of.

7.2 The curves $\mathcal{C}_N^\infty$ and their bifurcation points in $\mathcal{A}_{\rm odd}$

In this section, we restrict the analysis to the curves $\mathcal{C}_N^\infty$ in $\mathcal{A}_{\rm odd}$ *i.e.*, N must be odd. The more general setting will be considered in Section 7.3. The asymptotic approach of Section 5 gives detailed information on the bifurcation curves $\mathcal{C}_N^\infty$ for α large enough. Therefore, we define the region

$$\tilde{\mathcal{A}}_{\rm odd} = \{(\alpha,\beta) \in \overline{\mathcal{A}}_{\rm odd} : \alpha \leq \tilde{\alpha}\} \tag{7.5}$$

where $\tilde{\alpha}$ is sufficiently large that the results of Section 5 apply for $\alpha \geq \tilde{\alpha}$. Note that by choosing $\tilde{\alpha}$, we also implicitly choose a bound on N, since N must be $\mathcal{O}(1)$ with respect to $1/\tilde{\alpha}$.

Now, it is known from Theorem 6.1 that the curves $\mathcal{C}_N^\infty$ are smooth. Therefore, we may introduce the arc-length parametrization of each $\mathcal{C}_N^\infty \subset \tilde{\mathcal{A}}_{\rm odd}$ by

$$\mathcal{C}_N^\infty = \{(\alpha_N^\infty(s),\beta_N^\infty(s)) : s \in [0,L)\}, \tag{7.6}$$

where $\alpha_N^\infty(0) = \tilde{\alpha}$ and L is the length of the curve $\mathcal{C}_N^\infty$ inside $\tilde{\mathcal{A}}_{\rm odd}$. Note that $L = \infty$ is *a priori* possible and that – in this case – the arc-length parametrization may only give a part of $\mathcal{C}_N^\infty \subset \tilde{\mathcal{A}}_{\rm odd}$. It follows from Section 3 that $(\alpha_N^\infty(s),\beta_N^\infty(s)) \in \tilde{\mathcal{A}}_{\rm odd}$ for all $s \in [0,L)$. We now establish

Lemma 7.2 *The limit* $\lim_{s\to L}(\alpha_N^\infty(s),\beta_N^\infty(s))$ *exists for* $L < \infty$ *and for* $L = \infty$, *and it is defined as*

$$\lim_{s\to L}(\alpha_N^\infty(s),\beta_N^\infty(s)) = (\alpha_N^*,\beta_N^*) \in \tilde{\mathcal{A}}_{\rm odd}. \tag{7.7}$$

Moreover, if $L < \infty$, *then* (α_N^*,β_N^*) *is the unique bifurcation point of* $\mathcal{C}_N^\infty$ *in* $\tilde{\mathcal{A}}_{\rm odd}$.

Note that it is not claimed in this lemma that (α_N^*,β_N^*) is a bifurcation point when $L = \infty$, because the possibility that $(\alpha_N^*,\beta_N^*) \in \mathcal{C}_N^\infty$ if $L = \infty$ is not excluded by the upcoming proof. However, we will show in Lemma 7.4 that $L < \infty$, so that it will indeed follow from Lemma 7.2 that (α_N^*,β_N^*) is the unique bifurcation point of $\mathcal{C}_N^\infty$ in $\tilde{\mathcal{A}}_{\rm odd}$ (see also Theorem 7.1).

Proof If $L < \infty$, then it follows from Corollary 6.1 that the limit (7.7) must exist and that the associated orbit $\Gamma_N(x;(\alpha_N^*,\beta_N^*))$ is homoclinic to $\mathcal{M}$. By construction, we have that $(\alpha_N^*,\beta_N^*) \in \overline{\mathcal{C}_N^\infty}$. Now, if it is assumed that $(\alpha_N^\infty(L),\beta_N^\infty(L)) \in \mathcal{C}_N^\infty$, *i.e.*, that this point lies inside the set, and not just in its closure, then it follows from the continuation

result of Theorem 6.1 that the length of $\mathcal{C}_N^\infty$ in $\tilde{\mathcal{A}}_{\text{odd}}$ is at least $L + s_1$ for a certain $s_1 > 0$, which contradicts the assumption that the length of $\mathcal{C}_N^\infty$ inside $\tilde{\mathcal{A}}_{\text{odd}}$ is L. Thus, (α_N^*, β_N^*) is indeed the (unique) bifurcation point of $\mathcal{C}_N^\infty$.

If $L = \infty$, then we choose a sequence $\{s_j\}_{j=1}^\infty$ such that $s_j \to \infty$ as $j \to \infty$. Herewith, we define the sequence $\{(\alpha_N^\infty(s_j), \beta_N^\infty(s_j))\}_{j=1}^\infty \subset \tilde{\mathcal{A}}_{\text{odd}}$. Since $\tilde{\mathcal{A}}_{\text{odd}}$ is compact, it follows that $\{(\alpha_N^\infty(s_j), \beta_N^\infty(s_j))\}_{j=1}^\infty$ must have an accumulation point $(\alpha_N^*, \beta_N^*) \in \overline{\mathcal{C}}_N^\infty \subset \tilde{\mathcal{A}}_{\text{odd}}$. Now, we assume that there are two such sequences, $\{s_{1,j}\}_{j=1}^\infty$ and $\{s_{2,j}\}_{j=1}^\infty$, that generate two distinct accumulation points, $(\alpha_{1,N}^*, \beta_{1,N}^*)$ and $(\alpha_{2,N}^*, \beta_{2,N}^*)$, respectively, and derive a contradiction.

It may be assumed without loss of generality that

$$s_{1,j} < s_{2,j} < s_{1,j+1} < s_{2,j+1} \quad \text{for all} \quad j \geq 1. \tag{7.8}$$

Let ℓ^* be the line segment that connects $(\alpha_{1,N}^*, \beta_{1,N}^*)$ to $(\alpha_{2,N}^*, \beta_{2,N}^*)$, *i.e.*,

$$\ell^* = \{(\alpha^*(\lambda), \beta^*(\lambda)) = \big((1-\lambda)\alpha_{1,N}^* + \lambda\alpha_{2,N}^*, (1-\lambda)\beta_{1,N}^* + \lambda\beta_{2,N}^*\big),\ \lambda \in [0,1]\}, \tag{7.9}$$

and let n_λ^* be the line normal to ℓ^* for each $\lambda \in [0,1]$ so that $n_\lambda^* \cap \ell^* = (\alpha^*(\lambda), \beta^*(\lambda))$, as in (7.9). Choose a $\lambda \in (0,1)$. It follows from the smoothness of the curve $\mathcal{C}_N^\infty$ (Theorem 6.1) and from the ordering (7.8) that, for $j \geq J_\lambda$ with some J_λ large enough, there exist $s_{\lambda,j}$ such that $s_{1,j} < s_{\lambda,j} < s_{2,j}$ and $(\alpha_N^\infty(s_{\lambda,j}), \beta_N^\infty(s_{\lambda,j})) \in \mathcal{C}_N^\infty \cap n_\lambda^*$. Now, the curve $\mathcal{C}_N^\infty$ cannot have any self-intersections (Theorem 6.1), and hence the (bounded) sequence $\{(\alpha_N^\infty(s_{\lambda,j}), \beta_N^\infty(s_{\lambda,j}))\}_{j=J_\lambda}^\infty$ must have a limit point on n_λ^*, *i.e.*,

$$\lim_{j\to\infty} (\alpha_N^\infty(s_{\lambda,j}), \beta_N^\infty(s_{\lambda,j})) = (\alpha_n^*(\lambda), \beta_n^*(\lambda)) \in n_\lambda^*.$$

The application of Corollary 6.1 to the sequence $\{(\alpha_N^\infty(s_{\lambda,j}), \beta_N^\infty(s_{\lambda,j}))\}_{j=J_\lambda}^\infty$ implies that there is a subsequence $\{\tilde{s}_{\lambda,j}\}_{j=1}^\infty$ of $\{s_{\lambda,j}\}_{j=1}^\infty$ and a smooth curve through $(\alpha_n^*(\lambda), \beta_n^*(\lambda))$ such that the points $(\alpha_N^\infty(\tilde{s}_{\lambda,j}), \beta_N^\infty(\tilde{s}_{\lambda,j}))$ lie in n_λ^*, which is part of $\mathcal{C}_N^\infty$.

The above argument holds for any $\lambda \in (0,1)$, since the choice of λ was arbitrary, which implies that $\mathcal{C}_N^\infty \supset U$, an open region in the (α, β)-plane. However, this contradicts Theorem 6.1 and Corollary 6.1, which established that $\mathcal{C}_N^\infty$ is a 1-dimensional curve. Therefore, the assumption that the two sequences have distinct accumulation points is incorrect, and the lemma is proven. □

Lemma 7.3 *The limit* $\lim_{s\to L}(\frac{d}{ds}\alpha_N^\infty(s), \frac{d}{ds}\beta_N^\infty(s))$ *exists, both for* $L < \infty$ *and for* $L = \infty$*).*

This lemma implies that $\mathcal{C}_N^\infty$ can locally – near its limit/bifurcation point (α_N^*, β_N^*) – be approximated by a linear expression, and thus that $\mathcal{C}_N^\infty$ cannot spiral toward (α_N^*, β_N^*).

Proof In this proof, we do not distinguish between the cases $L < \infty$ and $L = \infty$, *i.e.*, L may be either finite or infinite in the forthcoming arguments.

Consider two sequences $\{s_{1,j}\}_{j=1}^\infty$ and $\{s_{2,j}\}_{j=1}^\infty$ that are ordered as in (7.8), so that $s_{i,j} \to L$ as $j \to \infty$ $(i = 1, 2)$. Both associated sequences $(\alpha_N^\infty(s_{i,j}), \beta_N^\infty(s_{i,j}))$

of points on $\mathcal{C}_N^\infty$ (7.6) must limit on (α_N^*, β_N^*) by Lemma 7.2. Moreover, it follows from Corollary 6.1 that there is a local parametrization $(\alpha_{i,N}^\infty(\sigma_i), \beta_{i,N}^\infty(\sigma_i))$ of $\mathcal{C}_N^\infty$ with $(\alpha_{i,N}^\infty(0), \beta_{i,N}^\infty(0)) = (\alpha_N^*, \beta_N^*)$, that is smooth for $\sigma_i \in [-\sigma_{i,1}, 0)$ for some $\sigma_{i,1} > 0$, such that $(\alpha_N^\infty(\tilde{s}_{i,j}), \beta_N^\infty(\tilde{s}_{i,j})) \in \{(\alpha_{i,N}^\infty(\sigma_i), \beta_{i,N}^\infty(\sigma_i)); \sigma_i \in [-\sigma_{i,1}, 0)\}$ for a subsequence $\{\tilde{s}_{i,j}\}_{j=1}^\infty$ of $\{s_{i,j}\}_{j=1}^\infty$ $(i = 1, 2)$. Without loss of generality, we may identify $\{\tilde{s}_{i,j}\}_{j=1}^\infty$ with $\{s_{i,j}\}_{j=1}^\infty$ and assume that (7.8) still holds. Furthermore, Corollary 6.1 also implies that the limits

$$\lim_{\sigma_i \uparrow 0} \left(\frac{d}{ds}\alpha_{i,N}^\infty(\sigma_i), \frac{d}{ds}\beta_{i,N}^\infty(\sigma_i)\right) \stackrel{\text{def}}{=} (\alpha_{i,N}^{t,*}, \beta_{i,N}^{t,*}),\ i = 1, 2,$$

exist. The assumption that $(\alpha_{1,N}^{t,*}, \beta_{1,N}^{t,*}) \neq (\alpha_{2,N}^{t,*}, \beta_{2,N}^{t,*})$ yields a contradiction by arguments that are similar to those in the proof of Lemma 7.2, as we now show.

Let $\{h_\lambda^*\}_{\lambda \in (0,1)}$ be a 'fan' of half-lines parameterized by λ such that each half-line h_λ^* has (α_N^*, β_N^*) as endpoint, and that the fan has the half-lines spanned by $(\alpha_{1,N}^{t,*}, \beta_{1,N}^{t,*})$ and $(\alpha_{2,N}^{t,*}, \beta_{2,N}^{t,*})$ as boundaries (as $\lambda \downarrow 0$ or $\lambda \uparrow 1$), *i.e.*, $\{h_\lambda^*\}_{\lambda \in (0,1)}$ fills the wedge between the half-lines determined by the endpoint (α_N^*, β_N^*) and the vectors $(\alpha_{1,N}^{t,*}, \beta_{1,N}^{t,*})$ and $(\alpha_{2,N}^{t,*}, \beta_{2,N}^{t,*})$. Choose a $\lambda \in (0, 1)$. It follows from the smoothness of $\mathcal{C}_N^\infty$ and the ordering (7.8) that, for $j \geq J_\lambda$ with some J_λ large enough, there exist $s_{\lambda,j}$ such that $s_{1,j} < s_{\lambda,j} < s_{2,j}$ and $(\alpha_N^\infty(s_{\lambda,j}), \beta_N^\infty(s_{\lambda,j})) \in \mathcal{C}_N^\infty \cap h_\lambda^*$. The sequence $\{(\alpha_N^\infty(s_{\lambda,j}), \beta_N^\infty(s_{\lambda,j}))\}_{j=J_\lambda}^\infty$ must limit on $(\alpha^*(\lambda), \beta^*(\lambda))$, so that Corollary 6.1 implies that there is a curve through $(\alpha^*(\lambda), \beta^*(\lambda))$ and the points $(\alpha_N^\infty(\tilde{s}_{\lambda,j}), \beta_N^\infty(\tilde{s}_{\lambda,j})) \in h_\lambda^*$ that is part of $\mathcal{C}_N^\infty$ – here the $\tilde{s}_{\lambda,j}$'s form a subsequence of the original $s_{\lambda,j}$ sequence. By varying λ, we generate an open region U in the wedge spanned by the h_λ^*'s that must be $\subset \mathcal{C}_N^\infty$. This again is in contradiction with the fact that $\mathcal{C}_N^\infty$ is a 1-dimensional curve. □

Lemma 7.4 *The length L of $\mathcal{C}_N^\infty$ inside $\tilde{\mathcal{A}}_{\text{odd}}$ is finite.*

Proof Assume that $L = \infty$. Let $\delta > 0$, and define the ball B_δ^* as the ball with radius δ and center (α_N^*, β_N^*). Since $(\alpha_N^\infty(s), \beta_N^\infty(s)) \to (\alpha_N^*, \beta_N^*)$ as $s \to \infty$ (Lemma 7.2), there must be an $s_\delta < \infty$ such that

$$(\alpha_N^\infty(s), \beta_N^\infty(s)) \subset B_\delta^* \text{ for all } s > s_\delta.$$

Thus, for any $\delta > 0$, the length of $\mathcal{C}_N^\infty$ inside B_δ^* must be ∞. Moreover, by Lemma 7.3 there are two smooth curves, C^u and C^l, given by

$$C^{u,l} = \{(\alpha^{u,l}(\sigma), \beta^{u,l}(\sigma)) : \sigma \geq 0\},$$

with $(\alpha^{u,l}(0), \beta^{u,l}(0)) = (\alpha_N^*, \beta_N^*)$, $(\frac{d}{ds}\alpha^{u,l}(0), \frac{d}{ds}\beta^{u,l}(0)) = (\alpha_N^{t,*}, \beta_N^{t,*})$, and $C^u \cap C^l = (\alpha_N^*, \beta_N^*)$, such that for all $s > s_\delta$, $(\alpha_N^\infty(s), \beta_N^\infty(s)) \subset$ the cusped triangle with boundaries $C^u \cap B_\delta^*$, $C^l \cap B_\delta^*$, and the part of ∂B_δ^* between C^u and C^l. Since $\mathcal{C}_N^\infty$ must be of infinite length in this cusped triangle (that has a surface area $\ll \delta^3$), it must oscillate wildly.

We can now apply an argument based on Corollary 6.1 along the lines of the proofs of Lemmas 7.2 and 7.3 to show that this implies that $\mathcal{C}_N^\infty$ must contain an open subset U. □

7.3 The structure and bifurcation points of the branches $\mathcal{C}_{k,N}$

Lemmas 7.2, 7.3, and 7.4 do not depend on the characteristics of the curve $\mathcal{C}_N^\infty$, or on the fact that N is assumed to be odd in Section 7.2. The arguments in the proofs of these lemmas can be applied to any branch $\mathcal{C}_{k,N}$ (7.3), (7.4) of homoclinic N-pulse orbits for any k or N. It is essential for these proofs that the full $\mathcal{C}_{k,N}$ branch remains in a bounded part of the (α,β)-plane. Now, for $\mathcal{C}_{k,N}$ with $k \geq 2$ – recall that $\mathcal{C}_{1,N} = \mathcal{C}_N^\infty$ by definition – this is known via the analysis of Sections 3 and 4, and in particular Corollaries 3.1 and 4.1, and the fact that the only $\mathcal{C}_{k,N}$ branches that can persist as $\alpha \to \infty$ are the $\mathcal{C}_{1,N}$, recall Section 5. For $k = 1$, we have full control on $\mathcal{C}_N^\infty$ for α large enough (Section 5), and here we introduce the bounded subregions $\tilde{\mathcal{A}}_{\rm odd} \subset \mathcal{A}_{\rm odd}$ and $\tilde{\mathcal{A}}_{\rm even} \subset \mathcal{A}_{\rm even}$ as in Section 7.2, (7.5) and define

$$\tilde{\mathcal{A}} = \tilde{\mathcal{A}}_{\rm odd} \cup \tilde{\mathcal{A}}_{\rm even}. \tag{7.10}$$

We know from the asymptotic analysis of Section 5 that we may restrict our attention to $\tilde{\mathcal{A}}$ for the bifurcation analysis.

Theorem 7.1 *The family Σ_N of all symmetric N-pulse orbits consists of finitely many smooth branches $\mathcal{C}_{k,N}$, $k = 1, 2, ..., K_N < \infty$ that do not intersect, i.e., $\mathcal{C}_{k,N} \cap \mathcal{C}_{l,M} = \emptyset$ if $(k,N) \neq (l,M)$.*

- *For $k = 1$, the branch $\mathcal{C}_{1,N} = \mathcal{C}_N^\infty$ is unbounded. Inside $\tilde{\mathcal{A}}$, $\mathcal{C}_{1,N}$ has the arc-length parametrization,*

$$\mathcal{C}_{1,N} = \{(\alpha_{1,N}(s), \beta_{1,N}(s)) : \ s \in [0, \tilde{L}_{1,N})\},$$

where $\tilde{L}_{1,N}$ – the length of $\mathcal{C}_{1,N}$ in $\tilde{\mathcal{A}}$ – is finite. The limits

$$\lim_{s \to \tilde{L}_{1,N}} (\alpha_{1,N}(s), \beta_{1,N}(s)) = (\alpha_{1,N}^*, \beta_{1,N}^*), \quad \lim_{s \to \tilde{L}_{1,N}} (\frac{d}{ds}\alpha_{1,N}(s), \frac{d}{ds}\beta_{1,N}(s)) = (\alpha_{1,N}^{t,*}, \beta_{1,N}^{t,*}),$$

both exist. The endpoint $(\alpha_{1,N}^*, \beta_{1,N}^*)$ is the unique bifurcation point of $\mathcal{C}_{1,N}$.

- *For $k > 1$, the branch $\mathcal{C}_{k,N}$ is bounded and has the arc-length parametrization,*

$$\mathcal{C}_{k,N} = \{(\alpha_{k,N}(s), \beta_{k,N}(s)) : \ s \in (-\frac{1}{2}L_{k,N}, \frac{1}{2}L_{k,N})\},$$

and the length $L_{k,N}$ of $\mathcal{C}_{k,N}$ is finite. The limits

$$\lim_{s \to \pm\frac{1}{2}L_{k,N}} (\alpha_{k,N}(s), \beta_{k,N}(s)) = (\alpha_{k,N}^{\pm,*}, \beta_{k,N}^{\pm,*}), \lim_{s \to \pm\frac{1}{2}L_{k,N}} (\frac{d}{ds}\alpha_{k,N}(s), \frac{d}{ds}\beta_{k,N}(s)) = (\alpha_{k,N}^{\pm,t,*}, \beta_{k,N}^{\pm,t,*}),$$

all exist. The endpoints $(\alpha_{k,N}^{\pm,*}, \beta_{k,N}^{\pm,*})$ are the bifurcation points of $\mathcal{C}_{k,N}$.

Each branch $\mathcal{C}_{k,N}$ can be extended beyond each of its bifurcation points into another branch of symmetric homoclinic M-pulse orbits.

Proof All but two of the statements in this Theorem follow from arguments that are identical to those in the proofs of Lemmas 7.2, 7.3, 7.4, or directly from Corollary

6.1. The first statement whose proof needs a few additional words is that two distinct branches $\mathcal{C}_{k,N}$ and $\mathcal{C}_{l,M}$ cannot intersect when $k \neq l$, irrespective of whether $N = M$ or $N \neq M$; but, this statement must hold since otherwise there would be a contradiction with the definition of the curves (if $N \neq M$) or with Theorem 6.1 (if $N = M$). The second statement is that $K_N < \infty$, and we now prove it, hence completing the proof of this Theorem.

Assume that $K_N = \infty$, *i.e.,* that $\mathcal{C}_N$ consists of infinitely many (smooth, bounded) non-intersecting branches $\mathcal{C}_{k,N}$. Clearly, $\mathcal{C}_{k,N} \subset \tilde{\mathcal{A}}$ for $k > 1$ and $\mathcal{C}_{1,N} \cap \tilde{\mathcal{A}} \neq \emptyset$. Therefore, we may choose on any $\mathcal{C}_{k,N}$ a point $(\alpha_{k,N}, \beta_{k,N}) \in \tilde{\mathcal{A}}$. Since $\tilde{\mathcal{A}}$ is compact, the sequence $\{(\alpha_{k,N}, \beta_{k,N})\}_{k=1}^{\infty}$ must have an accumulation point $(\alpha_{\mathrm{acc},N}, \beta_{\mathrm{acc},N}) \in \tilde{\mathcal{A}}$.

We may now apply Corollary 6.1 to conclude that there is a smooth curve $\mathcal{C}_{\mathrm{acc},N}$ that represents symmetric homoclinic N-pulse orbits, and that $(\tilde{\alpha}_{k,N}, \tilde{\beta}_{k,N}) \in \mathcal{C}_{\mathrm{acc},N}$ for all elements of a subsequence $\{(\tilde{\alpha}_{k,N}, \tilde{\beta}_{k,N})\}_{k=1}^{\infty}$ of $\{(\alpha_{k,N}, \beta_{k,N})\}_{k=1}^{\infty}$. Hence, $\mathcal{C}_{\mathrm{acc},N}$ intersects countably many branches $\mathcal{C}_{k,N}$, which contradicts Theorem 6.1. □

We define the open, connected region $\tilde{\mathcal{A}}_{\mathrm{inner}}$ as the interior of $\tilde{\mathcal{A}}$ (7.10), *i.e.*,

$$\tilde{\mathcal{A}}_{\mathrm{inner}} = \tilde{\mathcal{A}} \setminus \partial\tilde{\mathcal{A}},$$

see Figure 1.

Lemma 7.5 *For all k and N, $(\alpha^*_{k,N}, \beta^*_{k,N}) \in \tilde{\mathcal{A}}_{\mathrm{inner}}$.*

Note that this in particular implies that $\alpha^*_{k,N} > 0$ for all k, N.

Proof It follows from Theorem 7.1 that $(\alpha^*_{k,N}, \beta^*_{k,N}) \in \tilde{A}$, hence we only have to show that $(\alpha^*_{k,N}, \beta^*_{k,N}) \notin \partial\tilde{\mathcal{A}}$. We know from the analysis in Sections 3 and 4 that

$$\partial\tilde{\mathcal{A}} = \{\alpha = 0, \beta \in [0, \beta_{\mathrm{cap}}]\} \cup \mathcal{B}_{\mathrm{cap}} \cup \tilde{\mathcal{K}}_1 \cup \tilde{\mathcal{B}}_{\mathrm{upper}} \cup \{\alpha = \tilde{\alpha}, \beta \in [\tilde{\beta}_{\mathrm{lower}}, \tilde{\beta}_{\mathrm{upper}}]\} \cup \tilde{\mathcal{B}}_{\mathrm{upper}},$$

with $\tilde{\mathcal{K}}_1 = \mathcal{K}_1 \cap \partial\tilde{\mathcal{A}}$, etc., and the natural definitions for $\tilde{\beta}_{\mathrm{lower}}, \tilde{\beta}_{\mathrm{upper}}$ – see Figure 1. By construction, $(\alpha^*_{k,N}, \beta^*_{k,N}) \notin \mathcal{B}_{\mathrm{cap}}, \tilde{\mathcal{B}}_{\mathrm{upper}}, \tilde{\mathcal{B}}_{\mathrm{lower}}$ (Sections 3 and 4); $\alpha^*_{k,N} \neq \tilde{\alpha}$ by definition – recall that $\tilde{\alpha}$ is assumed to be so large that the asymptotic analysis of Section 5 is valid for $\alpha \geq \tilde{\alpha}$. The fact that $(\alpha^*_{k,N}, \beta^*_{k,N}) \notin \tilde{\mathcal{K}}_1$ is a consequence of Lemma 7.6 that will be proved below.

Thus, we only need to show that a bifurcation point cannot have $\alpha^*_{k,N} = 0$. If $\alpha^*_{k,N} = 0$, then its associated orbit $\Gamma(x; (0, \beta))$ can be determined explicitly, it is – by definition – a solution of system (1.12) with initial condition $\Gamma(0; (0, \beta)) = (0, 0, \beta, 0)$, *i.e.*,

$$\Gamma(x; (0, \beta)) = (0, 0, \frac{1}{2}\beta \cosh x, \frac{1}{2}\beta \sinh x).$$

This orbit is not homoclinic to $\mathcal{M}$. Bifurcation points (α^*, β^*) must correspond to orbits $\Gamma(x; (\alpha^*, \beta^*))$ that are homoclinic to $\mathcal{M}$ by Corollary 6.1, hence no point $(0, \beta)$ can be a bifurcation point. □

We know from Corollary 7.1 that a bifurcation point (α^*, β^*) either corresponds to a homoclinic orbit $\Gamma(x; (\alpha^*, \beta^*))$ that has two symmetric degenerate extrema at its flanks, or to a $\Gamma(x; (\alpha^*, \beta^*))$ that has a degenerate maximum at $x = 0$. Note that both types of bifurcations appear in system (1.1) – see the numerical simulations discussed in the Introduction.

In the former case, *i.e.,* if $(\alpha^*, \beta^*) \in \tilde{\mathcal{A}}_{\text{inner}} \setminus \mathcal{K}_1$, the point (α^*, β^*) marks the transition from an N-pulse homoclinic orbit to a homoclinic orbit with a v-component that either has $N + 2$, $N - 2$ or again N maxima. As already stated in Theorem 7.1, each branch $\mathcal{C}_{k,N}$ can be extended beyond its bifurcation point(s) $(\alpha^*_{k,N}, \beta^*_{k,N})$ by Corollary 6.1. However, Corollary 6.1 (and its proof) do not give further information on the nature of this extension. It thus does not exclude the possibility that $\mathcal{C}_{k,N}$ extends into another branch of N-pulse homoclinic orbits $\mathcal{C}_{l,N}$, $l \neq k$.

In the case that $(\alpha^*_{k,N}, \beta^*_{k,N}) \in \mathcal{K}_1$, we can be more explicit.

Lemma 7.6 *Let $N = 2n$, where $n \geq 1$, and assume that there is a $k \in \{1, 2, ..., K_{2n}\}$ such that the branch $\mathcal{C}_{k,2n} \subset \mathcal{A}_{\text{even}}$ of symmetric $2n$-pulse homoclinic orbits has a bifurcation point $(\alpha^*_{k,2n}, \beta^*_{k,2n}) \in \mathcal{K}_1$. Then, there is a branch $\mathcal{C}_{l,2n-1} \subset \mathcal{A}_{\text{odd}}$ of symmetric $(2n-1)$-pulse homoclinic orbits with a bifurcation point $(\alpha^*_{l,2n-1}, \beta^*_{l,2n-1})$ such that*

$$(\alpha^*_{l,2n-1}, \beta^*_{l,2n-1}) = (\alpha^*_{k,2n}, \beta^*_{k,2n}) \in \mathcal{K}_1. \tag{7.11}$$

Thus, we may conclude from this lemma that a symmetric $2n$-pulse orbit that is associated to a point $(\alpha_{k,2n}(s), \beta_{k,2n}(s))$ on a branch $\mathcal{C}_{k,2}$ that has a bifurcation point on $\mathcal{K}_1$, transforms smoothly into a symmetric $(2n-1)$-pulse orbit as $(\alpha_{k,2n}(s), \beta_{k,2n}(s))$ approaches $\mathcal{K}_1$. Note that this lemma also provides a kind of (topological) transversality result, although the possibility that the combined curve $\mathcal{C}_{k,2n} \cup (\alpha^*_{k,2n}, \beta^*_{k,2n}) \cup \mathcal{C}_{l,2n-1}$ is tangent to $\mathcal{K}_1$ at the intersection $(\alpha^*_{k,2n}, \beta^*_{k,2n})$ is not excluded by the lemma.

Proof By Theorem 7.1 and the assumptions in the lemma, we know that there is an arc-length parametrization $(\alpha_{k,2n}(s), \beta_{k,2n}(s))$ of $\mathcal{C}_{k,2n}$, such that $(\alpha_{k,2n}(s), \beta_{k,2n}(s)) \to (\alpha^*_{k,2n}, \beta^*_{k,2n})$ as $s \to \frac{1}{2} L_{k,2n}$. Thus, s also parameterizes the associated homoclinic orbits,

$$\Gamma_{k,2n}(x; s) = (u_{k,2n}(x; s), p_{k,2n}(x; s), v_{k,2n}(x; s), q_{k,2n}(x; s)) = \Gamma_{2n}(x; (\alpha_{k,2n}(s), \beta_{k,2n}(s))),$$

and the extremal points $G^j_{k,2n} = G^j_{k,2n}(s)$ (7.1). The points $G^0_{k,2n}(s)$ and $G^{\pm 1}_{2n}(s)$ merge as $s \to \frac{1}{2} L_{k,2n}$, since the maximum at $x = 0$ is degenerate on $\mathcal{K}_1$ (Corollary 7.1). This implies that the intersection curves $\mathcal{I}^{2n} \cap \mathcal{I}^{-2n}$ and $\mathcal{I}^{2n+1} \cap \mathcal{I}^{-(2n-1)}$ also merge as $s \to \frac{1}{2} L_{k,2n}$ (7.2). Note that the intersections $\mathcal{I}^{N+j} \cap \mathcal{I}^{-(N-j)}$ also appear in separate branches, but we refrain from adding the extra labels. Note also that we do not (have to) take the branch spanned by the $G^{-1}_{k,2n}(s)$'s into account.

Since $\mathcal{I}^{2n} \cap \mathcal{I}^{-2n} \subset \{p = 0\}$, it follows that $\mathcal{I}^{2n+1} \cap \mathcal{I}^{-(2n-1)}$ approaches $\{p = 0\}$ as $s \to \frac{1}{2} L_{k,2n}$. More precise,

$$\mathcal{I}^{2n+1} \cap \mathcal{I}^{-(2n-1)} \to G^1_{k,2n}(\frac{1}{2} L_{k,2n}) = G^0_{k,2n}(\frac{1}{2} L_{k,2n}) \in \{p = 0\} \text{ as } s \to \frac{1}{2} L_{k,2n},$$

and, since $u_{k,2n}(0;s) = \alpha_{k,2n}(s)$ and $v_{k,2n}(0;s) = \beta_{k,2n}(s)$ by definition (7.3),

$$G^0_{k,2n}(\frac{1}{2}L_{k,2n}) = (\alpha_{k,2n}(\frac{1}{2}L_{k,2n}), 0, \beta_{k,2n}(\frac{1}{2}L_{k,2n})) = (\alpha^*_{k,2n}, 0, \beta^*_{k,2n}). \tag{7.12}$$

Next we observe that both $\mathcal{I}^{2n+1} \cap \mathcal{I}^{-(2n-1)} \subset \mathcal{I}^{-(2n-1)}$ and $\mathcal{I}^{2n-1} \cap \mathcal{I}^{-(2n-1)} \subset \mathcal{I}^{-(2n-1)}$, and that $\mathcal{I}^{2n-1} \cap \mathcal{I}^{-(2n-1)}$ corresponds to $\mathcal{C}_{l,2n-1}$ for some l (7.2), (7.3), (7.4). Moreover, by the symmetry in the system, $\mathcal{C}_{2n-1} = \mathcal{I}^{-(2n-1)} \cap \{p = 0\}$. Hence, if $\mathcal{I}^{2n+1} \cap \mathcal{I}^{-(2n-1)}$ approaches $\{p = 0\}$ as $s \to \frac{1}{2}L_{k,2n}$, then $\mathcal{I}^{2n+1} \cap \mathcal{I}^{-(2n-1)}$ must also approach the branch $\mathcal{C}_{l,2n-1}$ (interpreted as subset of $\{p = 0\}$) as $s \to \frac{1}{2}L_{k,2n}$. This implies that the three branches $\mathcal{I}^{2n} \cap \mathcal{I}^{-2n}$ ($\leftrightarrow \mathcal{C}_{k,2n}$), $\mathcal{I}^{2n+1} \cap \mathcal{I}^{-(2n-1)}$ and $\mathcal{I}^{2n-1} \cap \mathcal{I}^{-(2n-1)}$ ($\leftrightarrow \mathcal{C}_{l,2n-1}$) all limit on the same point $G^0_{k,2n}(\frac{1}{2}L_{k,2n}) = (\alpha^*_{k,2n}, 0, \beta^*_{k,2n})$ (7.12), where $(\alpha^*_{k,2n}, \beta^*_{k,2n}) \in \mathcal{K}_1$ is the bifurcation point of $\mathcal{C}_{k,2n}$.

Since all orbits $\Gamma_N(x,(\alpha,\beta))$ have a degenerate maximum at $x = 0$ if $(\alpha,\beta) \in \mathcal{K}_1$, $(\alpha^*_{k,2n}, \beta^*_{k,2n}) \in \overline{\mathcal{C}}_{l,2n-1}$ must also be a bifurcation point of $\mathcal{C}_{l,2n-1}$. This is equivalent to (7.11) by Theorem 7.1. □

8 The model problem and the phenomenon of pulse splitting

In this section, we examine the relation between the homoclinic orbits of the system of ordinary differential equations (1.1) studied in this paper and the onset of the self-replication process exhibited by the Gray-Scott system (1.14). Moreover, we discuss the phenomenon of pulse self-replication in a more general setting, *i.e.*, beyond the specific context of the Gray-Scott model.

8.1 Pulses and pulse bifurcations in the Gray-Scott model

Stationary solutions of the Gray-Scott equation (1.14) satisfy the following system of ordinary differential equations:

$$\begin{cases} U'' &= \varepsilon_1^2[UV^2 - \varepsilon_1\varepsilon_2(1 - \frac{\varepsilon_2}{\varepsilon_1}U)], \\ V'' &= V - UV^2, \end{cases} \tag{8.1}$$

where we used the parameter combinations

$$\varepsilon_1 = \frac{\sqrt{A}}{B}, \quad \varepsilon_2 = \sqrt{BD}, \tag{8.2}$$

and the scaling

$$x = \sqrt{\frac{D}{B}}\tilde{x}, \quad U(x) = B^{3/2}\sqrt{\frac{D}{A}}\tilde{U}(\tilde{x}), \quad V(x) = \sqrt{\frac{A}{BD}}\tilde{V}(\tilde{x}),$$

and where the tildes have been dropped. See [19, 20, 5], or the equivalent scalings of (1.14) in [24, 25, 26, 27, 30, 31]. Now, system (8.1) is a singularly perturbed system of

ordinary differential equations when

$$0 < \varepsilon_1, \varepsilon_2 \ll 1, \quad \text{and} \quad \varepsilon_2 \ll \varepsilon_1 \quad \text{or} \quad \varepsilon_2 = \mathcal{O}(\varepsilon_1),$$

and the existence and stability of (singular) homoclinic stationary pulse and multi-pulse solutions of the Gray-Scott system has been established in [6, 8, 11, 24, 25, 26, 27, 30, 31].

These singular, localized, stable pulses can be seen as the origin of the self-replication process. Starting with $0 < \varepsilon_1, \varepsilon_2 \ll 1$, this process can be initiated by increasing ε_1 to $\mathcal{O}(1)$ values, while keeping ε_2 fixed. At a certain, $\mathcal{O}(1)$, critical value ε_1^*, the pulse 'disappears' in a homoclinic saddle-node bifurcation, and this homoclinic saddle-node bifurcation marks the onset of the self-replication process [5, 6, 24, 25, 26, 30, 33, 40]. Now, near the bifurcation, (8.1) is no longer singularly perturbed, since U, V, and their derivatives vary on the same scale. However, by a simple further scaling ($U = \varepsilon_1 u$, $V = v/\varepsilon_1$), (8.1) is transformed into

$$\left\{ \begin{array}{lcl} u'' & = & uv^2 - \varepsilon_1^2 \varepsilon_2 (1 - \varepsilon_2 u), \\ v'' & = & v - uv^2, \end{array} \right. \tag{8.3}$$

in which $0 < \varepsilon_2 \ll 1$ is still an asymptotically small parameter, but $\varepsilon_1 = O(1)$.

The reduced problem (1.1) considered in this paper is the leading order part of (8.3), *i.e.*, (1.1) can be obtained from (8.3) by taking the limit $\varepsilon_2 \to 0$. By a similar motivation, a version of equation (1.1) has been derived in [30]; equation (1.1) is called 'the core problem' in [24, 25, 26]. Systems like (1.1) have also been studied as simple models for auto-catalysis in [2, 3].

The homoclinic solutions considered in this paper are directly related to pulse solutions of the Gray-Scott equation in the pulse-splitting regime, *i.e.*, to homoclinic solutions of (8.3) with $0 < \varepsilon_2 \ll 1$ and $\varepsilon_1 = \mathcal{O}(1)$. To see this, we note that

$$\mathcal{M}^\varepsilon = \{(u, p, v, q) | v = 0, q = 0\}$$

is an invariant manifold of (8.3) that is identical to that of (1.1), see (1.13), where here again $p = u'$ and $q = v'$. Away from $\mathcal{M}^\varepsilon$ and with $u = \mathcal{O}(1)$, the perturbation term '$-\varepsilon_1^2 \varepsilon_2 (1 - \varepsilon_2 u)$' in (8.3) is just a regular perturbation term. Therefore, the results of the previous sections on the location and structure of the set Σ and the branches $\mathcal{C}_{k,N}$ that represent homoclinic orbits to $\mathcal{M}$ in (1.1) are expected to carry over directly to yield the existence of a set Σ^ε consisting of branches $\mathcal{C}_{k,N}^\varepsilon$ representing symmetric orbits in (8.3) that are homoclinic to $\mathcal{M}^\varepsilon$. In fact, the distances between the curves $\mathcal{C}_{k,N}^\varepsilon$ and their leading order counterparts $\mathcal{C}_{k,N}$ will be $\mathcal{O}(\varepsilon_2)$.

A more technical version of this statement can be made rigorous by relatively standard arguments, but we do not intend to go into this here. We also refer to [24, 25, 26] for an analysis based on asymptotic matching of the relation between homoclinic orbits in (8.3) and homoclinic orbits in (1.1).

A solution of (8.3) that is homoclinic to $\mathcal{M}^\varepsilon$ is not necessarily a (stationary) pulse solution of the Gray-Scott equation (1.14). Indeed, orbits homoclinic to $\mathcal{M}^\varepsilon$ must also

satisfy an additional condition, namely they must lie in the intersection of the two-dimensional stable and unstable manifolds of the critical point $(u,p,v,q) = (1/\varepsilon_2, 0, 0, 0) \in \mathcal{M}^\varepsilon$, so that they are forward and backward asymptotic to this fixed point on $\mathcal{M}^\varepsilon$. Note that this critical point corresponds to the 'trivial pattern' $U \equiv 1$, $V \equiv 0$ in the (unscaled) Gray-Scott equation (1.14), which is the 'background state' for pulse solutions.

The perturbation term '$-\varepsilon_1^2\varepsilon_2(1-\varepsilon_2 u)$' in (8.3) changes the trivial, shear flow of (1.1) on $\mathcal{M}$ significantly. The flow on $\mathcal{M}^\varepsilon$ is linear and governed by

$$\left\{ \begin{array}{rcl} u' &=& p, \\ p' &=& -\varepsilon_1^2\varepsilon_2(1-\varepsilon_2 u), \end{array} \right. \tag{8.4}$$

This linear system has a saddle point $(1/\varepsilon_2, 0, 0, 0)$ with stable and unstable manifolds given by the lines $\ell_{s,u} \subset \mathcal{M}^\varepsilon$,

$$\ell_s = \{(u,p) \in \mathcal{M}^\varepsilon | p = +\varepsilon_1(1-\varepsilon_2 u)\}, \quad \ell_u = \{(u,p) \in \mathcal{M}^\varepsilon | p = -\varepsilon_1(1-\varepsilon_2 u)\}. \tag{8.5}$$

Thus, while the p-coordinates of the symmetric homoclinic orbits of (1.1) constructed in this paper approach a constant value $\pm p_\infty$ as $x \to \pm\infty$, the p-coordinates of their perturbed counterparts in (8.3) become unbounded as $x \to \pm\infty$, except for the co-dimension 1 set of orbits which are homoclinic to $(1/\varepsilon_2, 0, 0, 0)$.

Fenichel theory can be applied to determine whether these special co-dimension 1 orbits indeed exist. Moreover, this geometric point of view can can also be used to establish a direct relation between the bifurcations of the symmetric homoclinic orbits as discussed in Section 7 and the homoclinic (saddle-node) bifurcations that have been observed by numerical simulations in the Gray-Scott model as the parameter ε_1 varies [33, 25], as we now show.

It follows from Fenichel theory that, to any curve $\mathcal{C}^\varepsilon_{k,N} \subset \Sigma^\varepsilon$ in the (α,β)-plane of homoclinic orbits to $\mathcal{M}^\varepsilon$ in (8.3), there correspond two curves on $\mathcal{M}^\varepsilon$, the take-off curve $T_{\text{off}}(\mathcal{C}^\varepsilon_{k,N})$ and the touch-down curve $T_{\text{down}}(\mathcal{C}^\varepsilon_{k,N})$, that govern the behavior of orbits homoclinic to $\mathcal{M}^\varepsilon$ backward and forward asymptotically, respectively, see [11, 7]. These curves represent the families of base points of the Fenichel fibers associated to the family of orbits homoclinic to $\mathcal{M}^\varepsilon$, backward and forward asymptotically, respectively, described by $\mathcal{C}^\varepsilon_{k,N}$. More precisely, let $\Gamma(x;\Gamma_0)$ be a solution of (8.3) taken as 4-dimensional dynamical system, with $\Gamma(0;\Gamma_0) = \Gamma_0 = (\alpha, 0, \beta, 0)$ and $(\alpha,\beta) \in \mathcal{C}^\varepsilon_{k,N}$. Then, there exist two points $\Gamma_0^\pm \in \mathcal{M}^\varepsilon$, $\Gamma_0^- \in T_{\text{off}}(\mathcal{C}^\varepsilon_{k,N})$ and $\Gamma_0^+ \in T_{\text{down}}(\mathcal{C}^\varepsilon_{k,N})$, and two solutions $\Gamma^\pm(x;\Gamma_0^\pm) \subset \mathcal{M}^\varepsilon$ with $\Gamma_0^\pm$ as initial conditions, such that

$$\|\Gamma(x;\Gamma_0) - \Gamma^\pm(x;\Gamma_0^\pm)\| \to 0 \quad \text{exponentially} \quad \text{for} \quad x \to \pm\infty.$$

In other words, the orbits $\Gamma^\pm(x;\Gamma_0^\pm) \in \mathcal{M}^\varepsilon$ shadow the path of the homoclinic orbit $\Gamma(x;\Gamma_0)$ for x such that it is (exponentially) close to $\mathcal{M}^\varepsilon$. Therefore, if

$$\Gamma_0^+ \in \ell_s \cap T_{\text{down}}(\mathcal{C}^\varepsilon_{k,N}) \tag{8.6}$$

for some k, then we may conclude that the orbit $\Gamma(x;\Gamma_0)$ is an N-pulse orbit homoclinic to $(1/\varepsilon_2, 0, 0, 0)$, *i.e.*, it represents an N-pulse solution in the Gray-Scott system, since

in this case $\Gamma^+(x;\Gamma_0^+) \to (1/\varepsilon_2,0,0,0)$ as $x \to \infty$. Of course, the orbit is symmetric, and hence (8.6) is equivalent to $\Gamma_0^- \in \ell_u \cap T_{\text{off}}(\mathcal{C}_{k,N}^\varepsilon)$.

Again, we remark that the analysis required to make these statements – and the upcoming ones – rigorous is technical but straightforward.

If $(\alpha,\beta) \in \mathcal{C}_{k,N}^\varepsilon$ with $\alpha,\beta = \mathcal{O}(1)$ with respect to ε_2, then the (u,p)-coordinates of the associated point in $T_{\text{down}}(\mathcal{C}_{k,N}^\varepsilon)$ will also be $\mathcal{O}(1)$ with respect to ε_2. If $\alpha \gg 1$ then the system can again be brought into a singular perturbed form – as in Section 5 – and $T_{\text{down}}(\mathcal{C}_{k,N}^\varepsilon)$ can be determined explicitly. In fact, this is in essence equivalent to the analysis in [11, 5]. Since the distance between $\mathcal{C}_{k,N}^\varepsilon$ and $\mathcal{C}_{k,N}$ is $\mathcal{O}(\varepsilon_2)$, the position of $T_{\text{down}}(\mathcal{C}_{k,N}^\varepsilon) \subset \mathcal{M}^\varepsilon$ is $\mathcal{O}(\varepsilon_2)$ close to that of its equivalent $T_{\text{down}}(\mathcal{C}_{k,N}) \in \mathcal{M}$ that is defined for system (1.1). Moreover, the position of $T_{\text{down}}(\mathcal{C}_{k,N}^\varepsilon)$ will not change (to leading order) as the parameter ε_1 is varied.

For $\mathcal{O}(1)$ values of u, the stable and unstable manifolds, $\ell_{u,s} \subset \mathcal{M}^\varepsilon$, of $(1/\varepsilon_2,0,0,0)$ are given by

$$\ell_s = \{(u,p) \in \mathcal{M}^\varepsilon | p = +\varepsilon_1 + \mathcal{O}(\varepsilon_2)\}, \quad \ell_u = \{(u,p) \in \mathcal{M}^\varepsilon | p = -\varepsilon_1 + \mathcal{O}(\varepsilon_2)\},$$

recall (8.5). Thus, the intersection (8.6), which establishes the existence of homoclinic orbits to $(1/\varepsilon_2,0,0,0)$ in (8.3), can be traced directly as a function of the bifurcation parameter ε_1, since $\ell_s = \{p = \varepsilon_1\}$ and $T_{\text{down}}(\mathcal{C}_{k,N}^\varepsilon)$ is not influenced by ε_1 (to leading order in ε_2).

If ε_1 is small, then to each intersection point in (8.6) there is an associated point $(\alpha(\varepsilon_1),\beta(\varepsilon_1)) \in \mathcal{C}_{k,N}^\varepsilon$ such that $\alpha \gg 1$, which implies that $k=1$, *i.e.*, $\mathcal{C}_{k,N}^\varepsilon = \mathcal{C}_N^{\varepsilon,\infty}$. Thus, for small ε_1, we recover the N-pulse homoclinic orbits to $(1/\varepsilon_2,0,0,0)$ (or, unscaled, to the background pattern $(U \equiv 1, V \equiv 0)$ in (1.14)). This statement is completely equivalent to results in [11], and its proof may therefore be found there (although the parameter space of (1.14) considered in [11] is more restricted than it is here). A bifurcation point $(\alpha_{k,N}^*,\beta_{k,N}^*)$ of a curve $\mathcal{C}_{k,N}^\varepsilon$ corresponds to a bifurcation value $\varepsilon_{k,N}^*$ of ε_1 such that

$$(\alpha(\varepsilon_{k,N}^*),\beta(\varepsilon_{k,N}^*)) = (\alpha_{k,N}^*,\beta_{k,N}^*).$$

Thus, each bifurcation point in Σ^ε corresponds to a well-defined value of the bifurcation parameter ε_1. Moreover, any such bifurcation value of ε_1 by definition marks the transition from an N-pulse to an M-pulse homoclinic orbit in the Gray-Scott model (1.1). Hence, the results obtained in this paper can be translated into results on the existence and bifurcations of homoclinic N-pulse orbits in the Gray-Scott equation in the splitting regime, *i.e.*, for $\sqrt{A}/B = \mathcal{O}(1)$ (8.2).

The outermost branch in Figure 1, *i.e.*, the curve $\text{cl}\,(\mathcal{C}_1^\infty \cup \mathcal{C}_2^\infty)$, is the most important curve for the relation between model problem (1.1) and the initiation of the pulse-splitting process in the Gray-Scott system. We therefore consider its counterpart $\text{cl}\,(\mathcal{C}_1^{\varepsilon,\infty} \cup \mathcal{C}_2^{\varepsilon,\infty})$ for system (8.3). If ε_1 is small, then the intersection $T_{\text{down}}\,(\text{cl}(\mathcal{C}_1^{\varepsilon,\infty} \cup \mathcal{C}_2^{\varepsilon,\infty})) \cap \ell_s$ consists of two points. These points correspond to $(\alpha_1(\varepsilon_1),\beta_1(\varepsilon_1)) \in \mathcal{C}_1^{\varepsilon,\infty}$ and $(\alpha_2(\varepsilon_1),\beta_2(\varepsilon_1)) \in \mathcal{C}_2^{\varepsilon,\infty}$, respectively, that represent the singular 1-pulse and 2-pulse homoclinic orbits, respectively, in the Gray-Scott model that have already been studied

in [11]. See also [24]. As ε_1 increases, the points $(\alpha_1(\varepsilon_1), \beta_1(\varepsilon_1))$ and $(\alpha_2(\varepsilon_1), \beta_2(\varepsilon_1)))$ travel along the curve $\mathrm{cl}\,(\mathcal{C}_1^{\varepsilon,\infty} \cup \mathcal{C}_2^{\varepsilon,\infty})$, with α-coordinates $\alpha_{1,2}(\varepsilon_1)$ that must remain bounded. Since we know that $\mathrm{cl}\,(\mathcal{C}_1^{\varepsilon,\infty} \cup \mathcal{C}_2^{\varepsilon,\infty})$ is bounded for bounded α, and bounded away from $\{\alpha = 0\}$, we may conclude that there is a critical value ε_1^* of ε_1 such that

$$\ell_s \cap T_{\mathrm{down}}\,(\mathrm{cl}(\mathcal{C}_1^{\varepsilon,\infty} \cup \mathcal{C}_2^{\varepsilon,\infty})) = \emptyset \quad \text{for} \quad \varepsilon_1 > \varepsilon_1^*,$$

while the intersection contains (at least) the two points $(\alpha_{1,2}(\varepsilon_1), \beta_{1,2}(\varepsilon_1))$ for $\varepsilon_1 < \varepsilon_1^*$. Thus, as ε_1 increases through ε_1^*, two homoclinic orbits merge and there is a homoclinic saddle-node bifurcation (in the sense of dynamical systems theory, see for instance [28]). This is the saddle-node bifurcation that initiates the self-replication process in the Gray-Scott model [5, 6, 24, 25, 26, 30, 33, 40]. Note that there is no reason for the bifurcation point $(\alpha_{1,2}(\varepsilon_1^*), \beta_{1,2}(\varepsilon_1^*))$ to be equal to the bifurcation point $\overline{\mathcal{C}_1^{\varepsilon,\infty}} \backslash \mathcal{C}_1^{\varepsilon,\infty} = \overline{\mathcal{C}_2^{\varepsilon,\infty}} \backslash \mathcal{C}_2^{\varepsilon,\infty}$ at which the two pulses of 2-pulse orbit merge into one pulse. In fact, numerical simulations indicate that this is indeed not the case (see also [25]).

This scenario has also been studied in detail, numerically and asymptotically ($0 < \varepsilon_1 \ll 1$ or equivalently $\alpha \gg 1$), in [24]. The analysis in this paper provides a rigorous foundation for the continuation of the curves $\mathcal{C}_{1,2}^{\varepsilon,\infty}$ into the region $\alpha = \mathcal{O}(1)$ (Section 6). Moreover, it follows from the results of this paper that the curves $\mathcal{C}_{1,2}^{\varepsilon,\infty}$ are smooth, bounded, and of finite length for α bounded (Sections 3, 4, and 7), which implies that there must be a value of ε_1 above which neither the 1- nor the 2-pulse orbits can exist in (8.3), *i.e.*, in the Gray-Scott model. However, we have not proved the numerically obvious fact that the 1-pulse and 2-pulse orbits do not undergo any other bifurcations ([33, 24] and Figure 1).

The 1- and 2-pulse orbits are naturally embedded in a family of N-pulse orbits (see Section 5 and [11], and Section 8.2 below, as well as [7], for a similar result for the Gierer-Meinhardt equation). We have shown in this paper that the equivalent scenario in which a $(2m-1)$-pulse can only bifurcate into a $2m$-pulse, *i.e.* in which $\overline{\mathcal{C}_{2m-1}^{\infty}} \cap \overline{\mathcal{C}_{2m}^{\infty}} \neq \emptyset$, is not correct for general higher order pulses. In fact, our numerical simulations indicate that this only happens for $m = 1, 2, 3$, and that other bifurcations take place for $m \geq 4$ (section 1). The analysis in this paper supplies a foundation for further research of the intriguing bifurcation structure of the multi-pulse homoclinic orbits in system (1.1) and in the Gray-Scott system (1.14).

8.2 The onset of pulse self-replication

Recently, it has been shown that the phenomenon of self-replication of pulses is not restricted to the Gray-Scott model. In [33] an 'artificial' model that exhibits pulse self-replication was constructed. Moreover, it was found in [12] that pulse self-replication also appears in the Gierer-Meinhardt model,

$$\begin{cases} \varepsilon^2 U_t &= U_{xx} - \varepsilon^2 \mu U + V^2 \\ V_t &= \varepsilon^2 V_{xx} - V + \frac{V^2}{U}, \end{cases} \tag{8.7}$$

with parameters $\varepsilon, \mu > 0$ [17, 32], and in the generalized Gierer-Meinhardt equations (see also [25]). Self-replication of pulses was observed also in [10] in several other models

of Gierer-Meinhardt type, as well as in generalizations of the Gray-Scott model, see [38]. It may thus be concluded that self-replication of pulses is a generic phenomenon. There are several ingredients that appear to be necessary for the self-replication process [33, 40, 13, 5, 25]. The existence of a family of symmetric 1- and 2-pulse orbits is one of them [11, 7, 25], it is called the 'multi-bump transition condition' in [25]. This latter ingredient is perhaps the aspect of pulse self-replication that is most suitable for a full analytical approach. Note that such an analysis cannot be restricted to only 1- and 2-pulse orbits. For instance, to prove that a 1-pulse homoclinic orbit must bifurcate into a 2-pulse orbit one must exclude the possibility that the 1-pulse develops extra pulses on its flanks, *i.e.*, that it bifurcates into a 3-pulse orbit, etc... Moreover, in all known examples of systems that exhibit pulse self-replication, the families of 1- and 2-pulse orbits are naturally embedded in a larger family of N-pulse orbits ($N \geq 1$) – see also the discussion below on self-replication in the Gierer-Meinhardt equations.

Thus, the onset of pulse self-replication is in general strongly linked to bifurcations of N-pulse homoclinic orbits. This gives a further motivation to study the existence and bifurcations of the family of homoclinic orbits in the a priori simple model problem (1.1).

The onset of pulse-self-replication in the Gierer-Meinhardt equation (8.7), and in models of (generalized) Gierer-Meinhardt type, is similar to that in the Gray-Scott system. The existence and stability of singular symmetric, stationary homoclinic multi-pulse solutions to (8.7) can be established if $0 < \varepsilon \ll 1$ is an asymptotically small parameter [4, 7, 22]. Note that these pulse solutions are homoclinic to the background state ($U \equiv 0, V \equiv 0$) and that the N-pulse homoclinic orbits are unstable as solutions of equation (8.7) if $0 < \varepsilon \ll 1$ and $N \geq 2$ [7].

It is shown in [12] that the multi-pulse orbits cannot exist for $\mu \gg 1/\varepsilon^4$, and that the methods developed in [7] can be applied up to $0 < \mu \ll 1/\varepsilon^4$, which establishes the existence of multi-pulse orbits for these values of μ. Hence, one expects homoclinic saddle-node bifurcations in the region $\mu = \mathcal{O}(1/\varepsilon^4)$. As in the Gray-Scott case, the self-replication is initiated by these saddle-node bifurcations, as was numerically confirmed in [12, 25].

In the scaling of the Gierer-Meinhardt equation chosen in (8.7), the U- and V-components of the pulses have $\mathcal{O}(1)$ amplitudes with respect to ε, however these amplitudes scale with $\sqrt{\mu}$ as μ is varied. To study the homoclinic saddle-node bifurcations it is therefore natural to introduce the $\mathcal{O}(1)$ parameter $\tilde{\mu}$ by $\mu = \tilde{\mu}/\varepsilon^4$, to scale U and V as

$$U(x) = \varepsilon^{-2} u, \quad V(x) = \varepsilon^{-2} v,$$

and set $x = \varepsilon \tilde{x}$. These scalings transform the stationary problem associated to (8.7) into

$$\left\{ \begin{array}{rcl} u'' & = & \tilde{\mu} u - v^2 \\ v'' & = & v - \frac{v^2}{u}. \end{array} \right. \tag{8.8}$$

Hence, the homoclinic saddle-node bifurcations and the onset of pulse self-replication occur in the Gierer-Meinhardt system for parameter combinations at which the stationary problem no longer has a singularly perturbed nature. This is completely similar to the Gray-Scott case (compare (8.8) to (8.3)). However, in the Gray-Scott problem, (8.3)

could be further simplified to the reduced, or core, problem (1.1). It is a priori not clear whether (8.8) can also be further simplified, since the term '$\tilde{\mu}$u' in (8.8) is not small, while the term '$-\varepsilon_1^2\varepsilon_2(1-\varepsilon_2)u$' is a higher order term in (8.3).

Nevertheless, although equations (8.3) and (8.8) are quite different, they exhibit two similar families of multi-pulse homoclinic orbits that play crucial and similar roles in the onset of pulse self-replication. It is expected that further investigation of the geometric structures that are responsible for the existence of the families of multi-pulse homoclinic orbits and their bifurcations may provide a fundamental understanding of the similarities between systems (8.3) and (8.8), and thus of the generic nature of the phenomenon of pulse self-replication.

Acknowledgements. We thank Nico Temme for pointing us to the modified Mathieu equation needed in Remark 4.1. A.D. thanks the Organization for Scientific Research (NWO) for financial support, T.K. thanks the National Science Foundation (NSF) for support through grants DMS-0072596 and DMS-0306523 and the Center for Mathematics and Computer Science (CWI) in Amsterdam for its hospitality, and A.D. and L.A.P. thank the Department of Mathematics at Boston University for its hospitality.

References

[1] M. Abramovitz and I. Stegun [1972], *Handbook of mathematical functions with formulas, graphs, and mathematical tables,* Dover.

[2] J. Billingham and D.J. Needham [1991] The development of traveling waves in quadratic and cubic autocatalysis with unequal diffusion rates. I. Permanent form traveling waves. *Phil. Trans. Roy. Soc. Lond. A* **334** 1–24.

[3] J. Billingham and D.J. Needham [1991], The development of travelling waves in quadratic and cubic autocatalysis with unequal diffusion rates. II. An initial value problem with an immobilized or nearly immobilized autocatalyst. *Phil. Trans. Roy. Soc. Lond.* **336**, 497–539.

[4] M. del Pino, M. Kowalczyk, and X. Chen [2001], The Gierer-Meinhardt system: the breaking of homoclinics and multi-bump ground states, *Commun. Contemp. Math.* **3** 419–439.

[5] A. Doelman, W. Eckhaus, and T.J. Kaper [2001], Slowly-modulated two-pulse solutions in the Gray-Scott model II: Geometric theory, bifurcations, and splitting dynamics, *SIAM J Appl. Math.* **61** 2036–2062.

[6] A. Doelman, R. A. Gardner, and T.J. Kaper [1998], Stability analysis of singular patterns in the 1-D Gray–Scott model: a matched asymptotics approach, *Physica D* **122** 1–36.

[7] A. Doelman, R. A. Gardner, and T.J. Kaper [2001], Large stable pulse solutions in reaction-diffusion equations, *Ind. Univ. Math. J.* **50** 443–507.

[8] A. Doelman, R. A. Gardner and T.J. Kaper [2002], A stability index analysis of 1-D patterns of the Gray–Scott model, *Memoirs AMS* **155**.

[9] A. Doelman, P. Holmes [1996], Homoclinic explosions and implosions, *Phil. Trans. Roy. Soc. Lond. A* **354** 845–893.

[10] A. Doelman and T.J. Kaper [2003], Semi-strong pulse interactions in a class of coupled reaction-diffusion equations, *SIAM J. Appl. Dyn. Syst.* **2** 53–96.

[11] A. Doelman, T.J. Kaper, and P. Zegeling [1997], Pattern formation in the one-dimensional Gray-Scott model, *Nonlinearity* **10** 523–563.

[12] A. Doelman and H. v.d. Ploeg [2002], Homoclinic stripe patterns, *SIAM J. Appl. Dyn. Sys.* **1** 65–104.

[13] S.-I. Ei, Y. Nishiura, and K.-I. Ueda [2001], 2^n-splitting or edge-splitting? A manner of splitting in dissipative systems, *Japan J. Indust. Appl. Math.* **18** 181–205.

[14] B. Ermentrout [2002], *Simulating, analyzing, and animating dynamical systems: A guide to XPPAUT for researchers and students,* SIAM, Philadelphia, PA.

[15] N. Fenichel [1971], Persistence and smoothness of invariant manifolds for flows, *Ind. Univ. Math. J.* **21** 193–226.

[16] N. Fenichel [1979], Geometrical singular perturbation theory for ordinary differential equations, *J. Diff. Eq.* **31** 53–98.

[17] A. Gierer and H. Meinhardt [1972], A theory of biological pattern formation, *Kybernetik* **12** 30–39.

[18] P. Gray and S.K. Scott [1984], Autocatalytic reactions in the isothermal, continuous stirred tank reactor: oscillations and instabilities in the system A + 2B $\rightarrow$ 3B, B $\rightarrow$ C, *Chem. Eng. Sci.* **39** 1087–1097.

[19] J.K. Hale, L.A. Peletier, and W.C. Troy [1999], Stability and instability in the Gray-Scott model: the case of equal diffusivities. *Appl. Math. Lett.* **12** 59–65.

[20] J.K. Hale, L.A. Peletier, and W.C. Troy [2000], Exact homoclinic and heteroclinic solutions of the Gray-Scott model for autocatalysis, *SIAM J. Appl. Math.* **61** 102–130.

[21] M.W. Hirsch, C.C. Pugh, and M. Shub [1977], *Invariant Manifolds*, LNM **583**, Springer-Verlag, New York, 1976.

[22] D. Iron, M.J. Ward, and J. Wei [2001], The stability of spike solutions to the one-dimensional Gierer-Meinhardt model, *Physica D* **150** 25–62.

[23] C.K.R.T. Jones [1994], Geometric singular perturbation theory, in *Dynamical systems, Montecatibi Terme, 1994*, Lecture Notes in Mathematics, **1609**, R. Johnson (ed.), Springer-Verlag.

[24] T. Kolokolnikov, M. Ward, and J. Wei [2005], The existence and stability of spike equilibria in the one-dimensional Gray-Scott model: the pulse-splitting regime, *Physica D* **202** 258–293.

[25] T. Kolokolnikov, M.J. Ward, and J. Wei [2005] Pulse-splitting for some reaction-diffusion systems in one-space dimension, *Stud. Appl. Math.* **114** 115–165.

[26] T. Kolokolnikov, M.J. Ward, and J. Wei [2005], The existence and stability of spike equilibria in the one-dimensional Gray-Scott model on a finite domain. *Appl. Math. Lett.* **18**, 951–956.

[27] T. Kolokolnikov, M.J. Ward, and J. Wei [2005], The existence and stability of spike equilibria in the one-dimensional Gray-Scott model: the low feed-rate regime. *Stud. Appl. Math.* **115** 21–71.

[28] Y. Kuznetsov [1995], *Elements of Applied Bifurcation Theory,* Applied Mathematical Sciences **112**, Springer-Verlag, New York, NY.

[29] K.-J. Lin, W.D. McCormick, J.E. Pearson, and H.L. Swinney [1994], Experimental observation of self-replicating spots in a reaction-diffusion system, *Nature* **369** (6477) 215–218.

[30] C.B. Muratov and V.V. Osipov [2000], Static spike autosolitons in the Gray-Scott model, *J. Phys. A* **33** 8893–8916.

[31] C.B. Muratov and V.V. Osipov [2002], Stability of the static spike autosolitons in the Gray-Scott model, *SIAM J. Appl. Math.* **62** 1463–1487.

[32] W.-M. Ni [1998], Diffusion, cross-diffusion, and their spike-layer steady states, *Notices AMS* **45**(1) 9–18.

[33] Y. Nishiura and D. Ueyama [1999], A skeleton structure for self-replication dynamics, *Physica D* **130**, 73–104.

[34] J.E. Pearson [1993], Complex patterns in a simple system, *Science* **261** 189–192.

[35] L.A. Peletier and W.C. Troy [2001], *Spatial patterns. Higher order models in physics and mechanics.* Progress in Nonlinear Differential Equations and their Applications, **45**, Birkhäuser Boston, Boston, MA.

[36] V. Petrov, S.K. Scott, and K. Showalter [1994], Excitability, wave reflection, and wave splitting in a cubic autocatalysis reaction-diffusion system, *Phil. Trans. Roy. Soc. Lond. A* **347** 631–642.

[37] W.N. Reynolds, J.E. Pearson, and S. Ponce-Dawson [1994], Dynamics of self-replicating patterns in reaction diffusion systems, *Phys. Rev. Lett.* **72** 2797–2800.

[38] W.N. Reynolds, S. Ponce-Dawson, and J.E. Pearson [1997], Self-replicating spots in reaction-diffusion systems, *Phys. Rev. E* **56**, 185–198.

[39] K. Sakamoto [1990], Invariant manifolds in singular perturbation problems for ordinary differential equations, *Proc. Roy. Soc. Edinb., A-Math.* **116**, 45–78.

[40] D. Ueyama [1999], Dynamics of self-replicating patterns in the one-dimensional Gray-Scott model, *Hokkaido Math. J.* **28** 175–210.

A The proofs of Lemmas 4.1 and 4.2

In this appendix, we prove Lemmas 4.1 and 4.2, which establish lower bounds on $z(x)$ and $y'(x)$, respectively. We begin by recalling the governing equations (4.2) from Section 4,

$$y'' = \beta^2 y z^2 \quad \text{and} \quad z'' = z - \alpha\beta y z^2, \quad \text{with} \quad y(0) = 1, y'(0) = 0, z(0) = 1, z'(0) = 0. \tag{A.1}$$

Also, we recall that $z_0(x) = \cosh(x)$ is the solution of

$$z_0'' - z_0 = 0, \qquad z_0(0) = 1, \;\; z_0'(0) = 0$$

and that $y_0(x) = C_0(\beta \sinh(x))$ is the solution of

$$y_0'' = \beta^2(\cosh^2(x))y_0 \qquad y_0(0) = 1 \;\text{ and }\; y_0'(0) = 0. \tag{A.2}$$

In order to prove the desired lower bounds, we need to derive the following *upper* bounds on z and y first.

Proposition A.1 *For $x > 0$,*

$$z(x) < z_0(x) \qquad \text{and} \qquad 0 < y(x) < y_0(x) < \cosh(\beta \sinh(x)). \tag{A.3}$$

Proof of Proposition A.1 Let $Z = z - z_0$. Then,

$$Z'' - Z = -\alpha\beta y z^2 < 0, \qquad Z(0) = 0, \;\; Z'(0) = 0.$$

Hence, $Z''(0) = -\alpha\beta < 0$, and we see that $Z' < 0$ and $Z < 0$ in a right neighborhood of the origin. Moreover, it also follows, by a standard argument by contradiction, that Z'', Z', and Z remain negative for all $x > 0$. Therefore, we may conclude as desired that $z(x) < z_0(x) = \cosh(x)$ for $x > 0$.

Next, observe that $y(x) > 0$, which follows directly from equation (A.1) for y. We now derive an upper bound for y. Since $z < z_0$, the y equation in (A.1) implies

$$y'' < \beta^2 y z_0^2.$$

Let $Y = y - y_0$. This difference variable satisfies

$$Y'' < \beta^2 z_0^2 Y \quad \text{for} \;\; x > 0, \qquad Y(0) = 0, \qquad Y'(0) = 0,$$

from which we deduce that $Y(x) < 0$ on $x > 0$ and, hence, $y < y_0$, as desired.

This upper bound on $y(x)$ is the sharper of the two stated in the lemma here, and it is purely for the benefit of later calculations that we also derive a bound on $y_0(x)$, which is a less sharp bound on y itself but which is much easier to work with. Let

$$t = \beta \sinh(x) \qquad \text{and} \qquad \eta(t) = y_0(x). \tag{A.4}$$

Then, $\eta(t)$ satisfies the modified Mathieu equation (A.2), which we may write as

$$\ddot{\eta} - \eta = -\frac{t}{\beta^2 + t^2}\dot{\eta}, \tag{A.5}$$

with $\eta(0) = 1$, $\dot{\eta}(0) = 0$, and the overdot now denotes the derivative with respect to t.

We observe that $\dot{\eta}(t) > 0$ at least for small values of t, because $\ddot{\eta}(0) = \eta(0) > 0$. Now, we claim that $\dot{\eta}(t) > 0$ for all values of $t > 0$. Suppose to the contrary that $\dot{\eta}(t) > 0$ for $t \in (0, t_0)$ for some t_0 and that $\dot{\eta}(t_0) = 0$. Then, it would be the case that $\ddot{\eta}(t_0) \leq 0$. However, the equation directly reveals that, if $\dot{\eta}(t_0) = 0$, then $\ddot{\eta}(t_0) = \eta(t_0) > 0$. Therefore, the initial supposition leads to a contradiction, and hence $\dot{\eta}(t) > 0$ for all $t > 0$.

As a consequence, we see that

$$\ddot{\eta} - \eta < 0 \qquad \text{for all } \; t > 0.$$

and hence that

$$\eta(t) < \cosh(t) \qquad \text{for } \; t > 0,$$

by comparison. Translating back to the x variable, we have shown the desired result that $y_0(x) < \cosh(\beta \sinh(x))$ for all $x > 0$, which completes the proof. □

Now, we are in a position to prove Lemma 4.1, which we recall states that

$$z(x) > z_1(x) \equiv z_0(x) - \alpha\beta\zeta_1(x), \qquad \text{as long as } z_1 > 0, \tag{A.6}$$

where

$$\zeta_1(x) = \int_0^x \sinh(x - s)\cosh(\beta \sinh(s))z_0^2(s)ds. \tag{A.7}$$

Proof of Lemma 4.1 We use a comparison argument. We insert the upper bounds for y and z found above in Proposition A.1 into the z equation of (A.1) to obtain

$$z'' - z > -\alpha\beta \cosh(\beta \sinh(x))z_0^2. \tag{A.8}$$

Hence, it is useful to examine the problem

$$z_1'' - z_1 = -\alpha\beta \cosh(\beta \sinh x)z_0^2, \qquad z_1(0) = 1, \qquad z_1'(0) = 0. \tag{A.9}$$

The homogeneous solution that satisfies the initial conditions is $z_0(x) = \cosh(x)$, and the particular solution is $-\alpha\beta\zeta_1(x)$, noting the minus sign, where $\zeta_1(x)$ is given by (A.7) above, namely by the solution of $\zeta_1'' - \zeta_1 = \cosh(\beta \sinh x)z_0^2$, with $\zeta_1(0) = 0$ and $\zeta_1'(0) = 0$. Therefore, we have

$$z_1(x) = z_0(x) - \alpha\beta\zeta_1(x). \tag{A.10}$$

Now, comparing the equations for z and z_1, namely (A.1) and (A.9), and recalling (A.8), we find that $z(x) > z_1(x)$, which completes the proof. □

Remark A.1 The sharper of the two upper bounds on y, namely $y < y_0$, from Proposition A.1 could also be used in this proof. That would lead to a slightly sharper lower bound on z, namely to the same expression for z_1 but with the modified Mathieu function $y_0(x) = C_0(\beta \sinh(x))$ in place of the term $\cosh(\beta \sinh(x))$ in the definition of ζ_1. However, the integrals are easier to evaluate with the weaker bound. Finally, to compare the two bounds, we found that the numerical values given by the sharper estimate are close. In fact, for the same values of α as reported in Table 2 we find $\xi(z_1)$= 1.419, 1.177, 1.051, 0.974, 0.917, 0.874, and $\xi(\mathcal{H}_1)$= 0.8564, 0.6095, 0.4762, 0.3842, 0.3088, 0.2410 (in increasing order of α).

To conclude this appendix we prove Lemma 4.2, which we recall establishes that $y(x) > y_1(x)$ and $y'(x) > y_1'(x)$, where y_1 satisfies

$$y_1'' - \beta^2 z_0^2(x) y_1 = -2\alpha\beta^3 \cosh(\beta \sinh(x)) z_0(x) \zeta_1(x), \qquad y_1(0) = 1, \quad y_1'(0) = 0. \tag{A.11}$$

Proof of Lemma 4.2 Again, we use comparison arguments. We recall from (A.1) that y satisfies

$$y'' = \beta^2 y z^2.$$

Substituting the lower bound $z(x) > z_1(x)$, obtained in the previous lemma, into the right member of this equation and recalling that $y(x) > 0$, we find

$$y'' > \beta^2 (z_0 - \alpha\beta\zeta_1)^2 y > \beta^2 (z_0^2 - 2\alpha\beta z_0 \zeta_1) y.$$

Then, recalling the upper bound $y(x) < \cosh(\beta \sinh(x))$ obtained in Proposition A.1, we find

$$y'' - \beta^2 z_0^2 y > -2\alpha\beta^3 \cosh(\beta \sinh(x)) z_0 \zeta_1, \qquad \text{for } 0 < x < \xi(z_1). \tag{A.12}$$

Clearly, since y_1 is defined to be the solution of the problem (A.11), we obtain the desired result that $y(x) > y_1(x)$, by comparison.

Finally, we show that $y'(x) > y_1'(x)$. Substituting the lower bound $z(x) > z_1(x)$ from the previous lemma into the equation for y, we find

$$y'' > \beta^2 z_1^2 y \qquad \text{on} \quad x > 0. \tag{A.13}$$

By integrating, we find

$$y'(x) > \int_0^x \beta^2 z_1^2(s) y(s) ds.$$

Next, we use the lower bound $y(x) > y_1(x)$ that was just established and expand the z_1^2 term using the definition of z_1 (recall (A.6)) to obtain

$$y'(x) > \int_0^x \beta^2 (z_0^2(s) - 2\alpha\beta z_0(s)\zeta_1(s) + \alpha^2\beta^2 \zeta_1^2(s)) y_1(s) ds.$$

In addition, we recall that $y(x) < y_0(x) < \cosh(\beta \sinh(x))$ from Proposition A.1 and observe that the third term in the right member of the lower bound on y' is positive. Hence,

$$y'(x) > \int_0^x (\beta^2 z_0^2(s) y_1(s) - 2\alpha\beta z_0(s)\zeta_1(s)\cosh(\beta\sinh(s)))ds.$$

Finally, we observe that the term in square brackets is precisely $y_1''(s)$ by (A.11). Hence,

$$y'(x) > \int_0^x y_1''(s)ds = y_1'(x), \tag{A.14}$$

which completes the proof. □

B The proof of Lemma 4.4: the asymptotics of the zeroes $\xi(z_1)$ and $\xi(\mathcal{H}_1)$

In this appendix, we prove Lemma 4.4, which gives the asymptotics of the first positive zeroes, $\xi(z_1)$ and $\xi(\mathcal{H}_1)$, of $z_1(x)$ and $\mathcal{H}_1(x)$, respectively, in the limit as $\alpha \to 0$. It also shows that at $x = \xi^*$, defined by (4.11), the three quantities $y'(x)$, $z(x)$ and $\mathcal{H}_1(x)$ are strictly positive.

The zeroes diverge as $\alpha \to 0$. Hence, we are interested in the asymptotics for large x throughout the proof. Moreover, we warn the reader that the asymptotics need to be carried out to fairly high order, so that some of the calculations are rather long.

Proof of Lemma 4.4

Part I. The asymptotics of $\xi(z_1)$. We start by recalling the definition of $z_1(x)$, the lower bound on $z(x)$,

$$z_1(x) = z_0(x) - \alpha\beta\zeta_1(x), \tag{B.1}$$

from (4.6). Here, the function

$$\zeta_1(x) = \int_0^x \sinh(x-t)\cosh^2(t)\cosh(\beta\sinh(t))dt \tag{B.2}$$

is the solution of the problem

$$\zeta_1'' - \zeta_1 = z_0^2(x)\cosh(\beta\sinh(x)), \qquad \text{with} \quad \zeta_1(0) = 0 \quad \text{and} \quad \zeta_1'(0) = 0.$$

A more useful formula for ζ_1 is obtained by using the addition formula for sinh, as follows:

$$\zeta_1(x) = \sinh(x)\phi_1(x) - \cosh(x)\phi_2(x), \tag{B.3}$$

where

$$\begin{aligned}
\phi_1(x) &= \int_0^x \cosh^3(t)\cosh(\beta\sinh(t))dt = \int_0^{\sinh(x)} (1+s^2)\cosh(\beta s)ds \\
\phi_2(x) &= \int_0^x \sinh(t)\cosh^2(t)\cosh(\beta\sinh(t))dt = \int_0^{\sinh(x)} s\sqrt{1+s^2}\cosh(\beta s)ds.
\end{aligned}$$

Next, set

$$r = \sinh(x) \qquad \text{and} \qquad \Phi_i(r) = \phi_i(x),\ i = 1, 2.$$

Then,

$$\Phi_1(r) = \frac{1}{\beta}\left(1 + \frac{2}{\beta^2} + r^2\right)\sinh(\beta r) - \frac{2}{\beta^2} r\cosh(\beta r),$$

which implies that to leading order

$$\Phi_1(r) = \frac{e^{\beta r}}{2\beta}\left(r^2 - \frac{2}{\beta}r + \frac{2}{\beta^2} + 1\right) \qquad \text{as} \qquad r \to \infty.$$

Hence, we have one of the two main ingredients for the asymptotics of $\zeta_1(x)$; to leading order,

$$r\Phi_1(r) = \frac{e^{\beta r}}{2\beta}\left(r^3 - \frac{2}{\beta}r^2 + \frac{2}{\beta^2}r + r\right). \tag{B.4}$$

Next, we turn to the function $\Phi_2(r)$. Note that

$$s\sqrt{1+s^2} = s^2\left\{1 + \frac{1}{2}s^{-2} - \frac{1}{8}s^{-4} + \frac{1}{16}s^{-6} + O(s^{-8})\right\}.$$

Hence,

$$\Phi_2(r) = \frac{1}{\beta}\left(r^2 + \frac{2}{\beta^2} + \frac{1}{2} - \frac{1}{8r^2}\right)\sinh(\beta r) - \frac{2}{\beta^2} r\cosh(\beta r) + \cdots,$$

which implies that to leading order

$$\Phi_2(r) = \frac{e^{\beta r}}{2\beta}\left(r^2 - \frac{2}{\beta}r + \frac{2}{\beta^2} + \frac{1}{2} - \frac{1}{8}r^{-2}\right) \qquad \text{as} \qquad r \to \infty.$$

Hence, the second of the two main ingredients for the asymptotics of $\zeta_1(x)$ is also in hand, namely to leading order

$$\sqrt{1+r^2}\Phi_2(r) = \frac{e^{\beta r}}{2\beta}\left(r^3 - \frac{2}{\beta}r^2 + \frac{2}{\beta^2}r + r - \frac{1}{\beta} + \frac{1}{\beta^2}r^{-1}\right) \tag{B.5}$$

Asymptotically, therefore, $\tilde{\zeta}_1(r) = \zeta_1(x)$ is given by subtracting (B.5) from (B.4),

$$\tilde{\zeta}_1(r) = \frac{e^{\beta r}}{2\beta^2}\left\{1 - \frac{1}{\beta}r^{-1} + \mathcal{O}(r^{-2})\right\}, \quad \text{where} \quad r = \sinh(x) \to \infty, \tag{B.6}$$

In turn, this result for ζ_1 enables us to obtain the desired asymptotics of $\xi = \xi(z_1)$, the first zero of $z_1(x)$, as follows. Setting $z_1(x) = 0$ in (B.1), we have $z_0(\xi) = \alpha\beta\zeta_1(\xi)$. In the limit of large r, this becomes

$$\sqrt{1+r^2} = \frac{\alpha}{2\beta}e^{\beta r},$$

which is equivalent, asymptotically, to

$$e^{\beta r} = \frac{2\beta}{\alpha}r, \qquad \text{as} \quad r \to \infty.$$

After an elementary computation, we find, to leading order,

$$r = \frac{1}{\beta} \ln\left(\frac{1}{\alpha}\right) + \frac{1}{\beta} \ln\left[\ln\left(\frac{1}{\alpha}\right)\right].$$

Therefore, recalling $r = \sinh(x)$, we wind up with the desired first formula in Lemma 4.4; namely, to leading order,

$$\xi(z_1) = \left(\ln \frac{2}{\beta}\left[\ln\left(\frac{1}{\alpha}\right)\right]\right)\left(1 + \left[\ln\left(\frac{1}{\alpha}\right)\right]^{-1}\right), \qquad \text{as} \qquad \alpha \to 0. \tag{B.7}$$

See also Table 3 below.

Part II. The asymptotics of $\xi(\mathcal{H}_1)$, the first zero of $\mathcal{H}_1$. We turn to $\mathcal{H}_1$, which we recall from (4.10) is given by

$$\mathcal{H}_1(x) \equiv -\frac{1}{2} + \frac{\alpha\beta}{3} + \frac{\alpha\beta}{3}\int_0^x y_1'(s) z_1^3(s) ds. \tag{B.8}$$

The goal is to find lower and upper bounds on the asymptotics of the first zero, $\xi(\mathcal{H}_1)$.

We begin with a lower bound on $\xi(\mathcal{H}_1)$. This lower bound will be the first zero of an upper bound on $\mathcal{H}_1$, and we label it ξ_0. We recall that $y_1'(x) < y'(x) < y_0'(x)$ and that $z_1(x) = z_0(x) - \alpha\beta\zeta_1(x) < z_0(x)$, as long as $y_1'(x) > 0$ and $z_1(x) > 0$. Hence, for these same values of x,

$$\mathcal{H}_1(x) < -\frac{1}{2} + \frac{\alpha\beta}{3} + \frac{\alpha\beta}{3} X_0(x), \qquad \text{where} \quad X_0(x) \equiv \int_0^x y_0'(s) z_0^3(s) ds. \tag{B.9}$$

Set $t = \beta \sinh(x)$. To leading order,

$$y_0'(x) \sim \frac{1}{\sqrt{2\pi}} e^t \sqrt{t}\left(1 - \frac{3}{8} t^{-1}\right) \qquad \text{as} \quad x \to \infty. \tag{B.10}$$

Also,

$$z_0(x) = \frac{1}{\beta}\sqrt{\beta^2 + t^2},$$

and the differential element for the integral defining X_0 is $ds = dt/\sqrt{\beta^2 + t^2}$. Hence, we find

$$X_0(x) = \frac{1}{\sqrt{2\pi}\beta^3} \int_0^t e^r r^{1/2}\left(1 - \frac{3}{8} r^{-1}\right)(\beta^2 + r^2) dr,$$

which, after some integration by parts, yields to leading order

$$X_0(x) = \frac{1}{\sqrt{2\pi\beta^3}} e^t t^{\frac{5}{2}}\left(1 - \frac{23}{8} t^{-1}\right), \qquad \text{where} \quad t = \beta \sinh(x). \tag{B.11}$$

Now, the upper bound on $\mathcal{H}_1$ first vanishes, to leading order, when

$$e^t t^{\frac{5}{2}}\left(1 - \frac{23}{8} t^{-1}\right) = \frac{K}{\alpha}, \qquad \text{as} \quad \alpha \to 0, \qquad \text{where} \quad K = \frac{3\beta^2\sqrt{2\pi}}{2}. \tag{B.12}$$

Taking the logarithm and Taylor expanding the natural logarithm of the third term in the left member (noting, a posteriori, that quadratic terms in this expansion are higher order), we find to leading order

$$t + \frac{5}{2}\ln(t) - \frac{23}{8}t^{-1} = \ln\left(\frac{1}{\alpha}\right) + \ln(K).$$

After some computations, we find that the first three terms in the asymptotic expansion of t are

$$t = \ln\left(\frac{1}{\alpha}\right) - \frac{5}{2}\ln\left[\ln\left(\frac{1}{\alpha}\right)\right] + \ln(K) \qquad \text{as} \quad \alpha \to 0. \tag{B.13}$$

Remark B.1 The next two terms are

$$\frac{25}{4}\left[\ln\left[\ln\left(\frac{1}{\alpha}\right)\right]\right]\left[\ln(1/\alpha)\right]^{-1} + \frac{5}{2}\left(\frac{23}{20} - \ln(K)\right)\left[\ln(1/\alpha)\right]^{-1}$$

with a remainder strictly

$$\mathcal{O}\left(\left[\ln\left[\ln\left(\frac{1}{\alpha}\right)\right]\right]\left[\ln(1/\alpha)\right]^{-2}\right).$$

Finally, recalling that $t = \beta\sinh(x) \sim (\beta/2)e^x$, we translate this result back into the original x variable to obtain the asymptotics of ξ_0,

$$\xi_0 \sim \ln\left[\ln\left(\frac{1}{\alpha}\right)\right] + \ln\left(\frac{2}{\beta}\right) - \frac{5}{2}\left[\ln\left[\ln\left(\frac{1}{\alpha}\right)\right]\right]\left[\ln\left(\frac{1}{\alpha}\right)\right]^{-1} + \left[\ln(K)\right]\left[\ln\left(\frac{1}{\alpha}\right)\right]^{-1}, \tag{B.14}$$

as $\alpha \to 0$. This completes the analysis of the lower bound, and hence also of the first half of the proof of Part II.

In this second half of the proof, we derive an upper bound for $\xi(\mathcal{H}_1)$ and the asymptotic expansion of this upper bound will turn out to agree with that of the lower bound, ξ_0, at least in the first five nontrivial terms, and hence the leading order asymptotics for $\xi(\mathcal{H}_1)$ will be as claimed in the second formula of this lemma.

In particular, we derive a lower bound on $\mathcal{H}_1$, and then, by construction, the first zero of this lower bound will be the desired upper bound on $\xi(\mathcal{H}_1)$. We label this zero ξ_U. Recall that $y_1'(x) < y'(x)$, as long as $z_1(x) > 0$, and that y_1 satisfies (4.9),

$$y_1'' - \beta^2 z_0^2(x) y_1 = -2\alpha\beta^3\cosh(\beta\sinh(x))z_0(x)\zeta_1(x), \qquad y_1(0) = 1, \quad y_1'(0) = 0. \tag{B.15}$$

Let $t = \beta\sinh(x)$ and $\eta_1(t) = y_1(x)$. This equation becomes

$$\ddot{\eta}_1 + \frac{t}{\beta^2 + t^2}\dot{\eta}_1 - \eta_1 = -f(t), \qquad \eta_1(0) = 1, \quad \dot{\eta}_1(0) = 0, \tag{B.16}$$

where

$$f(t) = \frac{2\alpha\beta^2}{\sqrt{\beta^2 + t^2}}\cosh(t)\zeta_1(t) \qquad \text{and} \qquad \zeta_1(t) = \frac{t}{\beta}\phi_1(t) - \sqrt{1 + \frac{t^2}{\beta^2}}\phi_2(t).$$

It is useful to compare the left member to the left member of the simpler, modified Bessel equation. Namely, we observe that

$$\ddot{\eta}_1 + \frac{1}{t}\dot{\eta}_1 - \eta_1 = -f(t) + \left(\frac{1}{t} - \frac{t}{\beta^2 + t^2}\right)\dot{\eta}_1 > -f(t), \qquad \text{as long as } \dot{\eta}_1 > 0 \quad \text{(B.17)}$$

Hence, we study the inhomogeneous modified Bessel equation,

$$\ddot{\eta}_2 + \frac{1}{t}\dot{\eta}_2 - \eta_2 = -f(t), \qquad \eta_2(0) = 1, \quad \dot{\eta}_2(0) = 0; \qquad \text{(B.18)}$$

and, from the comparison (B.17), we see that

$$\eta_2(t) < \eta_1(t) \qquad \text{and} \qquad \dot{\eta}_2(t) < \dot{\eta}_1(t), \quad \text{as long as } \dot{\eta}_1 > 0.$$

Moreover, letting $y_2(x) = \eta_2(t)$, we find the desired lower bound on $\mathcal{H}_1$,

$$\mathcal{H}_2(x) \equiv -\frac{1}{2} + \frac{\alpha\beta}{3} + \frac{\alpha\beta}{3} X_L(x) < \mathcal{H}_1(x), \qquad \text{where} \quad X_L(x) \equiv \int_0^x y_2'(s) z_1^3(s) ds. \quad \text{(B.19)}$$

The asymptotics of this lower bound are obtained as follows.

The solution of (B.18) that satisfies the initial conditions is

$$\eta_2(t) = I_0(t) + \tilde{\eta}_2(t), \quad \text{where} \quad \tilde{\eta}_2(t) = -I_0(t)\int_0^t r K_0(r) f(r) dr + K_0(t)\int_0^t r I_0(r) f(r) dr, \qquad \text{(B.20)}$$

and I_0 and K_0 are the modified Bessel functions of order zero. Writing η_2 in this manner as the sum of the homogeneous solution, $I_0(t)$, and the particular solution, $\tilde{\eta}_2(t)$, is advantageoues for keeping track of the asymptotics, as we will now see. The large t asymptotics are

$$\begin{aligned} I_0(t) &\sim \frac{e^t}{\sqrt{2\pi t}}\left(1 + \frac{1}{8}t^{-1} + \frac{9}{128}t^{-2}\right) \\ K_0(t) &\sim \sqrt{\frac{\pi}{2t}} e^{-t}\left(1 - \frac{1}{8}t^{-1} + \frac{9}{128}t^{-2}\right) \\ \zeta_1(t) &\sim \frac{e^t}{2\beta^2}\left(1 - t^{-1} + \frac{\beta^2}{4}t^{-2}\right), \end{aligned} \qquad \text{(B.21)}$$

where we recall (B.6). Hence, after some computation, we find

$$\eta_2(t) = \frac{e^t}{\sqrt{2\pi t}}\left(1 + \frac{1}{8}t^{-1} + \mathcal{O}(t^{-2})\right) - \frac{\alpha e^{2t}}{6t}\left(1 - \frac{1}{2}t^{-1} + \mathcal{O}(t^{-2})\right), \qquad \text{as} \quad t \to \infty$$

and also

$$\dot{\eta}_2(t) = \frac{e^t}{\sqrt{2\pi t}}\left(1 - \frac{3}{8}t^{-1} + \mathcal{O}(t^{-2})\right) - \frac{\alpha e^{2t}}{3t}\left(1 + \mathcal{O}(t^{-1})\right), \qquad \text{as} \quad t \to \infty$$

Converting this expression back into one in terms of the original x variable, we find

$$y_2'(x) = \dot{\eta}_2(t)\sqrt{\beta^2 + t^2} = \frac{e^t}{\sqrt{2\pi}}\sqrt{t}\left(1 - \frac{3}{8}t^{-1} + \mathcal{O}(t^{-2})\right) - \frac{\alpha e^{2t}}{3}\left(1 + \mathcal{O}(t^{-1})\right),$$

as $t = \beta \sinh(x) \to \infty$. A central observation now is that the first two terms, at least, in the asymptotic expansion of that part of y_2' that stems from the homogeneous solution coincide with the first two terms of the asymptotic expansion of y_0' above, recall (B.10). This observation will be essential to determining the asymptotics of the lower bound on $\mathcal{H}_1$, as well as on its first zero, as we show below. On a technical note, we will keep only these first two terms, as well as the dominant term from the particular solution.

For $\mathcal{H}_2$, the other two ingredients (expressed in terms of t) are

$$z_1(x) = z_0(x) - \alpha\beta\zeta_1(x) = \frac{1}{\beta}\sqrt{\beta^2 + t^2} - \alpha\beta\tilde{\zeta}_1(t).$$

and $dx = dt/\sqrt{\beta^2 + t^2}$. Hence, $X_L(x)$, the integral in $\mathcal{H}_2$, becomes

$$X_L(x) = X_1(x) - 3\alpha\beta X_2(x) + 3\alpha^2\beta^2 X_3(x) - \alpha^3\beta^3 X_4(x), \tag{B.22}$$

where $t = \beta \sinh(x)$ and

$$X_1(x) = \frac{1}{\beta^3}\int_0^t \left[\frac{1}{\sqrt{2\pi}}\sqrt{r}e^r\left(1 - \frac{3}{8}r^{-1}\right) - \frac{\alpha}{3}e^{2r}\right]\left(\beta^2 + r^2\right)dr \tag{B.23}$$

$$X_2(x) = \frac{1}{2\beta^4}\int_0^t \left[\frac{1}{\sqrt{2\pi}}\sqrt{r}e^r\left(1 - \frac{3}{8}r^{-1}\right) - \frac{\alpha}{3}e^{2r}\right]\sqrt{\beta^2 + r^2}e^r dr \tag{B.24}$$

$$X_3(x) = \frac{1}{4\beta^5}\int_0^t \left[\frac{1}{\sqrt{2\pi}}\sqrt{r}e^r\left(1 - \frac{3}{8}r^{-1}\right) - \frac{\alpha}{3}e^{2r}\right]e^{2r}dr \tag{B.25}$$

$$X_4(x) = \frac{1}{8\beta^6}\int_0^t \left[\frac{1}{\sqrt{2\pi}}\sqrt{r}e^r\left(1 - \frac{3}{8}r^{-1}\right) - \frac{\alpha}{3}e^{2r}\right]\frac{e^{3r}}{\sqrt{\beta^2 + r^2}}dr. \tag{B.26}$$

In the formula for $X_L(x)$, the stated terms from $X_1(x)$ are the dominant ones on the time scales over which $y_1'(x) > 0$ that we are interested in, and we recall that the integrals of these first terms were already found above in the computation of $X_0(x)$. Integrating the last term also, we find

$$X_L(x) \sim \frac{1}{\beta^3}\left[\frac{1}{\sqrt{2\pi}}t^{5/2}e^t\left(1 - \frac{23}{8}t^{-1}\right) - \frac{\alpha}{6}t^2e^{2t}\right]. \tag{B.27}$$

Moreover, ξ_U, the zero of the lower bound on $\mathcal{H}_1$, is given to leading order by the solution of

$$X_L(x) = \frac{3}{2\alpha\beta}.$$

We solve this equation, following the procedure used above. However, there is one significant difference. We have

$$e^t t^{\frac{5}{2}}\left(1 - \frac{23}{8}t^{-1} - \frac{\alpha\sqrt{2\pi}}{6}e^t t^{-\frac{1}{2}}\right) = \frac{K}{\alpha},$$

where the constant K is as before. The exponential term inside the parentheses is the significant difference. We will see that it is higher order, as follows. Taking the logarithm

and Taylor expanding (noting that the quadratic terms in this expansion are higher order, although here there is one more quadratic term that could have been important *a priori* but is not), we find

$$t + \frac{5}{2}\ln(t) - \frac{23}{8}t^{-1} - \frac{\alpha\sqrt{2\pi}}{6}e^t t^{-\frac{1}{2}} = \ln\left(\frac{1}{\alpha}\right) + \ln(K).$$

Since the leading order solution is $t = \ln(1/\alpha)$, we set

$$t = \ln\left(\frac{1}{\alpha}\right)(1+w), \tag{B.28}$$

to also find the relative error w. Substituting this into the equation, we find

$$\begin{aligned}&\left[\ln\left(\frac{1}{\alpha}\right)\right]w + \frac{5}{2}\left[\ln\left[\ln\left(\frac{1}{\alpha}\right)\right]\right] + \frac{5}{2}w - \frac{23}{8}\left[\ln\left(\frac{1}{\alpha}\right)\right]^{-1}(1-w)\\ &-\frac{\sqrt{2\pi}}{6}\left(\frac{1}{\alpha}\right)^w\left(1-\frac{w}{2}\right)\left[\ln\left(\frac{1}{\alpha}\right)\right]^{-\frac{1}{2}} = \ln(K)\end{aligned}$$

where we expanded $\ln(1+w) \sim w$ and $(1+w)^{-1/2} \sim 1 - (w/2)$. Next, we observe that

$$\left(\frac{1}{\alpha}\right)^w = e^{w\ln\left(\frac{1}{\alpha}\right)} \sim e^{-\frac{5}{2}\left[\ln\left[\ln\left(\frac{1}{\alpha}\right)\right]\right]} = \left[\ln\left(\frac{1}{\alpha}\right)\right]^{-\frac{5}{2}},$$

where we profited from looking ahead at the leading order asymptotics of w. Therefore, solving for w and recalling (B.28), we find that, as $\alpha \to 0$,

$$\begin{aligned}\xi_U &= \ln\left[\ln\left(\frac{1}{\alpha}\right)\right] + \ln\left(\frac{2}{\beta}\right) - \frac{5}{2}\left[\ln\left[\ln\left(\frac{1}{\alpha}\right)\right]\right]\left[\ln\left(\frac{1}{\alpha}\right)\right]^{-1} + [\ln(K)]\left[\ln\left(\frac{1}{\alpha}\right)\right]^{-1} + \cdots\\ &+ \mathcal{O}\left(\left[\ln\left[\ln\left(\frac{1}{\alpha}\right)\right]\right]\left[\ln\left(\frac{1}{\alpha}\right)\right]^{-3}\right).\end{aligned}$$

Now, by construction, ξ_U is an upper bound on $\xi(\mathcal{H}_1)$. But, we see that the first several terms in its asymptotic expansion agree with those of the lower bound ξ_0 found above. Moreover, they first differ in the term $\mathcal{O}\left(\left[\ln\left[\ln\left(\frac{1}{\alpha}\right)\right]\right]\left[\ln\left(\frac{1}{\alpha}\right)\right]^{-3}\right)$, which is in ξ_U, and which arises due to the fact that $X_0(x) - X_1(x)$, the difference between the integrals involved in the upper and lower bounds on $\mathcal{H}_1$, respectively, is to leading order $\frac{\alpha}{6}t^2e^{2t}$, which is a higher order term. Hence, the asymptotic expansion of $\xi(\mathcal{H}_1)$, which lies between ξ_0 and ξ_U, agrees with those of these bounds, at least to within the order stated, and is as given in the statement of the lemma.

Remark B.2 The other terms involving $X_2(x)$, $X_3(x)$, and $X_4(x)$ and the remaining terms obtained from integrating by parts in $X_1(x)$ correspond to higher order terms. For example,

$$-3\alpha\beta X_1(x) \sim -\frac{3\alpha}{2\beta^3}\left[\frac{1}{2\sqrt{2\pi}}t^{3/2}e^{2t} - \frac{\alpha}{9}te^{3t}\right].$$

However, these terms are higher order only by factors powers of $\ln(1/\alpha)$, which arise due to the differences in the fractional powers of t. In fact, the exponential terms all

lead to the same asymptotic expression; namely, we note that, for each integer $m > 0$, $\alpha^m e^{(m+1)t} = \alpha^{-1}$ at $t = \ln(1/\alpha)$, *i.e.*, at $x = \ln((2/\beta)\ln(1/\alpha))$.

Part III. Finally, we show that y_1', z_1, and $\mathcal{H}_1$ are positive at ξ^* for sufficiently small values of α. Recall that the 'time' ξ^* is defined implicitly by

$$\beta \sinh(\xi^*) = \ln\left(\frac{1}{\alpha}\right). \tag{B.29}$$

The equivalent explicit definition is

$$\xi^* = \xi^*(\alpha) = \sinh^{-1}\left\{\frac{1}{\beta}\ln\left(\frac{1}{\alpha}\right)\right\}.$$

Direct calculation using the above asymptotics for y_1', z_1, and $\mathcal{H}_1$ implies:

$$\begin{aligned}
y_1'(\xi^*) &= \frac{1}{\sqrt{2\pi}}\frac{\sqrt{\ln\left(\frac{1}{\alpha}\right)}}{\alpha}\left\{1 + \mathcal{O}\left(\frac{1}{\sqrt{\ln\left(\frac{1}{\alpha}\right)}}\right)\right\} \\
z_1(\xi^*) &= \frac{1}{2\beta}\ln\left(\frac{1}{\alpha}\right) + \mathcal{O}(1) \\
\mathcal{H}_1(\xi^*) &= \frac{1}{3\sqrt{2\pi}\beta^2}\left\{\ln\left(\frac{1}{\alpha}\right)\right\}^{5/2}\left\{1 + \mathcal{O}\left(\frac{1}{\sqrt{\ln\left(\frac{1}{\alpha}\right)}}\right)\right\} \qquad \text{as } \alpha \to 0.
\end{aligned} \tag{B.30}$$

This concludes the proof of the lemma. □

To confirm the above asymptotics, we compared the values of $\xi(z_1)$ and $\xi(\mathcal{H}_1)$ as computed by direct numerical simulations and by evaluation of the asymptotic formulas. The data is presented for the case $\beta = 4$ in Table 3.

α	$\xi(z_1)$ (num)	$\xi(z_1)$ (asymp)	$\xi(\mathcal{H}_1)$ (num)	$\xi(\mathcal{H}_1)$ (asymp)
10^{-4}	1.902	1.693	1.372	1.369
10^{-5}	2.076	1.902	1.565	1.576
10^{-6}	2.223	2.073	1.744	1.754
10^{-7}	2.341	2.216	1.890	1.910
10^{-8}	2.458	2.341	2.025	2.047
10^{-9}	2.551	2.451	2.152	2.170

Table 3. The values of $\xi(z_1)$ and $\xi(\mathcal{H}_1)$ as computed via direct numerical simulations (num) and via evaluation of the asymptotic formulas (asymp), recall (B.7) and the lower bound given by (B.14). Here $\beta = 4$.

C The proof of Lemma 4.5: the nontrivial lower bound $\mathcal{B}_{\text{lower}}$ on $\mathcal{A}_{\text{even}}$

In this appendix, we prove Lemma 4.5, which we recall establishes the curve $\mathcal{B}_{\text{lower}}$. In particular, for each $\alpha > 0$, there exists a $\beta_L(\alpha)$ such that there are no homoclinic orbits for $\beta < \beta_L(\alpha)$. Also, after the proof of this lemma, the asymptotics of $\beta_L(\alpha)$ are presented both for $\alpha \to \infty$ and for $\alpha \to 0$.

It will be convenient first to normalize u and v by scaling the dependent variables as we did in the proof of Lemma 4.3. Let

$$u(x) = \alpha y(x) \qquad \text{and} \qquad v(x) = \beta z(x). \tag{C.1}$$

We recall that the equations become

$$y'' = \beta^2 y z^2 \qquad \text{and} \qquad z'' = z(1 - \alpha\beta\, yz), \tag{C.2}$$

with initial data $y(0) = 1$, $y'(0) = 0$, $z(0) = 1$, and $z'(0) = 0$, and the energy function is

$$\mathcal{H}(y, y', z, z') = \frac{1}{2} z'^2 - \frac{1}{2} z^2 + \frac{1}{3} \alpha\beta y z^3.$$

Now,

$$\mathcal{H}'(x) = \frac{1}{3} \alpha\beta\, y'(x) z^3(x);$$

and, hence, $\mathcal{H}$ increases along homoclinic orbits, because $z(x) > 0$ by assumption for homoclinic orbits and $y'(x) > 0$ by (C.2). Moreover, for any $x > 0$, one finds

$$\mathcal{H}(x) = \mathcal{H}(0) + \frac{1}{3} \alpha\beta \int_0^x y'(t) z^3(t)\, dt; \qquad \mathcal{H}(0) = -\frac{1}{2} + \frac{1}{3} \alpha\beta. \tag{C.3}$$

The proof will be by contradiction. We will show that, for any $\alpha > 0$, there exists a $\beta_L(\alpha)$ such that, if β is smaller than $\beta_L(\alpha)$, then there is some finite value of x, which we will label $\xi(\beta)$, such that $\mathcal{H}(\xi(\beta)) > 0$. (The variable ξ here is different from that used earlier.) This will in turn yield a contradiction with the fact $\mathcal{H}(x) \to 0^-$ as $x \to \infty$ along a homoclinic orbit.

Proof of Lemma 4.5 Let

$$\xi = \xi(\beta) = k \log\Big(\frac{1}{\beta}\Big), \qquad \frac{3}{5} < k < 1. \tag{C.4}$$

We will show that for each $\alpha > 0$ there exists a $\beta_L(\alpha)$ such that

$$\mathcal{H}(\xi) > 0 \qquad \text{for} \qquad \beta \in (0, \beta_L(\alpha)). \tag{C.5}$$

We follow the by-now standard strategy, namely we first derive upper bounds on the components $z(x)$ and $y(x)$ for all $x \in [0, \xi(\beta)]$, and then we use these to help derive lower bounds on both $z(x)$ and $y'(x)$, the two key ingredients in $\mathcal{H}'(x)$.

Since $y(x) > 0$ for all x, it follows from (C.2) that

$$y(x) > 1 \qquad \text{and} \qquad z(x) < \cosh(x) \qquad \text{for} \qquad x > 0.$$

Therefore, one directly obtains the following upper bound on z:

$$z(x) < \cosh(\xi) \leq e^{\xi} = \beta^{-k} \qquad \text{for} \qquad 0 < x \leq \xi. \tag{C.6}$$

Next, we seek an upper bound on $y(x)$. Substitution of (C.6) into (C.2) yields

$$y'' < \beta^{2(1-k)} y \qquad \text{for} \qquad 0 < x \leq \xi.$$

Integration of this inequality then yields

$$y(x) < \cosh(\beta^{1-k}x) \leq \cosh(\beta^{1-k}\xi) < \exp(\beta^{1-k}\xi) \stackrel{\text{def}}{=} \eta(\beta) \qquad \text{for} \qquad 0 < x \leq \xi. \tag{C.7}$$

Also, $\lim_{\beta \to 0} \eta(\beta) = 1$, since $k < 1$ and

$$\beta^{1-k}\xi = k\beta^{1-k} \log\left(\frac{1}{\beta}\right) \to 0 \quad \text{as} \quad \beta \to 0.$$

Now, we bound $z(x)$ from below. Substitution of (C.6) and (C.7) into (C.2) yields

$$z'' > \mu^2 z, \qquad \mu = \sqrt{1 - \alpha\beta^{1-k}\eta(\beta)}. \tag{C.8}$$

Therefore,

$$z(x) > \cosh(\mu\, x) \qquad \text{for} \qquad 0 < x \leq \xi, \tag{C.9}$$

which is the desired lower bound.

Remark C.1. $\mu(\beta) \to 1^-$ as $\beta \to 0^+$.

Finally, we estimate y' from below. By putting the lower bound (C.9) for z into (C.2) and recalling that $y(x) > 1$ for $x > 0$, we obtain

$$y'' > \beta^2 \cosh^2(\mu\, x) \qquad \text{for} \qquad 0 < x \leq \xi.$$

Hence,

$$y'(x) > \beta^2 \int_0^x \cosh^2(\mu\, t)\, dt > \frac{\beta^2}{4} \sinh(2\mu x) \qquad \text{for} \qquad 0 < x \leq \xi. \tag{C.10}$$

We now have the two necessary ingredients, (C.9) and (C.10), to derive a lower bound on $\mathcal{H}(\xi)$. Substituting these into the formula (C.3) for $\mathcal{H}(\xi)$, we find

$$\begin{aligned} \mathcal{H}(\xi) &> \frac{1}{12}\alpha\beta^3 \int_0^{\xi} \sinh(2\mu t) \cosh^3(\mu t)\, dt + \mathcal{H}(0) \\ &= \frac{\alpha\beta^3}{30\mu}\{\cosh^5(\mu\xi) - 1\} + \mathcal{H}(0) \\ &> \frac{\alpha\beta^{3-5\mu k}}{2^6 \cdot 15\mu}(1 - 32\beta^{5\mu k}) - \frac{1}{2} + \frac{1}{3}\alpha\beta. \end{aligned} \tag{C.11}$$

Evidently, we have to choose k and β such that

$$3 - 5\mu k < 0. \tag{C.12}$$

Since we have fixed $k > \frac{3}{5}$, and $\mu(\beta) \to 1^-$ as $\beta \to 0^+$, there exists a $\beta_1 > 0$ such that (C.12) is satisfied. Also, by taking β sufficiently small, i.e. smaller than some $\beta_2 > 0$, we can ensure that $\mathcal{H}(\xi) > 0$, as desired. Therefore, by taking $\beta_L = \min\{\beta_1, \beta_2\}$, we have shown that for $\beta < \beta_L$ homoclinic orbits cannot exist. □

As we will now show, the curve $\mathcal{B}_{\text{lower}}$ is a sharp lower bound in the limit that $\alpha \to \infty$. Consider the curve

$$\Gamma_\nu : \quad \{(\alpha, \beta) : \alpha = K\beta^{-\nu}\}, \qquad \nu > 0,$$

for any positive, $\mathcal{O}(1)$ constant K, and repeat the above argument while α and β stay on Γ_ν as $\beta \to 0$. We find that we now need to fix k, β and ν such that

$$3 - 5\mu k - \nu < 0 \qquad \text{and} \qquad k < 1 - \nu.$$

Since $\mu(\beta) \to 1$ as $\beta \to 0$, it is possible for any $\nu < \frac{1}{2}$ to find k and β_1 so that these two inequalities are satisfied for $\beta < \beta_1$. Like before, this implies the existence of a constant $\beta_L \in (0, \beta_1]$ such that no homoclinic orbit can exist for $\beta < \beta_L$. Moreover, recalling that the curve $\mathcal{C}_2$ is given asymptotically by $\beta = \beta_2(\alpha) = \frac{6\sqrt{2}}{\sqrt{5}} \frac{1}{\alpha^2}$ as $\alpha \to \infty$, we see that $\mathcal{B}_{\text{lower}}$ is a sharp lower bound, because the above estimate holds for any $0 < \nu < \frac{1}{2}$, and hence for any $\beta_L \ll \frac{K^2}{\alpha^2}$.

Finally, we also briefly examine the $\alpha \to 0$ asymptotics of $\beta_L(\alpha)$. To this end, consider

$$\tilde{\Gamma}_\nu : \quad \{(\alpha, \beta) : \alpha = K\beta^{\nu}\}, \qquad \nu > 0, K > 0.$$

The conditions are now

$$3 - 5\mu k + \nu < 0 \qquad \text{and} \qquad k < 1.$$

Since $\mu(\beta) \to 1$ as $\beta \to 0$, it follows that for any $\nu \in (0, 2)$ it is possible to find constants k and β_1 such that for any $\beta \in (0, \beta_1)$ the two inequalities are satisfied. This completes our analysis of the curve $\mathcal{B}_{\text{lower}}$ and this appendix.